

REACTIVITY OF THE $[\text{B}_{20}\text{H}_{18}]^{2-}$ ION WITH CARBON NUCLEOPHILES
FOR POTENTIAL APPLICATION IN BNCT

THESIS

Presented to the Graduate Council of
Texas State University-San Marcos
in Partial Fulfillment
of the Requirements

for the Degree

Master of SCIENCE

by

Martin J. Mantz, B.S.

San Marcos, Texas
December 2013

REACTIVITY OF THE $[\text{B}_{20}\text{H}_{18}]^{2-}$ ION WITH CARBON NUCLEOPHILES
FOR POTENTIAL APPLICATION IN BNCT

Committee Members Approved:

Debra A. Feakes

Todd Hudnall

Chad Booth

Approved:

Andrea Golato
Dean of the Graduate College

COPYRIGHT

by

Martin J. Mantz

2013

FAIR USE AND AUTHOR'S PERMISSION STATEMENT

Fair Use

This work is protected by the Copyright Laws of the United States (Public Law 94-553, section 107). Consistent with fair use as defined in the Copyright Laws, brief quotations from this material are allowed with proper acknowledgment. Use of this material for financial gain without the author's express written permission is not allowed.

Duplication Permission

As the copyright holder of this work I, Martin J. Mantz, refuse permission to copy in excess of the "Fair Use" exemption without my written permission.

ACKNOWLEDGEMENTS

I would like to acknowledge my committee members: Dr. Hudnall and Dr. Booth for their guidance in my graduate career. I would also like to give special thanks to Dr. Feakes for her consistent enthusiasm towards the nature of chemistry. I would like to thank Jaci Smits for the preliminary observation of the *n*-butyllithium carbon nucleophile reaction which served as the basis for this thesis work. Airybel Rodriguez deserves credit for her assistance in the laboratory. I would also like to thank the Department of Chemistry and Biochemistry for financial support during my graduate studies. Dan Milikan deserves thanks for his efforts supporting NMR data collection.

I would like to recognize my mother and father for their support during my career. I would also like to thank Dustin Guilbeaux, a friend.

This manuscript was submitted on August 7th, 2013.

TABLE OF CONTENTS

	Page
ACKNOWLEDGEMENTS.....	v
LIST OF FIGURES	ix
ABSTRACT.....	xi
CHAPTER	
I. INTRODUCTION	1
1.1 Boron Hydrides.....	1
1.2 Nucleophilic Attack on the [<i>trans</i> -B ₂₀ H ₁₈] ²⁻ Ion.....	7
1.3 Carbon Nucleophiles.....	12
1.4 BNCT.....	14
1.5 Liposomal Delivery	15
II. STATEMENT OF PROBLEM	18
III. EXPERIMENTAL.....	20
3.1 Materials	20
3.2 Physical Measurements.....	20
3.3 Synthetic Procedures.....	21
Preparation of (Et ₃ NH) ₂ [<i>closo</i> -B ₁₀ H ₁₀].....	21
Preparation of (Et ₃ NH) ₂ [<i>trans</i> -B ₂₀ H ₁₈]	22
Preparation of Rb ₄ [<i>ae</i> -B ₂₀ H ₁₇ (CH ₂) ₃ CH ₃].....	22
Preparation of Rb ₄ [<i>ae</i> -B ₂₀ H ₁₇ C ₂ H]	23
Preparation of Rb ₄ [<i>ae</i> -B ₂₀ H ₁₇ CH ₂ CN].....	24
Preparation of Rb ₄ [<i>a</i> ² -B ₂₀ H ₁₇ (CH ₂) ₃ CH ₃].....	25
Preparation of Rb ₄ [<i>a</i> ² -B ₂₀ H ₁₇ C ₂ H].....	25
Preparation of Rb ₄ [<i>a</i> ² -B ₂₀ H ₁₇ CH ₂ CN]	26
Preparation of (Me ₄ N) ₂ [B ₂₀ H ₁₇ (CH ₂) ₃ CH ₃].....	26
Preparation of (Bu ₄ N) ₂ [B ₂₀ H ₁₇ C ₂ H]	27
Preparation of (Bu ₄ N) ₂ [B ₂₀ H ₁₇ CH ₂ CN].....	28
IV. RESULTS and DISCUSSION.....	29

4.1 Reduced Derivatives	30
Results regarding $\text{Rb}_4[\text{ae-B}_{20}\text{H}_{17}(\text{CH}_2)_3\text{CH}_3]$	30
Results regarding $\text{Rb}_4[\text{a}^2\text{-B}_{20}\text{H}_{17}(\text{CH}_2)_3\text{CH}_3]$	33
Results regarding $\text{Rb}_4[\text{ae-B}_{20}\text{H}_{17}\text{C}_2\text{H}]$	35
Results regarding $\text{Rb}_4[\text{a}^2\text{-B}_{20}\text{H}_{17}\text{C}_2\text{H}]$	37
Results regarding $\text{Rb}_4[\text{ae-B}_{20}\text{H}_{17}\text{CH}_2\text{CN}]$	39
Results regarding $\text{Rb}_4[\text{a}^2\text{-B}_{20}\text{H}_{17}\text{CH}_2\text{CN}]$	42
4.2 Oxidized Derivatives	45
Results regarding $(\text{Me}_4\text{N})_2[\text{B}_{20}\text{H}_{17}(\text{CH}_2)_3\text{CH}_3]$	46
Results regarding $(\text{Bu}_4\text{N})_2[\text{B}_{20}\text{H}_{17}\text{C}_2\text{H}]$	49
Results regarding $(\text{Bu}_4\text{N})_2[\text{B}_{20}\text{H}_{17}\text{CH}_2\text{CN}]$	52
V. CONCLUSIONS	54
VI. FUTURE WORKS	58
6.1 Acetonitrile Derivatives	58
6.2 Acetylide Derivatives	60
6.3 Amino Acid Coupling	60
APPENDIX: SPECTRA	62
REFERENCES	101

LIST OF FIGURES

Figure	Page
1. Structure of decaborane, B ₁₀ H ₁₄	2
2. Structure of the [<i>closo</i> -B ₁₀ H ₁₀] ²⁻ anion.	3
3. Oxidation of the [B ₁₀ H ₁₀] ²⁻ ion to form the [B ₂₀ H ₁₈] ²⁻ anion. ● = B; ○ = BH.....	3
4. Structures of the three known isomers of the [B ₂₀ H ₁₈] ²⁻ ion. ● = B; ○ = BH.	4
5. Isomers of the reduced [B ₂₀ H ₁₈] ⁴⁻ ion. ● = B; ○ = BH	5
6. Redox reaction of [<i>ae</i> -B ₂₀ H ₁₈] ⁴⁻ to [<i>trans</i> -B ₂₀ H ₁₈] ²⁻	6
7. Mechanism of nucleophilic attack proposed by Hawthorne in 1965. ● = B; ○ = BH.	7
8. Rearrangement of the <i>ae</i> -isomer to the <i>a</i> ² -isomer. ● = B; ○ = BH.....	8
9. ¹¹ B NMR spectrum of the [<i>trans</i> -B ₂₀ H ₁₈] ²⁻ ion.....	9
10. Representative ¹¹ B NMR spectrum of an apical-equatorial isomer of [B ₂₀ H ₁₇ X] ⁴⁻ (X is a generic nucleophile) indicating the apical or substituted region and the equatorial region of the spectrum.....	10
11. Representative ¹¹ B NMR spectrum of an apical-apical isomer of [B ₂₀ H ₁₇ X] ⁴⁻ (X is a generic nucleophile) indicating the apical or substituted region and the equatorial region of the spectrum.....	11
12. Oxidation of [<i>ae</i> -B ₂₀ H ₁₇ OH] ⁴⁻ to [<i>trans</i> -B ₂₀ H ₁₇ OH] ²⁻	12
13. Reaction of the <i>n</i> -butyl ion with [<i>trans</i> -B ₂₀ H ₁₈] ²⁻	31
14. ¹¹ B{ ¹ H} and ¹¹ B NMR spectra of Rb ₄ [<i>ae</i> -B ₂₀ H ₁₇ (CH ₂) ₃ CH ₃].....	32
15. Isomerization of [B ₂₀ H ₁₇ (CH ₂) ₃ CH ₃] ⁴⁻	33
16. ¹¹ B{ ¹ H} and ¹¹ B NMR spectra of Rb ₄ [<i>a</i> ² -B ₂₀ H ₁₇ (CH ₂) ₃ CH ₃].....	34
17. Reaction of the acetylide ion with [<i>trans</i> -B ₂₀ H ₁₈] ²⁻	36

18. $^{11}\text{B}\{^1\text{H}\}$ and ^{11}B NMR spectra of $\text{Rb}_4[\text{ae-B}_{20}\text{H}_{17}\text{C}_2\text{H}]$	36
19. Isomerization of $[\text{B}_{20}\text{H}_{17}\text{C}\equiv\text{CH}]^{4-}$	38
20. $^{11}\text{B}\{^1\text{H}\}$ and ^{11}B NMR spectra of $\text{Rb}_4[\alpha^2\text{-B}_{20}\text{H}_{17}\text{C}_2\text{H}]$	38
21. Reaction of $^-\text{CH}_2\text{CN}$ with $[\text{trans-B}_{20}\text{H}_{18}]^{2-}$	40
22. $^{11}\text{B}\{^1\text{H}\}$ and ^{11}B NMR spectra of $\text{Rb}_4[\text{ae-B}_{20}\text{H}_{17}\text{CH}_2\text{CN}]$	41
23. Isomerization of $[\text{B}_{20}\text{H}_{17}\text{CH}_2\text{CN}]^{4-}$	42
24. $^{11}\text{B}\{^1\text{H}\}$ and ^{11}B NMR spectra of $\text{Rb}_4[\alpha^2\text{-B}_{20}\text{H}_{17}\text{CH}_2\text{CN}]$	43
25. Oxidation of $[\text{ae-B}_{20}\text{H}_{17}(\text{CH}_2)_3\text{CH}_3]^{4-}$ to $[\text{trans-B}_{20}\text{H}_{17}(\text{CH}_2)_3\text{CH}_3]^{2-}$	46
26. $^{11}\text{B}\{^1\text{H}\}$ and ^{11}B NMR spectra of $(\text{Me}_4\text{N})_2[\text{B}_{20}\text{H}_{17}(\text{CH}_2)_3\text{CH}_3]$	48
27. Oxidation of $[\text{ae-B}_{20}\text{H}_{17}(\text{C}_2\text{H})]^{4-}$ to $[\text{trans-B}_{20}\text{H}_{17}(\text{C}_2\text{H})]^{2-}$	49
28. $^{11}\text{B}\{^1\text{H}\}$ and ^{11}B NMR spectra of $(\text{Bu}_4\text{N})_2[\text{B}_{20}\text{H}_{17}\text{C}_2\text{H}]$	51
29. $^{11}\text{B}\{^1\text{H}\}$ and ^{11}B NMR spectra of $(\text{Bu}_4\text{N})_2[\text{B}_{20}\text{H}_{17}\text{CH}_2\text{CN}]$	52
30. $^{11}\text{B}\{^1\text{H}\}$ and ^{11}B NMR spectra of $(\text{Bu}_4\text{N})_2[\text{B}_{20}\text{H}_{17}\text{CH}_2\text{CN}]$	53
31. Hydrolysis of $[\text{B}_{20}\text{H}_{17}\text{CH}_2\text{CN}]^{4-}$	59
32. Oxidation of the acetylide functional group of $[\text{trans-B}_{20}\text{H}_{17}\text{C}_2\text{H}]^{2-}$	60
33. Coupling of carboxylic acid derivative to a representative amino acid, the ethyl ester of tyrosine.....	61

ABSTRACT

REACTIVITY OF THE $[B_{20}H_{18}]^{2-}$ ION WITH CARBON NUCLEOPHILES FOR POTENTIAL APPLICATION IN BNCT

by

Martin J. Mantz, B.S.

Texas State University-San Marcos

December 2013

SUPERVISING PROFESSOR: DEBRA A. FEAKES

Boron neutron capture therapy is a field of interdisciplinary medicine. The well-known binary nuclear reaction of the boron isotope, boron-10, with a thermal neutron is used as the basis of all research in this field. When a neutron comes into contact with the boron-10 nucleus an unstable atom is created which undergoes fission to produce a Li^{3+} ion, a He^{2+} ion, and a gamma photon. The process releases 2.28 MeV of kinetic energy, which is distributed between the He^{2+} ion and the Li^{3+} ion. The kinetic energy of the resulting ions is the valuable product towards the therapeutic benefits of this reaction. When this reaction is carried out in the cell mass of a tumor, the energetic ions cause ionization tracking and cellular damage resulting in toxicity within a radius of 10 micrometers. As a result of both the localization of the boron-10 nuclei in the tumor cells and the localized distribution of kinetic energy resulting from the neutron capture reaction, the irradiated tumor cells should be destroyed without damage to bordering normal cells. A boron target compound is necessary for boron-10 enrichment and

subsequent irradiation with thermal neutrons. The [*trans*-B₂₀H₁₈]²⁻ anion has been of particular interest due to its large boron content per unit charge and an electron deficient region within its structure. This region is characterized by dual three-center two-electron bonds which are susceptible to nucleophilic attack. While nucleophilic attack on the [*trans*-B₂₀H₁₈]²⁻ anion has been reported for the hydroxide ion, alkoxide ions, amide ions, and thiolate ions, no literature reports have been made regarding the susceptibility of the electron-deficient bonds to nucleophilic attack by carbanions. Therefore, the specific aims of the proposed research are to:

- 1) develop a synthetic route to evaluate the reactivity of the [*trans*-B₂₀H₁₈]²⁻ anion with the selected carbon nucleophiles to produce a series of substituted isomers, of the [B₂₀H₁₇X]⁴⁻ ion where X is the selected carbon nucleophile.
- 2) investigate the ability of the resulting reduced polyhedral borane anions to undergo oxidation and restore the three center, two electron bonds that are susceptible to further nucleophilic attack, producing substituted isomers of the [B₂₀H₁₇X]²⁻ ion where X is the selected carbon nucleophile

In order for this anion and derivatives of the anion to fulfill their potential use towards BNCT, a method must be available by which their accumulation is possible in therapeutic concentrations inside the tumor. Compounds which have the potential to bind to intracellular proteins remain within the tumor in *in vivo* biodistribution experiments. Therefore, the synthesis of a series of boron-rich compounds with the potential to bind to intracellular proteins is the goal of this research.

CHAPTER I

INTRODUCTION

1.1 Boron Hydrides

Being to the left of carbon on the periodic table, boron has one less valence electron and, as a result, is less electronegative than its more popular neighbor, carbon. Nonetheless, the chemistry of these two elements can be compared. For example, both boron and carbon are known to bond with themselves, catenating to form families of binary hydrides. With boron, the binary hydrides are known as boranes as opposed to carbon and its associated alkanes.¹ In addition, hydrides of both carbon and boron are known to exhibit aromaticity. The planar structure of the arenes formed by carbon is much different than the three dimensional aromatic *closo* cluster compounds formed by boron. While not all of the cluster compounds demonstrate aromaticity, they are all known as polyhedral boranes and their structures are classified by Wade's rules.² Polyhedral borane species containing a large numbers of boron atoms are of interest for potential application in BNCT, a proposed cancer treatment based on the ability of the boron-10 isotope to capture thermal neutrons.³

Alfred Stock pioneered the synthesis of boron hydrides.¹ Stock has been attributed with the development of air-sensitive techniques which were essential in the preparation of the volatile and potentially explosive borane compounds B_2H_6 , B_4H_6 , B_5H_{11} , and B_6H_{10} .⁴ The synthesis of the relatively stable, yet extremely hazardous,

$B_{10}H_{14}$, known as decaborane, is also attributed to Stock.^{4,5} Decaborane is characterized by ten B-H vertices linked through a series of B-B-B and B-H-B bonds in a *nido* structure (Figure 1).⁴ The compound is produced by the pyrolysis of smaller boron hydride clusters under vacuum and purified by sublimation to form a white crystalline solid.⁵

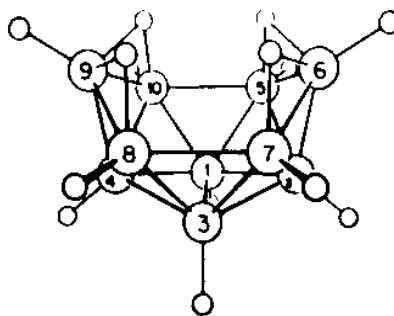


Figure 1: Structure of decaborane, $B_{10}H_{14}$.⁴

Professor William Lipscomb received the 1976 Nobel Prize in Chemistry for his research on the structure and bonding of boron-containing compounds.⁴ Lipscomb's investigations of boron compounds containing three-center two-electron bonds have been quintessential to the development and understanding of boron hydride chemistry. He developed the theory which has been used to explain the types of bonds within the boron framework of a borane structure, ultimately leading to the evolution of new reaction mechanisms.⁴ His molecular orbital studies on boranes set forth vital guidelines for chemists working with boron hydride compounds and the enigmatic ability of boron to bond through unconventional means.⁴

In cooperation with theoretical investigations by Hoffman and Lipscomb, aromatic polyhedral borane chemistry was established as a new field of chemistry.⁶ The

aromatic species are now classified as *closo* structures, based upon their $n+1$ bonding orbitals, where n is the number of polyhedral vertices.² The $[closo-B_{10}H_{10}]^{2-}$ ion^{7,8} (**Figure 2**) and the $[closo-B_{12}H_{12}]^{2-}$ ion⁹ were discovered in 1959 and 1960, respectively. The preferred synthetic route to prepare the $[closo-B_{10}H_{10}]^{2-}$ anion, particularly for the proposed research is the reaction of decaborane with triethylamine.¹⁰

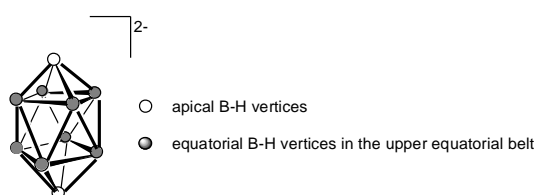


Figure 2: Structure of the $[closo-B_{10}H_{10}]^{2-}$ anion.⁷

The difference in reactivity between these two dianions, $[closo-B_{10}H_{10}]^{2-}$ and $[closo-B_{12}H_{12}]^{2-}$, is evident when either ion is introduced to oxidative conditions with reagents such as Ce^{4+} and Fe^{3+} in aqueous solution; $[closo-B_{12}H_{12}]^{2-}$ is unreactive while $[closo-B_{10}H_{10}]^{2-}$ undergoes oxidative conversion to form $[B_{20}H_{18}]^{2-}$.³ The normal isomer of the $[B_{20}H_{18}]^{2-}$ anion (**Figure 3**), designated $[n-B_{20}H_{18}]^{2-}$, was first prepared by Kaczmarczyk and co-workers in 1962 using Fe^{3+} as the oxidizing agent.¹¹

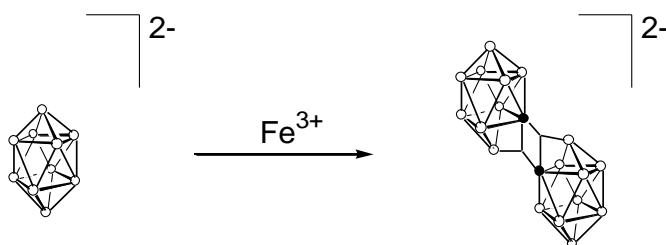


Figure 3: Oxidation of the $[B_{10}H_{10}]^{2-}$ ion to form the $[B_{20}H_{18}]^{2-}$ anion.¹¹ ● = B; ○ = BH

In the proposed mechanism for this reaction, it is the equatorial (*e*) boron atom that loses its terminal (*exo*) hydrogen atom during the oxidation, rather than the apical (*a*) boron atom.¹ The ferric ion oxidation of the polyhedral [*closo*-B₁₀H₁₀]²⁻ ion was previously reported to produce the [*n*-B₂₀H₁₈]²⁻ ion, and Lipscomb suggested a doubly H-bridged structure for this ion. The currently established structure of [*n*-B₂₀H₁₈]²⁻ is known to be linked by dual three center two electron bonds.¹²

Three isomers of the [B₂₀H₁₈]²⁻ anion are known, each consisting of two polyhedral [B₁₀H₉]⁻ anions linked by a pair of three-center two-electron bonds (**Figure 4**).¹¹⁻¹⁵ The relative location and composition of the unique bonding region determines the isomeric assignment of the polyhedral borane isomer. The [*trans*-B₂₀H₁₈]²⁻, equivalent to the normal isomer, [*n*-B₂₀H₁₈]²⁻, and the [*cis*-B₂₀H₁₈]²⁻ isomers are both characterized by the presence of B-B-B linkages at the intercage region while the [*iso*-B₂₀H₁₈]²⁻ isomer is characterized by a set of B-H-B linkages between two parallel [B₁₀H₉]⁻ cages.¹¹⁻¹⁵

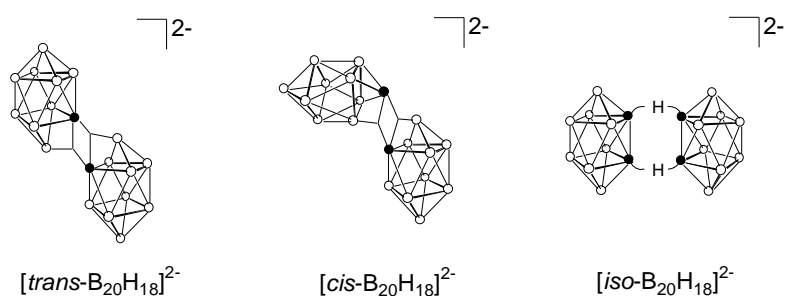


Figure 4: Structures of the three known isomers of the [B₂₀H₁₈]²⁻ ion.¹¹ ● = B; ○ = BH.

The known isomers of the [B₂₀H₁₈]²⁻ anion are produced by different means. The [*trans*-B₂₀H₁₈]²⁻ isomer, first reported in 1962, was produced by the oxidation of the

$[\text{B}_{10}\text{H}_{10}]^{2-}$ anion with the Fe^{3+} ion.^{11,13} The pale yellow color of the $[\text{trans-B}_{20}\text{H}_{18}]^{2-}$ is due to a pair of strong electronic absorptions at 232 and 292 nm.¹³ Irradiation of the $[\text{trans-B}_{20}\text{H}_{18}]^{2-}$ anion with ultraviolet light in acetonitrile results in the production of the symmetric $[\text{iso-B}_{20}\text{H}_{18}]^{2-}$ species, a photoisomer of $[\text{trans-B}_{20}\text{H}_{18}]^{2-}$.¹⁴ Salts of the photoisomer will revert to the normal isomer by thermal soaking at 110°C for 36 hours.¹⁴ The most recently discovered isomer is the $[\text{cis-B}_{20}\text{H}_{18}]^{2-}$ anion.¹⁵ The *cis* isomer can be produced directly by the low temperature oxidation of an $[\text{ae-B}_{20}\text{H}_{18}]^{4-}$ anion with Fe^{3+} .¹⁶ The *cis* isomer can be converted to the $[\text{trans-B}_{20}\text{H}_{18}]^{2-}$ ion by heating or by the addition of catalytic amounts of HCl. It can be converted to the $[\text{iso-B}_{20}\text{H}_{18}]^{2-}$ anion, through a photoisomerization process.¹

The ferric ion oxidation of $[\text{closio-B}_{10}\text{H}_{10}]^{2-}$ produced the $[\text{trans-B}_{20}\text{H}_{18}]^{2-}$ and a $[\text{B}_{20}\text{H}_{19}]^{3-}$ ion, a protonated $[\text{B}_{20}\text{H}_{18}]^{4-}$ ion.¹⁷ Reaction of $[\text{trans-B}_{20}\text{H}_{18}]^{2-}$ with sodium in liquid ammonia produces the reduced $[\text{B}_{20}\text{H}_{18}]^{4-}$ ion having an equatorial-equatorial (e^2) two-center linkage (**Figure 5**) between the polyhedral cages and designated $[\text{e}^2\text{-B}_{20}\text{H}_{18}]^{4-}$. The anion can be isolated as the potassium salt. Subsequent acid-catalyzed rearrangement of the $[\text{e}^2\text{-B}_{20}\text{H}_{18}]^{4-}$ isomer produced two other isomers of $[\text{B}_{20}\text{H}_{18}]^{4-}$. These isomers were characterized by apical-equatorial (*ae*) or apical-apical (a^2) two-center linkages.¹²

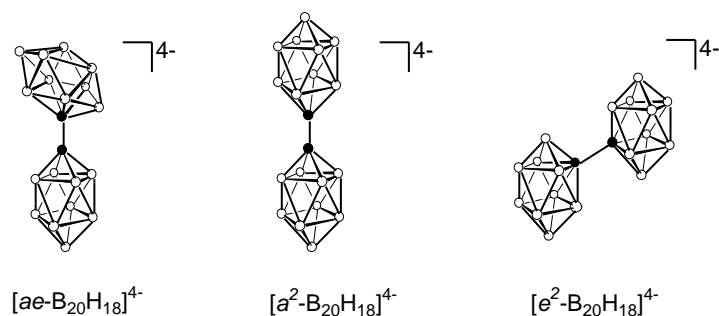


Figure 5: Isomers of the reduced $[\text{B}_{20}\text{H}_{18}]^{4-}$ ion.¹² ● = B; ○ = BH.

In most solvents, protonated $[\text{B}_{20}\text{H}_{18}]^{4-}$ derivatives, $[\text{B}_{20}\text{H}_{19}]^{3-}$, exist as a mixture of isomers. The ^{11}B NMR spectrum is complex³ because the bridging proton is fluxional and $[\text{B}_{20}\text{H}_{19}]^{3-}$ is present in equilibrium concentrations. The rearrangements that lead to isomerization of the $[\text{B}_{20}\text{H}_{18}]^{4-}$ ion are not understood, but the migration of intact $[\text{closo-B}_{10}\text{H}_9]^{2-}$ clusters, promoted by acid catalysts and protic solvents, are believed to be involved.³ The aromatic character of the $[\text{closo-B}_{10}\text{H}_9]^{2-}$ cages is similar to that of the $[\text{closo-B}_{10}\text{H}_{10}]^{2-}$ cage.³ A mechanism for these rearrangement reactions has been proposed which requires $[\text{B}_{20}\text{H}_{19}]^{3-}$ intermediates.¹²

The reverse reaction is the oxidation of the $[\text{B}_{20}\text{H}_{18}]^{4-}$ ion to form the $[\text{trans-B}_{20}\text{H}_{18}]^{2-}$ ion (**Figure 6**). This type of oxidation is more facile than the oxidative coupling of $[\text{closo-B}_{10}\text{H}_{10}]^{2-}$ that produces the $[\text{trans-B}_{20}\text{H}_{18}]^{2-}$ ion.¹⁸ For example, all three isomers of $[\text{B}_{20}\text{H}_{18}]^{4-}$ will produce the $[\text{trans-B}_{20}\text{H}_{18}]^{2-}$ when oxidized with hot aqueous ferric ion.¹⁸ The *cis*-isomer is obtained as the kinetically controlled product when the oxidation of $[\text{ae-B}_{20}\text{H}_{18}]^{4-}$ is performed at 0°C in the presence of a precipitating counter ion, such as a tetramethylammonium ion, that removes the product from solution before reaction or rearrangement occurs.¹⁶ The mechanism of these facile oxidations has not been investigated due to the rapid rearrangement of the $[\text{B}_{20}\text{H}_{19}]^{3-}$ intermediates.¹

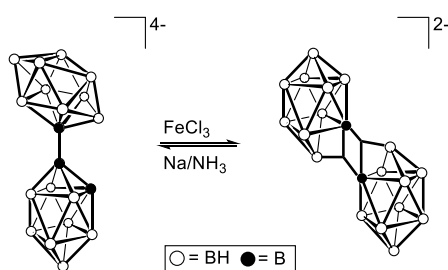


Figure 6: Redox reaction of $[\text{ae-B}_{20}\text{H}_{18}]^{4-}$ to $[\text{trans-B}_{20}\text{H}_{18}]^{2-}$.¹⁸

1.2 Nucleophilic Attack on the $[trans-B_{20}H_{18}]^{2-}$ Ion

The intercage linkages in all three of the known isomers of the $[B_{20}H_{18}]^{2-}$ anion provide an electron-deficient region which is susceptible to reactions with nucleophiles.¹ Nucleophilic attack on the electron-deficient region linking the cages results in a reductive substitution reaction. As a result, nucleophilic attack on the $[B_{20}H_{18}]^{2-}$ isomers allows for a wide variety of substituted derivatives to be formed.^{1,4,18,19,20} Hawthorne and co-workers proposed a mechanism for nucleophilic attack by hydroxide ions in 1965 which delineated the formation of the apical-equatorial (*ae*) isomer, the kinetic isomer (**Figure 7**).¹⁸

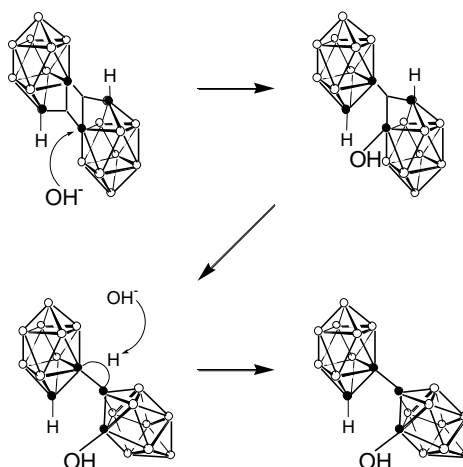


Figure 7: Mechanism of nucleophilic attack proposed by Hawthorne in 1965.¹⁸ ● = B; ○ = BH.

The first step of the mechanism is attack on the equatorial boron atom involved in the electron-deficient three-center two-electron bond by the hydroxide ion. The second step is the migration of the three-center edge bonded B_{10} boron cage by displacement of an apical proton to a neighboring edge. After the addition of a second equivalent of the

hydroxide ion the residual proton is removed resulting in the formation of the kinetic apical-equatorial isomer of $[\text{B}_{20}\text{H}_{17}\text{OH}]^{4-}$, designated $[\text{ae-B}_{20}\text{H}_{17}\text{OH}]^{4-}$. The hydroxide substituent is located on the equatorial belt near the intercage linkage. The $[\text{ae-B}_{20}\text{H}_{17}\text{OH}]^{4-}$ isomer is susceptible to subsequent acid-catalyzed rearrangement to form the thermodynamically stable, apical-apical isomer, designated $[\text{a}^2\text{-B}_{20}\text{H}_{17}\text{OH}]^{4-}$ (**Figure 8**).¹⁸

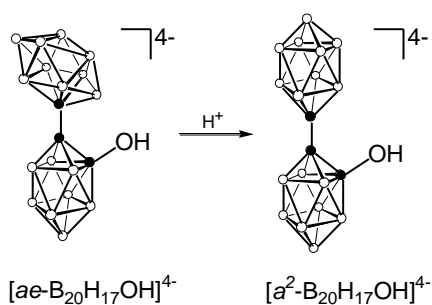


Figure 8: Rearrangement of the *ae*-isomer to the *a*²-isomer.¹⁸ $\bullet = \text{B}$; $\circ = \text{BH}$.

Reaction of the $[\text{trans-B}_{20}\text{H}_{18}]^{2-}$ isomers with nucleophiles is monitored by boron-11, or ^{11}B , nuclear magnetic resonance (NMR) spectroscopy. The starting material for the current investigations, $[\text{trans-B}_{20}\text{H}_{18}]^{2-}$ ion, has a characteristic seven peak $^{11}\text{B}\{^1\text{H}\}$ NMR spectrum (**Figure 9**).

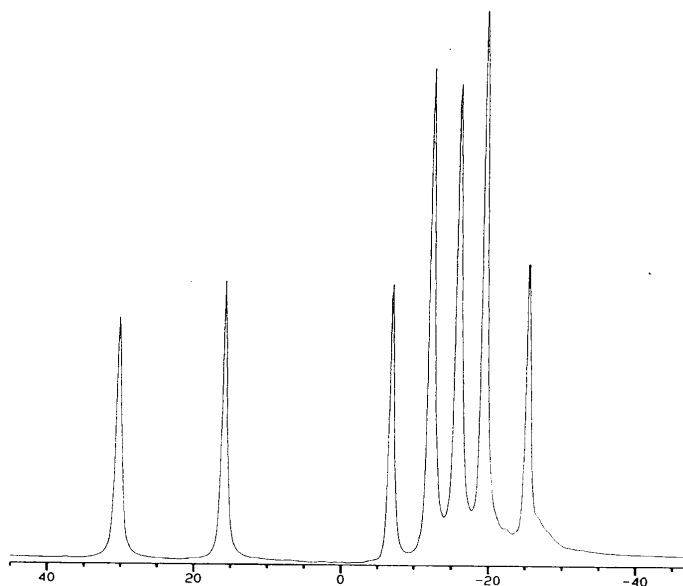


Figure 9: ^{11}B NMR spectrum of the $[\text{trans-B}_{20}\text{H}_{18}]^{2-}$ ion.

Isomeric assignment of the product (ae , a^2 , or e^2) can easily be made from the ^{11}B NMR spectrum. The signals associated with apical boron atoms and substituted boron atoms appear in the region above -15 ppm in the ^{11}B NMR spectrum. The signals associated with equatorial boron atoms appear upfield. An apical-equatorial isomer is characterized by three apical B-H vertices (**Figure 10**). The signals associated with the apical vertices will appear as singlets in the proton decoupled, abbreviated $^{11}\text{B}\{^1\text{H}\}$, NMR spectrum and as doublets in the proton coupled ^{11}B NMR spectrum. The signal for the substituted boron atom will also appear in this region as will the signal associated with the boron atoms in the intercage connection. Both of these signals, since the boron atom does not have a bonded hydrogen atom, are singlets in both the $^{11}\text{B}\{^1\text{H}\}$ and ^{11}B NMR spectrum.

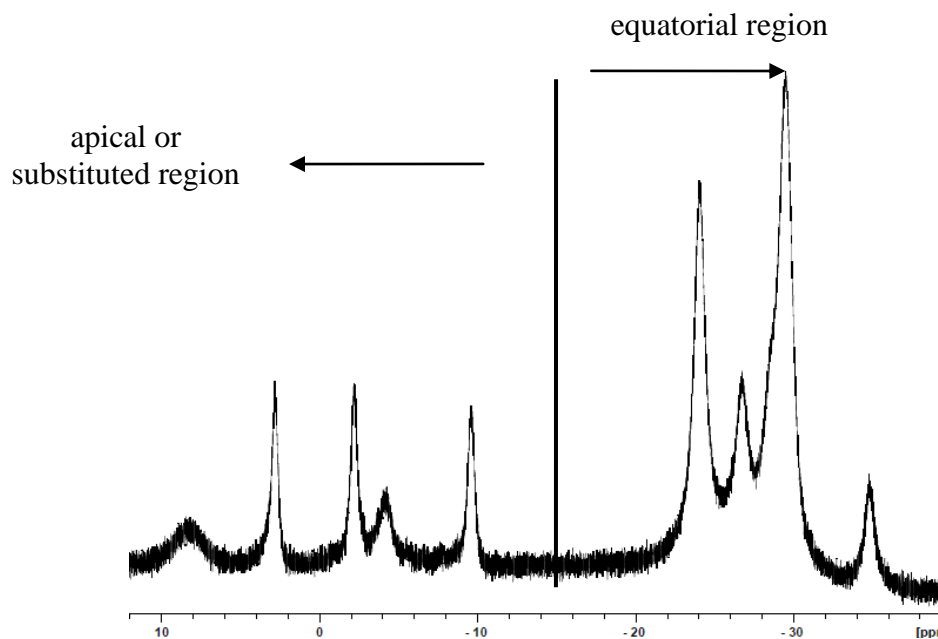


Figure 10: Representative ^{11}B NMR spectrum of an apical-equatorial isomer of $[\text{B}_{20}\text{H}_{17}\text{X}]^{4-}$ (X is a generic nucleophile) indicating the apical or substituted region and the equatorial region of the spectrum.

An apical-apical isomer is characterized by the presence of two apical B-H vertices (**Figure 11**). Two sharp signals are present in the apical region of the spectrum, which are singlets in the $^{11}\text{B}\{^1\text{H}\}$ NMR spectrum and doublets in the ^{11}B NMR spectrum. Again, the signal for the substituted boron atom will appear in this region as will the signal associated with the boron atoms in the intercage connection. Since the boron atom does not have a bonded hydrogen atom, both signals are singlets in the $^{11}\text{B}\{^1\text{H}\}$ and ^{11}B NMR spectrum.

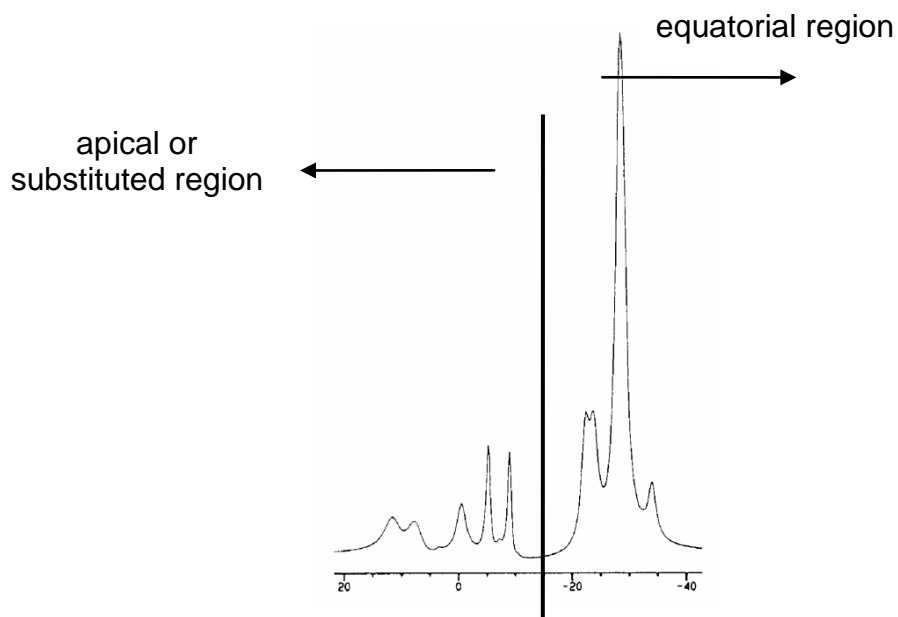


Figure 11: Representative ^{11}B NMR spectrum of an apical-apical isomer of $[\text{B}_{20}\text{H}_{17}\text{X}]^{4-}$ (X is a generic nucleophile) indicating the apical or substituted region and the equatorial region of the spectrum.

The $[e^2\text{-B}_{20}\text{H}_{17}\text{X}]^{4-}$ isomer is characterized by the presence of four apical B-H vertices. The ^{11}B NMR spectrum of an $[e^2\text{-B}_{20}\text{H}_{17}\text{X}]^{4-}$ isomer would have four sharp singlets and two broadened signals in the apical or substituted region of the proton-decoupled spectrum, one associated with the substituted boron atom and one associated with the boron atoms in the cage connection. The two broadened signals will not split in the ^{11}B NMR spectrum.

The availability of a variety of substituted derivatives of $[ae\text{-B}_{20}\text{H}_{17}\text{X}]^{4-}$, most notably the $[ae\text{-B}_{20}\text{H}_{17}\text{OH}]^{4-}$ has led to investigations of the fate of these ions when subjected to oxidizing conditions.¹ For example, the low temperature oxidation of $[ae\text{-B}_{20}\text{H}_{17}\text{OH}]^{4-}$, with aqueous ferric ion produced the $[trans\text{-B}_{20}\text{H}_{17}\text{OH}]^{2-}$ ion (**Figure 12**).¹⁸

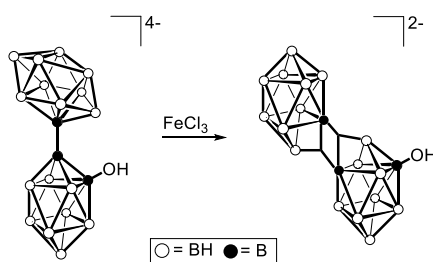


Figure 12: Oxidation of $[ae-B_{20}H_{17} OH]^{4-}$ to $[trans-B_{20}H_{17} OH]^{2-}$.¹⁸

Based on the oxidation of this well-known derivative, it is predicted that other derivatives of the nucleophilic attack on the $[trans-B_{20}H_{18}]^{2-}$ will behave in a similar fashion. Both the substituted $[B_{20}H_{17}X]^{4-}$ derivatives and the oxidized $[B_{20}H_{17}X]^{2-}$ derivatives have gained recent interest because of their potential application in BNCT. The oxidized derivatives have the potential to react directly with nucleophilic substituents on intracellular proteins by nucleophilic attack of the three center two electron bond and the reduced derivatives have the potential to oxidize *in vivo* to the more reactive oxidized ions which again are susceptible to nucleophilic attack.

1.3 Carbon Nucleophiles

Throughout the 1960's, investigations based on the reactivity of the polyhedral borane anions thrived. As the potential applications in the area of high energy fuels diminished, so did interest in polyhedral borane chemistry. In the early 1990's interest again increased, as a result of the potential for this class of compounds to be used for BNCT.^{21,22} During this time, researchers established that the $[trans-B_{20}H_{18}]^{2-}$ ion is susceptible to nucleophilic attack by amide ions^{20,23} and thiolate ions.²⁴ Also, the most

recently identified isomer, the $[cis-B_{20}H_{18}]^{2-}$ ion, was discovered.¹⁶ The result of these discoveries was an examination into the proposed mechanism of nucleophilic attack on the $[trans-B_{20}H_{18}]^{2-}$. The original mechanism cannot explain some of the observed chemistry.^{1,24} For example, reaction of the $[trans-B_{20}H_{18}]^{2-}$ ion with the protected nucleophile, $[SC(O)OC(CH_3)_3]^-$, produced directly, and in good yield, the apical-apical isomer rather than the anticipated apical-equatorial isomer. Additionally, the substituent appears, from two-dimensional ^{11}B NMR data, to be located on the equatorial belt adjacent to the boron apex rather than the equatorial belt adjacent to the intercage connection.²⁵ In another sequence of reactions, the anticipated nucleophilic attack did not occur, but a solvent-coordinated product was obtained.²⁵

While studying the reaction mechanism of the nucleophilic attack on the $[trans-B_{20}H_{18}]^{2-}$ anion in 2009, a new discovery was made. During the course of the base-mediated investigations, the formation of what may be the product formed by the reaction of the $[trans-B_{20}H_{18}]^{2-}$ anion and a carbon nucleophile was observed. Reaction of the $[trans-B_{20}H_{18}]^{2-}$ ion and *n*-butyllithium in tetrahydropyran lead to the formation of a substituted apical-equatorial derivative based on the ^{11}B NMR spectrum. The 1H spectrum for this compound yielded a singlet, consistent with the formation of the $[ae-B_{20}H_{17}C(CH_3)_3]^{4-}$ anion.²⁶ At the time, the hypothesis was made that a methyl shift resulted in a carbanion rearrangement to yield a tertiary alky substituent; however, this mechanism is unlikely because of the stability associated with the primary carbanion. The reaction was not repeated nor has the product been completely characterized. The ^{13}C NMR experiment was not performed to confirm the identity of the product.

Since the preparation of the $[trans-B_{20}H_{18}]^{2-}$ in the 1960's, no literature reports of

the reactivity of the $[trans\text{-B}_{20}\text{H}_{18}]^{2-}$ ion with carbon nucleophiles have been made. As a result, the research proposed herein is based on the investigation of the reactivity of the $[trans\text{-B}_{20}\text{H}_{18}]^{2-}$ ion with carbon nucleophiles and the preparation of a series of substituted $[\text{B}_{20}\text{H}_{18}]^{4-}$ and substituted $[\text{B}_{20}\text{H}_{18}]^{2-}$ ions with potential application in BNCT.

1.4 BNCT

Boron neutron capture therapy (BNCT) is a binary cancer therapy that requires the selective conglomeration of at least 15 micrograms of boron/g tumor of the boron-10 isotope in cancer cells. Irradiation of the locally concentrated boron-10 nuclei with thermal neutrons results in neutron capture and nuclear fission.²³ The reaction can be represented by the following equation ${}^{10}_5\text{B} + {}^1_0\text{n} \rightarrow {}^4_2\text{He}^{2+} + {}^7_3\text{Li}^{3+} + \gamma$.¹ The process releases 2.28 MeV of kinetic energy, which is distributed between the alpha particle (He^{2+}) and the Li^{3+} ion. As the particles pass through the interior of the cell, the energetic ions cause ionization tracking and cellular damage resulting in toxicity. The effective distance these two ions can travel in tumor tissue is limited to approximately one cell diameter.²⁷ The gamma photon (0.5 MeV) is less useful because its energy is inert.¹ The thermal neutron capture cross section of the boron-10 nucleus (approximately 3800 Barnes) is several orders of magnitude greater than that of the elements which comprise the bulk of mammalian tissues (C, H, N, O, P, Na, Ca, Cl, etc.).¹ As a result of both the localization of the boron-10 nuclei in the tumor cells and the localized distribution of kinetic energy resulting from the neutron capture reaction, the irradiated tumor cells should be destroyed without damage to bordering normal cells.²⁷ The application of BNCT depends on the identification of boron-containing compounds, which can be

accumulated in significant amounts in the tumor through natural mechanisms.²⁴

Alternatively, the identification of a tumor specific delivery scheme would enable the dispatch of boron-containing compounds that have no integrated tumor specificity. The optimal delivery scheme should be able to incorporate large quantities of boron atoms without affecting the selective delivery of the boron to the tumor.²⁴

BNCT has experienced dramatic advancements since it was first proposed by Locher in 1936.²⁸ The development of nuclear energy during World War II for purposes other than energy allowed the proposed therapy to become a reality. Advances in nuclear reactor technology led to a coincidental increase in the number of reactors potentially available for BNCT. The technological competition during the Cold War, known as the Space Race, generated the field of polyhedral borane chemistry. At the time, researchers were interested in these molecules as potential rocket fuels. More specifically, the field has been shifted toward the treatment of *glioblastoma multiforme* (GBM) and metastatic melanoma with some interest in other types of conditions.²⁸ While developments in nuclear physics, imaging technologies, and other analytical techniques have all moved the field of BNCT further, the lack of boron-containing compounds, which accumulate in significant quantities in the tumor, remains the limiting factor in the application of BNCT.

1.5 Liposomal Delivery

For any targeting strategy, the greatest difficulties to overcome are the delivery of therapeutic concentrations of boron atoms to the tumor, the lack of tumor cell specificity, and the moderation of the specificity once useful amounts of boron are in the target.²⁷

Liposomes composed of distearoyl phosphatidylcholine/cholesterol (1:1) with encapsulated hydrophilic salts of polyhedral borane ions have demonstrated success in the delivery of boron to murine tumors *in vivo*.^{23,24,27} Desired characteristics for liposomal delivery include high boron content with low osmotic stress, water solubility, hydrolytic stability, and a long intracellular residence time.^{23,27} Liposomal delivery has been used to conglomerate a large amount of target molecules in BALB/c mice bearing EMT6 tumors.^{23,24,27} A comparison of different compounds using the liposomal delivery method has shown that the retention of $\text{Na}_2\text{B}_{12}\text{H}_{11}\text{SH}$, a compound currently being used in the application of BNCT and abbreviated BSH, was increased in comparison to other target compounds.²⁷ Researchers have proposed that the retention of the anion is based on a mechanism of retention which includes the interaction of the target compound with intracellular proteins to form disulfide bonds.²⁷ In another study, liposomal delivery has shown to be an effective method to deliver $\text{Na}_3[\text{B}_{20}\text{H}_{17}\text{NH}_3]$, a previously synthesized derivative of the $[\textit{trans}\text{-B}_{20}\text{H}_{18}]^{2-}$ ion.²³ Retention of this molecule has been attributed to an *in vivo* oxidation to the reactive uninegative species $[\text{B}_{20}\text{H}_{17}\text{NH}_3]^{-}$.²³ One of the most promising water soluble polyhedral borane compounds studied thus far, using liposomal delivery, has been $\text{Na}_4[\text{B}_{20}\text{H}_{17}\text{SH}]$.²⁴ The biodistribution of $\text{Na}_4[\text{B}_{20}\text{H}_{17}\text{SH}]$ exhibits tumor boron concentrations that exceed therapeutically desired values at all time points of the biodistribution. Based on the proposed mechanism for the retention of $\text{Na}_2\text{B}_{12}\text{H}_{11}\text{SH}$ and $\text{Na}_3[\text{B}_{20}\text{H}_{17}\text{NH}_3]$, researchers have proposed that the thiol-containing compound could bind directly to protein residues through the formation of a disulfide bond and/or potentially oxidize to the more reactive $\text{Na}_2[\text{B}_{20}\text{H}_{17}\text{SH}]$ which would be susceptible to nucleophilic attack as well as the potential to form disulfide bonds.^{23,24,27}

Of the prospective boron agents that have been proposed and synthesized for application in BNCT, all have had at least one disqualifying feature or lacked biological evaluation competent to advance them to clinical trials. The challenge for the chemist is to design and synthesize boron-rich compounds which are relatively non-toxic, selectively delivered to tumor cells, and retained long enough to allow neutron irradiation.¹

CHAPTER II

STATEMENT OF PROBLEM

Although polyhedral borane anions have been investigated since the early 1960's, many questions regarding their reactivity, as well as the mechanisms of the reactions, remain unanswered. While nucleophilic attack on the [*trans*-B₂₀H₁₈]²⁻ anion has been reported for the hydroxide ion,^{18,19} alkoxide ions,^{18,19} amide ions,^{20,23} and thiolate ions,²⁴ no literature reports have been made regarding the susceptibility of the electron-deficient bonds to nucleophilic attack by carbanions. Therefore, the specific aims of the proposed research are to:

- 1) develop a synthetic route to evaluate the reactivity of the [*trans*-B₂₀H₁₈]²⁻ anion with the selected carbon nucleophiles to produce a series of substituted isomers, of the [B₂₀H₁₇X]⁴⁻ ion where X is the selected carbon nucleophile.
- 2) investigate the ability of the resulting reduced polyhedral borane anions to undergo oxidation and restore the three center, two electron bonds that are susceptible to further nucleophilic attack, producing substituted isomers of the [B₂₀H₁₇X]²⁻ ion where X is the selected carbon nucleophile

The proposed research will make a contribution to the existing body of literature in addition to the resulting compounds having the potential to be used as target compounds

in the interdisciplinary cancer therapy known as boron neutron capture therapy.

CHAPTER III

EXPERIMENTAL

3.1 Materials

Sublimed decaborane, B₁₀H₁₄, was obtained from Professor Lee J. Todd at Indiana University (Bloomington, IN). *Caution: decaborane is a highly toxic, impact sensitive compound that forms explosive mixtures especially when in contact with halogenated materials. A careful examination of the MSDS is recommended.* Sodium acetylide, *n*-butyllithium, rubidium acetate, and rubidium hydroxide were purchased from Alfa Aesar. Tetrabutylammonium bromide, tetramethylammonium bromide, and iron (III) chloride hexahydrate were purchased from Aldrich Chemical Co and all solid reagents were used without further purification. Triethylamine was dried over molecular sieves. Diethyl ether and acetonitrile were reagent grade and distilled in the presence of sodium metal and calcium hydride respectively, before use. All synthetic reactions were performed under argon in anhydrous conditions using Schlenk techniques.

3.2 Physical Measurements

One-dimensional ¹H, ¹³C, and ¹¹B Fourier transform nuclear magnetic resonance (NMR) spectra were obtained with a Bruker Avance III spectrometer, operating at 400 MHz, 100 MHz, and 128 MHz respectively. ¹¹B NMR spectra were obtained using quartz tubes. Proton chemical shifts were referenced to residual solvent protons. Carbon

shifts were referenced to CD_3CN or CH_3CN , added as an internal standard to aqueous samples. Boron chemical shifts were externally referenced to $\text{BF}_3 \cdot \text{Et}_2\text{O}$; peaks. All Fourier transform infrared (IR) spectra were obtained using a Perkin-Elmer Spectrum One instrument and were obtained as Nujol mulls.

3.3 Synthetic Procedures

Preparation of $(\text{Et}_3\text{NH})_2[\text{closo-B}_{10}\text{H}_{10}]$. The $(\text{Et}_3\text{NH})_2[\text{B}_{10}\text{H}_{10}]$ preparation was based on the technique developed by Hawthorne and coworkers.¹⁰ Sublimed decaborane (30.1 g, 0.249 mol) was added to a 1-Liter three neck flask that had been equipped with an argon inlet, a 250 mL pressure equalizing dropping funnel (PED), and an overhead stirrer. The flask was flushed with argon gas and placed into an oil bath. Xylene (~400 mL) was added to the reaction flask and triethylamine (94.0 mL, 674 mmol) was placed into the PED and added dropwise to the stirred decaborane solution. As the triethylamine was added, a yellow precipitate of the $\text{B}_{10}\text{H}_{12}(\text{NEt}_3)_2$ intermediate was produced. After all of the triethylamine had been added, the argon flow was increased and the PED was replaced with a thermometer adapter and thermometer. The temperature of the reaction mixture was raised to 100 °C and kept at that temperature for 3 hours. The argon flow was increased, the thermometer adapter was replaced with a condenser, and the reaction was allowed to reflux, while stirring, for an additional 5 hours. The reaction mixture was cooled in an ice bath and filtered. The light yellow solid was washed with isopropyl alcohol (5 x 50 mL), removing a majority of the yellow color. The white solid was washed with diethyl ether (2 x 100 mL) and transferred to a 1 liter round-bottom flask and dried *in vacuo*. The dried product was dissolved in approximately 90 mL of boiling

water and the solution was brought to a rolling boil. Absolute ethanol was added to the mixture until the boiling solution began to appear cloudy. The mixture was removed from the heat and allowed to cool to room temperature overnight. Filtration of the solution resulted in 60.2 grams of a white crystalline $(\text{Et}_3\text{NH})_2[\text{B}_{10}\text{H}_{10}]$ (75.6 % yield). $^{11}\text{B}\{^1\text{H}\}$ NMR (δ , acetonitrile) -1.4, -15.9, $([\text{B}_{12}\text{H}_{12}]^{2-})$ -29.4.

Preparation of $(\text{Et}_3\text{NH})_2[\text{trans-}\mathbf{B}_{20}\mathbf{H}_{18}]$. The $(\text{Et}_3\text{NH})_2[\text{B}_{20}\text{H}_{18}]$ preparation was based on the technique developed by Hawthorne and coworkers.¹² $(\text{Et}_3\text{NH})_2[\text{B}_{10}\text{H}_{10}]$ (30.0 g, 93.0 mmol) was placed in a 1 liter three-neck flask that that been equipped with a PED, and a stir bar. Distilled water (300 mL) was added to the reaction flask to dissolve the $(\text{Et}_3\text{NH})_2[\text{B}_{10}\text{H}_{10}]$ and the solution was brought to reflux. A solution of $\text{FeCl}_3 \cdot 6\text{H}_2\text{O}$ (75.0 g, 277 mmol) dissolved in a minimum amount of distilled water was prepared. The $\text{FeCl}_3 \cdot 6\text{H}_2\text{O}$ solution was transferred to the PED and added dropwise to the refluxing solution of $(\text{Et}_3\text{NH})_2[\text{B}_{10}\text{H}_{10}]$. After addition was complete, the reaction was allowed to reflux an additional 3 hours. The reaction mixture was cooled to room temperature and the solid was filtered. The residue was recrystallized from boiling water, cooled and filtered, resulting in the isolation of 15.4 g of pale yellow crystals of $(\text{Et}_3\text{NH})_2[\text{trans-}\mathbf{B}_{20}\mathbf{H}_{18}]$ (75.4% yield). $^{11}\text{B}\{^1\text{H}\}$ NMR (δ , acetonitrile) 29.9, 15.6, -7.3, -12.8, -16.3, -19.8, -26.0

Preparation of $\text{Rb}_4[\text{ae-}\mathbf{B}_{20}\mathbf{H}_{17}(\text{CH}_2)_3\text{CH}_3]$. A clean, dry 100 mL Schlenk flask was equipped with a stir bar, stoppered, and flushed with argon gas. Freshly distilled diethyl ether (15.0 mL) was added to the flask via syringe. A syringe was used to transfer a 2.5

M solution of n-butyllithium in hexanes (2.40 mL, 6.00 mmol) to the reaction flask and allowed to stir. The stopper was removed under an atmosphere of flowing argon and the starting material $(\text{Et}_3\text{NH})_2[\textit{trans}\text{-B}_{20}\text{H}_{18}]$ (0.513 g, 1.17 mmol) was added. The reaction proceeded at room temperature for three days. Complete reaction was confirmed by ^{11}B NMR spectroscopy. The reaction mixture was dried *in vacuo* and the light yellow solid $\text{Li}_4[\text{B}_{20}\text{H}_{17}(\text{CH}_2)_3\text{CH}_3]$ residue was dissolved in a minimum amount of room temperature distilled water. The desired anion was precipitated as a rubidium salt by adding a solution of 0.5 M $\text{RbC}_2\text{H}_3\text{O}_2$ (10.0 mL) in methanol to the aqueous product solution. The precipitate was filtered and recrystallized from water:methanol. The solid was filtered and dried *in vacuo* to yield the product resulting in the isolation of 0.436 g of a white flaky solid (60.6% yield). $^{11}\text{B}\{^1\text{H}\}$ NMR (δ , D_2O) 7.1, 2.7, -3.2, -6.1, -7.9, -9.8, -24.1, -24.1, -26.1, -29.6, -33.8. ^{13}C NMR (δ , D_2O) 65.5, 16.6. IR (cm^{-1} , *nujol*) 2440 (BH).

Preparation of $\text{Rb}_4[\textit{ae}\text{-B}_{20}\text{H}_{17}\text{C}_2\text{H}]$. A clean, dry 100 mL Schlenk flask was equipped with a stir bar, stoppered, and flushed with argon gas. Triethylamine (15.0 mL) was transferred to the reaction flask via syringe. An 18% by mass suspension of sodium acetylide (95% purity) in xylenes (3.00 mL, 9.24 mmol) was added to the reaction flask via syringe and allowed to stir. A paraffin oil bath was placed around the flask and the bath heated to 90 °C. The stopper was removed under an atmosphere of flowing argon and the starting material $(\text{Et}_3\text{NH})_2[\textit{trans}\text{-B}_{20}\text{H}_{18}]$ (0.537 g, 1.22 mmol) was added along with a condenser. The reaction was allowed to reflux for four days. Complete reaction was not achieved as confirmed by ^{11}B NMR spectroscopy; however the desired product was identified. The reaction mixture was dried *in vacuo*, dissolved in a minimum amount

of room temperature distilled water, and the desired anion was precipitated as a rubidium salt by adding a solution of $\text{RbC}_2\text{H}_3\text{O}_2$ (0.5 M, 10.0 mL) in methanol to the aqueous product solution. The precipitate was filtered and recrystallized from water:methanol. The pure solid was filtered and dried *in vacuo* to yield 0.375 g of a tan flaky solid in 54.8% yield. $^{11}\text{B}\{^1\text{H}\}$ NMR (δ , D_2O) 8.4, 2.8, -2.2, -4.3, -9.6, -24.0, -26.7, -29.5, -34.8. IR (cm^{-1} , nujol) 2438 (BH).

Preparation of $\text{Rb}_4[\text{ae-B}_{20}\text{H}_{17}\text{CH}_2\text{CN}]$. A clean, dry 100 mL Schlenk flask was equipped with a stir bar, stoppered, and flushed with argon gas. A syringe was used to transfer a 2.5 M solution of n-butyllithium in hexanes (2.40 mL, 6.00 mmol) to the reaction flask. The solution was dried *in vacuo* over night to remove the hexanes resulting in a dry white solid n-butyllithium. Freshly distilled diethyl ether (10.0 mL) was added to the flask via syringe. A dry ice-acetone bath was placed around the flask to cool the solution to $-78\text{ }^\circ\text{C}$. Freshly distilled acetonitrile (0.35 mL, 6.7 mmol) was added to the flask and the mixture was allowed to stir for 30 minutes. After this time, the bath was removed and the mixture warmed to room temperature over a period of two hours. After this period, the starting material, $(\text{Et}_3\text{NH})_2[\text{trans-B}_{20}\text{H}_{18}]$ was added (0.501 g, 1.14 mmol). The reaction proceeded at room temperature for three days. Complete reaction was confirmed by ^{11}B NMR spectroscopy. The reaction mixture was dried *in vacuo* and the dark rust colored solid $\text{Li}_4[\text{B}_{20}\text{H}_{17}\text{CH}_2\text{CN}]$ residue was dissolved in a minimum amount of room temperature distilled water. The desired anion was precipitated as a rubidium salt by adding excess $\text{RbC}_2\text{H}_3\text{O}_2$ (0.5 M, 10.0 mL) solution in methanol to the aqueous product solution. The precipitate was filtered and recrystallized from water:methanol. The

product was isolated by filtration and dried *in vacuo* to yield a white flaky solid (0.447 g, 72.6% yield). $^{11}\text{B}\{^1\text{H}\}$ NMR (δ , D_2O) 8.3, 2.4, -2.5, -4.6, -9.9, -24.4, -27.1, -29.8, -35.1. IR (cm^{-1} , nujol) 2438 (BH).

Preparation of $\text{Rb}_4[\text{a}^2\text{-B}_{20}\text{H}_{17}(\text{CH}_2)_3\text{CH}_3]$. A clean dry 100 mL round bottom flask was equipped with a stir bar. An aqueous solution of $\text{Rb}_4[\text{ae-B}_{20}\text{H}_{17}\text{CH}_2\text{CN}]$ prepared by the synthesis described previously was made by dissolving $\text{Rb}_4[\text{ae-B}_{20}\text{H}_{17}\text{CH}_2\text{CN}]$ (0.319 g, 0.504 mmol) in 20.0 mL of distilled water. An oil bath was placed around the flask and heated to 100°C . An aqueous 3M HCl solution was added dropwise until a pH of 1 was achieved as indicated by pH paper. After 1 hour, the solution was basified by adding a 20% solution of NaOH in methanol dropwise to the mixture until a pH of 13 was indicated by pH paper. The product was recrystallized by the addition of methanol. The product was isolated by filtration and dried *in vacuo* to yield a white flaky solid (0.187 g, 58.6% yield). $^{11}\text{B}\{^1\text{H}\}$ NMR (δ , D_2O) 12.0, 7.3, -2.4, -5.8, -7.8, -22.8, -24.4, -29.2, -32.4. ^{13}C NMR (ppm, D_2O) 66.0, 48.92, 16.7, 14.2, 6.6. IR (cm^{-1} , nujol) 2413 (BH).

Preparation of $\text{Rb}_4[\text{a}^2\text{-B}_{20}\text{H}_{17}\text{C}_2\text{H}]$. A clean dry 100 mL round bottom flask was equipped with a stir bar. An aqueous solution of $\text{Rb}_4[\text{ae-B}_{20}\text{H}_{17}\text{C}_2\text{H}]$ prepared by the synthesis described previously was made by dissolving $\text{Rb}_4[\text{ae-B}_{20}\text{H}_{17}\text{C}_2\text{H}]$ (0.299 g, 0.498 mmol) in 20.0 mL of distilled water. An oil bath was placed around the flask and heated to 100°C . An aqueous 3M HCl solution was added dropwise until a pH of 1 was achieved as indicated by pH paper. After 1 hour, the solution was basified by adding a 20% solution of NaOH in methanol dropwise to the mixture until a pH of 13 was

indicated by pH paper. The product was recrystallized by the addition of methanol. The product was isolated by filtration and dried *in vacuo* to yield a white flaky solid (0.154 g, 51.5% yield). $^{11}\text{B}\{^1\text{H}\}$ NMR (δ , D_2O) 11.9, -5.9, -23.3, -28.3, -29.1. IR (cm^{-1} , nujol) 2429 (BH).

Preparation of $\text{Rb}_4[\text{a}^2\text{-B}_{20}\text{H}_{17}\text{CH}_2\text{CN}]$. A clean dry 100 mL round bottom flask was equipped with a stir bar. An aqueous solution of $\text{Rb}_4[\text{ae-B}_{20}\text{H}_{17}\text{C}_2\text{H}]$ prepared by the synthesis described previously was made by dissolving $\text{Rb}_4[\text{ae-B}_{20}\text{H}_{17}\text{C}_2\text{H}]$ (0.268 g, 0.436 mmol) in 20.0 mL of distilled water. An oil bath was placed around the flask and heated to 100°C . An aqueous 3M HCl solution was added dropwise until a pH of 1 was achieved as indicated by pH paper. After 1 hour, the solution was basified by adding a 20% solution NaOH in methanol dropwise to the mixture until a pH of 13 was indicated by pH paper. The product was recrystallized by the addition of methanol. The product was isolated by filtration and dried *in vacuo* to yield a white flaky solid (0.173 g, 64.6% yield). $^{11}\text{B}\{^1\text{H}\}$ NMR (δ , D_2O) 10.8, -6.5, -8.9, 24.0, 29.8. IR (cm^{-1} , nujol) 2410 (BH).

Preparation of $(\text{Me}_4\text{N})_2[\text{B}_{20}\text{H}_{17}(\text{CH}_2)_3\text{CH}_3]$. A clean, dry 100 mL Schlenk flask was equipped with a stir bar, stoppered, and flushed with argon gas. An aqueous solution of crude $\text{Rb}_4[\text{B}_{20}\text{H}_{17}(\text{CH}_2)_3\text{CH}_3]$, prepared by the synthesis described previously was made by dissolving $\text{Rb}_4[\text{B}_{20}\text{H}_{17}(\text{CH}_2)_3\text{CH}_3]$ (0.377 g, 0.605 mmol) in 20.0 mL of distilled water. The stopper was removed under an atmosphere of flowing argon and the solution was added to the flask and allowed to stir. The flask was placed into an ice bath and the solution allowed to cool. The stopper was removed under an atmosphere of flowing argon

and a PED was inserted into the neck of the flask and filled with an aqueous solution of the oxidizing agent $\text{FeCl}_3 \cdot 6\text{H}_2\text{O}$ (1.16 g, 0.00429 mol). The solution was added dropwise to the reaction flask. As the iron is reduced, solid iron metal particulates form while the desired product remains in solution. The reaction was allowed to warm to room temperature overnight. In order to isolate the product, the iron metal was removed from the aqueous solution by filtration. The filtrate was saved and the oxidized product was precipitated as the Me_4N^+ salt by the addition of an aqueous solution of Me_4NBr (0.5 M, 5.0 mL). The product was filtered and recrystallized in boiling H_2O . The pure product was filtered and dried *in vacuo* resulting in 0.125 g, a 47.8% yield. $^{11}\text{B}\{^1\text{H}\}$ NMR (δ , acetonitrile) 13.6, 6.8, -9.9, -16.1, -20.7, -24.9, -26.9, -29.7. ^{13}C NMR (δ , acetonitrile) 78.0, 47.1, 14.0, 8.4. ^1H NMR (δ , acetonitrile) 4.1 (m), 3.3 (q), 1.3 (t). IR (cm^{-1} , nujol) 2477 (BH).

Preparation of $(\text{Bu}_4\text{N})_2[\text{B}_{20}\text{H}_{17}\text{C}_2\text{H}]$. A clean, dry 100 mL Schlenk flask was equipped with a stir bar, stoppered, and flushed with argon gas. An aqueous solution of crude $\text{Rb}_4[\text{B}_{20}\text{H}_{17}\text{C}_2\text{H}]$, prepared by the synthesis described previously, was made by dissolving $\text{Rb}_4[\text{B}_{20}\text{H}_{17}\text{C}_2\text{H}]$, (0.336 g, 0.560 mmol) in 20.0 ml of distilled water. The stopper was removed under an atmosphere of flowing argon and the solution was added to the flask and allowed to stir. The flask was placed into an ice bath and the solution allowed to cool. The stopper was removed under an atmosphere of flowing argon and a PED was inserted into the neck of the flask and filled with an aqueous solution of the oxidizing agent $\text{FeCl}_3 \cdot 6\text{H}_2\text{O}$ (1.04 g, 3.84 mmol). The solution was added dropwise to the reaction flask. As the iron is reduced solid iron metal particulates form while the desired product

remains in solution. The reaction was allowed warm to room temperature overnight. In order to isolate the product, the iron metal was removed from the aqueous solution by filtration. The filtrate was saved and the oxidized product was precipitated as the Bu_4N^+ salt by the addition of an aqueous solution of Bu_4NBr (0.5 M, 5.00 mL). The product was filtered and dried *in vacuo* to obtain 0.371 g of product, (89.1% yield). $^{11}\text{B}\{^1\text{H}\}$ NMR (δ , acetonitrile) 29.4, 27.9, 14.8, 4.8, -8.0, -11.9, -13.6, -16.0, -17.1, -20.5, -21.3, -23.8, 25.7, -26.8, -30.7, -26.8. ^1H NMR (δ , acetonitrile) 5.3 (m).

Preparation of $(\text{Bu}_4\text{N})_2[\text{B}_{20}\text{H}_{17}\text{CH}_2\text{CN}]$. A clean, dry 100 mL Schlenk flask was equipped with a stir bar, stoppered, and flushed with argon gas. An aqueous solution of crude $\text{Rb}_4[\text{B}_{20}\text{H}_{17}\text{CH}_2\text{CN}]$, prepared by the synthesis described previously, was made by dissolving $\text{Rb}_4[\text{B}_{20}\text{H}_{17}\text{CH}_2\text{CN}]$, (0.148 g, 0.195 mmol) in 20 mL of distilled water. The stopper was removed under an atmosphere of flowing argon and the solution was added to the flask and allowed to stir. The flask was placed into an ice bath and the solution allowed to cool. The stopper was removed under an atmosphere of flowing argon and a PED was inserted into the neck of the flask and filled with an aqueous solution of the oxidizing agent $\text{FeCl}_3 \cdot 6\text{H}_2\text{O}$ (0.538 g, 1.99 mmol). The solution was added dropwise to the reaction flask. The reaction was allowed to warm to room temperature and stirred overnight. The oxidized product was precipitated from solution as the Bu_4N^+ salt by the addition of an aqueous solution of Bu_4NBr (0.5 M, 5.00 mL). The product was filtered and dried *in vacuo* to obtain 0.0702 g, (37.5% yield). $^{11}\text{B}\{^1\text{H}\}$ NMR (δ , acetonitrile) 29.2, 27.9, 13.9, 12.8, 10.1, 3.5, -8.6, -11.9, -14.4, -16.0, -17.9, 21.3, -23.8, -25.8, -30.2. ^1H NMR (δ , acetonitrile) 5.3 (m).

CHAPTER IV

RESULTS and DISCUSSION

Nucleophilic attack on the $[trans\text{-B}_{20}\text{H}_{18}]^{2-}$ ion by hydroxide ions was first reported in 1963.¹⁹ In 1965 a preliminary mechanism was reported.¹⁸ The kinetic product of the reaction is the apical-equatorial isomer, designated as *ae*, and the thermodynamic product of the reaction is the apical-apical isomer, designated as *a*².¹⁸ With an increasing interest in the polyhedral borane anions, resulting from the growing interest in the anions for potential application in BNCT, other nucleophiles were investigated. These nucleophiles include alkoxide ions,^{18,19} amide ions,^{20,23} and thiolate ions²⁴; however, to date, no products from the reaction of the $[trans\text{-B}_{20}\text{H}_{18}]^{2-}$ ion with carbon-based nucleophiles have been reported in the literature. Carbon-based nucleophiles provide a means to prepare polyhedral borane anions which have substituents capable of reacting with intracellular protein substituents, such as carboxylic acid derivatives. Binding of the polyhedral borane anions to intracellular protein substituents is the predominant mechanism proposed for the retention of the polyhedral borane anions within the tumor mass, once delivered by unilamellar liposomes. As a result, the proposed research is based on the synthesis of a series of $[\text{B}_{20}\text{H}_{17}\text{X}]^{4-}$ and $[\text{B}_{20}\text{H}_{17}\text{X}]^{2-}$ ions formed from the reaction of the $[trans\text{-B}_{20}\text{H}_{18}]^{2-}$ ion with select carbon-based nucleophiles.

Three carbon nucleophiles were selected for investigation. The *n*-butyllithium nucleophile was selected based on a previous observation within our laboratory which reported the occurrence of a reaction between the [*trans*-B₂₀H₁₈]²⁻ ion and *n*-butyllithium. In that preliminary report, a [B₂₀H₁₇C(CH₃)₃]⁴⁺ ion was proposed based on interpretations of the ¹³C NMR spectrum. The *t*-butyl substituent is proposed to be the result of a carbanion rearrangement based on an unpublished result.²⁶ Two other carbon nucleophiles, the acetylide ion and deprotonated acetonitrile, were chosen because of the potential oxidation of the alkyne and cyano- functional groups to produce carboxylic acid and amide derivatives. Each of the carbon-based nucleophiles was investigated in the current research project and the results reported.

4.1 Reduced Derivatives

Results regarding Rb₄[*ae*-B₂₀H₁₇(CH₂)₃CH₃]. The *n*-butyl nucleophile was obtained by using a 2.5 M solution of *n*-butyllithium dissolved in hexanes. Reaction of the [*trans*-B₂₀H₁₈]²⁻ ion with the *n*-butyl ion nucleophile was completed in diethylether as the solvent. The alpha carbon on the *n*-butyl chain carries the negative charge and is the atom involved in covalent bond formation. Once the starting material, [*trans*-B₂₀H₁₈]²⁻, was added, the mixture was allowed to react for three days at room temperature. Formation of the [B₂₀H₁₇(CH₂)₃CH₃]⁴⁺ ion (**Figure 13**) was achieved by the reductive substitution reaction of the [*trans*-B₂₀H₁₈]²⁻ ion with the *n*-butyl anion as the nucleophile. The reaction was monitored by ¹¹B NMR spectroscopy and the reaction was complete after the allotted time period. The ¹¹B{¹H} NMR spectrum of the starting material is characterized by seven signals $\delta = 29.9, 15.6, -7.3, -12.8, -16.3, -19.8, \text{ and } -26.0$. The ¹¹B{¹H} NMR

spectrum of the resulting product was consistent with the formation of the *ae* isomer (**Figure 14**) which was identified by the presence of three sharp singlets located at 2.75, -3.19, and -9.84 ppm. These signals are observed as doublets in the ^{11}B NMR experiment. The signal for the substituted boron atom is not easily identified in the $^{11}\text{B}\{^1\text{H}\}$ NMR spectrum and may be present under one of the peaks corresponding to an apical boron atom. The ^1H NMR exhibited a complicated region between 4.5 ppm and 2.0 ppm which has not been observed in the spectrum of other substituted polyhedral borane anions. The complicated region may be attributed to the hydrogens on the *n*-butyl chain coupling to one or more boron atoms on the polyhedral borane anion framework. The ^{13}C NMR spectrum exhibited two signals at 65.5 and 16.6 ppm. These two signals correspond to two of the carbon atoms of the *n*-butyl chain. All four signals have been observed for this derivative in other samples and their spectra are included. The two signals present at 65.5 and 16.6 ppm for this purified sample are consistently at the same ppm with those in the other samples. The sample was referenced to acetonitrile and it is possible that these signals were not observed due to a low signal to noise ratio from the standard and low concentration of sample. IR spectroscopy confirmed the presence of the B-H stretch at 2441 cm^{-1} corresponding to the boron-hydrogen bonds present in the polyhedral borane cage.

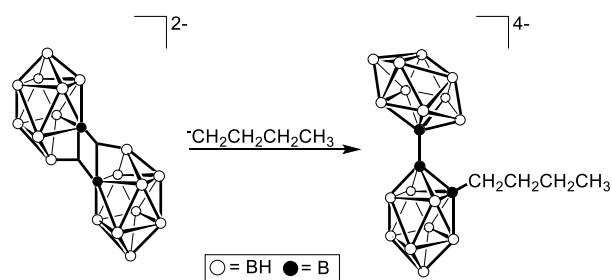


Figure 13: Reaction of the *n*-butyl ion with $[\text{trans-B}_{20}\text{H}_{18}]^{2-}$.

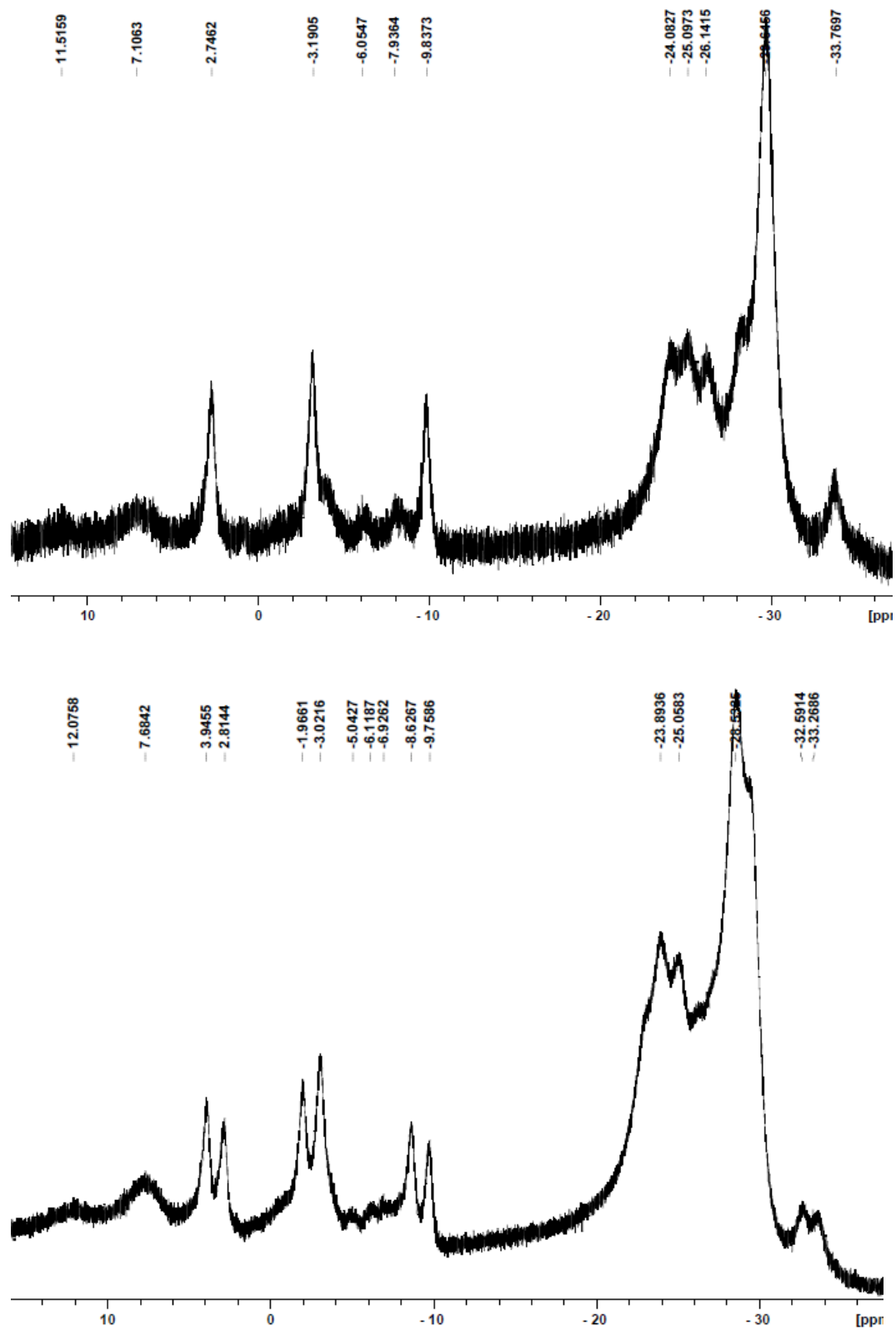


Figure 14: $^{11}\text{B}\{^1\text{H}\}$ and ^{11}B NMR spectra of $\text{Rb}_4[\text{ae-B}_{20}\text{H}_{17}(\text{CH}_2)_3\text{CH}_3]$.

Results regarding $Rb_4[a^2-B_{20}H_{17}(CH_2)_3CH_3]$. The resulting *ae* isomer was treated with heat and hydrochloric acid, followed by basification, to produce the thermodynamic isomer $[a^2-B_{20}H_{17}(CH_2)_3CH_3]^{4-}$ (**Figure 15**). The product was isolated, recrystallized from water:methanol, and characterized by NMR and IR spectroscopy. The a^2 thermal isomer was identified in the $^{11}B\{^1H\}$ NMR spectrum (**Figure 16**) by the presence of two singlets at -5.8 and -7.8 ppm which appear as doublets in the ^{11}B NMR experiment. In addition, the equatorial region of the spectrum demonstrates fewer peaks than the *ae* isomer, a result of the apical-apical bond changing the chemical shift equivalence of these nuclei. The 1H NMR also displays the same characteristic region between approximately 4.5 ppm and 2.0 ppm which may be due to the 1H - ^{11}B coupling. The ^{13}C NMR spectrum exhibited four signals at 66.0, 48.9, 16.7, and 14.2 ppm corresponding to the carbons of the *n*-butyl chain. IR spectroscopy confirmed the presence of the boron-hydrogen bonds which compose the polyhedral borane cage by the strong peak centered at 2413 cm^{-1} .

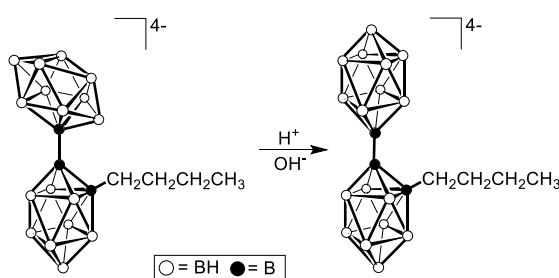


Figure 15: Isomerization of $[B_{20}H_{17}(CH_2)_3CH_3]^{4-}$.

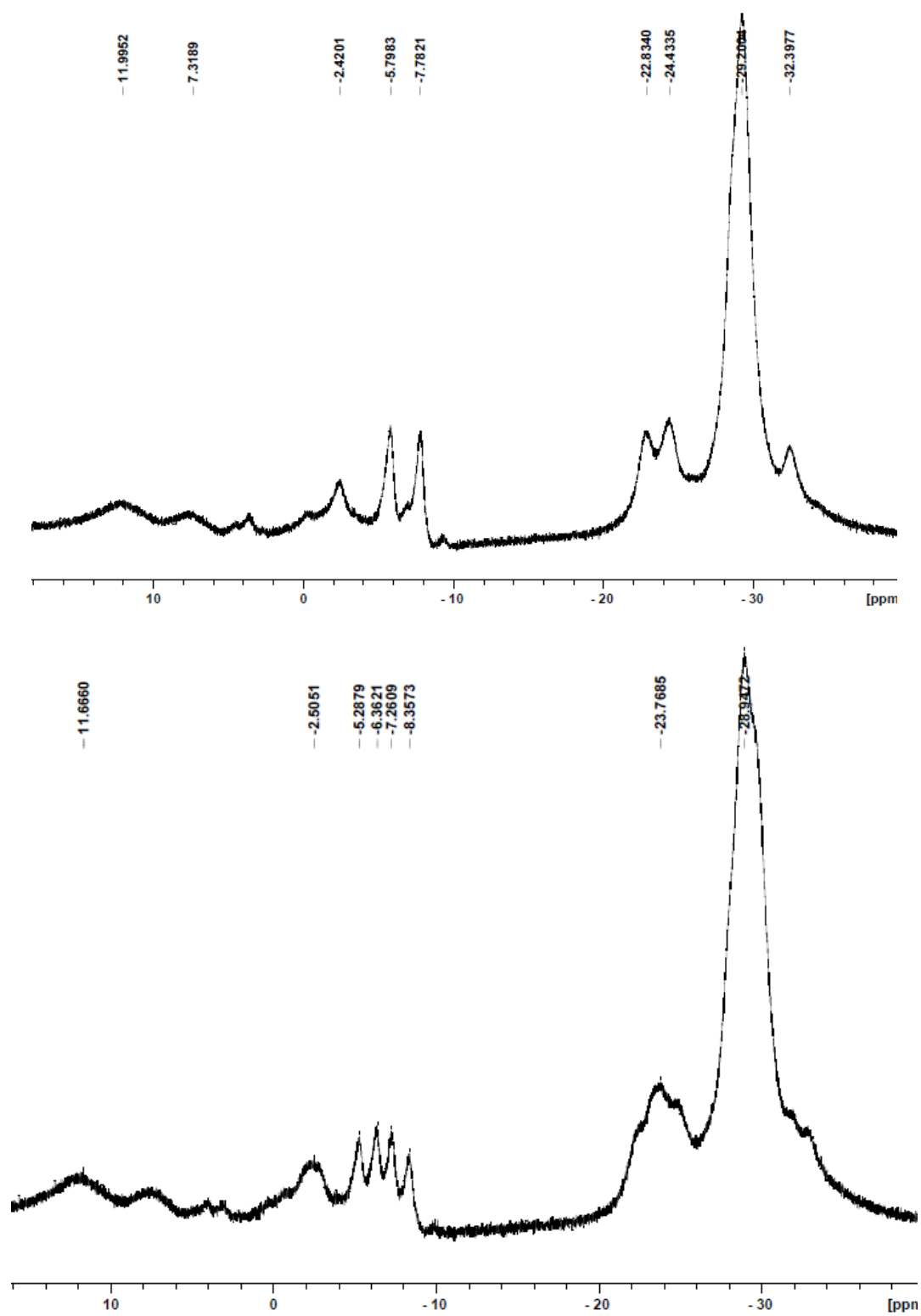


Figure 16: $^{11}\text{B}\{^1\text{H}\}$ and ^{11}B NMR spectra of $\text{Rb}_4[\text{a}^2\text{-B}_{20}\text{H}_{17}(\text{CH}_2)_3\text{CH}_3]$.

Results regarding $Rb_4[ae-B_{20}H_{17}C_2H]$. The $[B_{20}H_{17}C\equiv CH]^4+$ ion was prepared from the reaction of the $[trans-B_{20}H_{18}]^{2-}$ ion and the acetylide ion, $[C\equiv CH]^-$, as depicted in **Figure 17**. The source of the carbon containing nucleophile is a slurry of 18% sodium acetylide in xylenes. The reaction is carried out in triethylamine. The result is the formation of the *ae* isomer which has been identified by three signals at 2.8, -2.2, and -9.6 ppm in the $^{11}B\{^1H\}$ NMR experiment which appear as doublets in the ^{11}B NMR spectrum (**Figure 18**). The 1H NMR exhibited a complicated region between approximately 4.5 ppm and 2.0 ppm similar to that observed for the n-butyl derivative. The complicated region may be attributed to the hydrogen on the terminal alkyne coupling to one or more boron atoms on the polyhedral borane anion framework through the triple bond. It is not uncommon to observe long range coupling through a triple bond.²⁹ The ^{13}C spectrum does not exhibit any peaks. This may be a result of the low abundance of ^{13}C atoms and/or the potential peak corresponding to the alpha carbon bonded to the boron atom being broadened by coupling to the spin active nucleus. The beta carbon may not have been observed for the same reason and/or long range coupling to the boron nucleus known to occur through a triple bond. The carbon atoms in acetylide are expected between 65 and 90 ppm.²⁹ The strong peak at 2347 cm^{-1} in the IR spectrum corresponds to the B-H bonds present in the molecule. The presence of a weak alkyne band expected in the region of $2260\text{-}2100\text{ cm}^{-1}$ cannot be observed because of the overlap of the strong and broad B-H stretch in the same region.²⁹

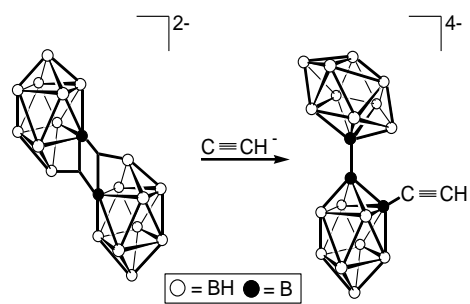


Figure 17: Reaction of the acetylide ion with $[\text{trans-B}_{20}\text{H}_{18}]^{2-}$.

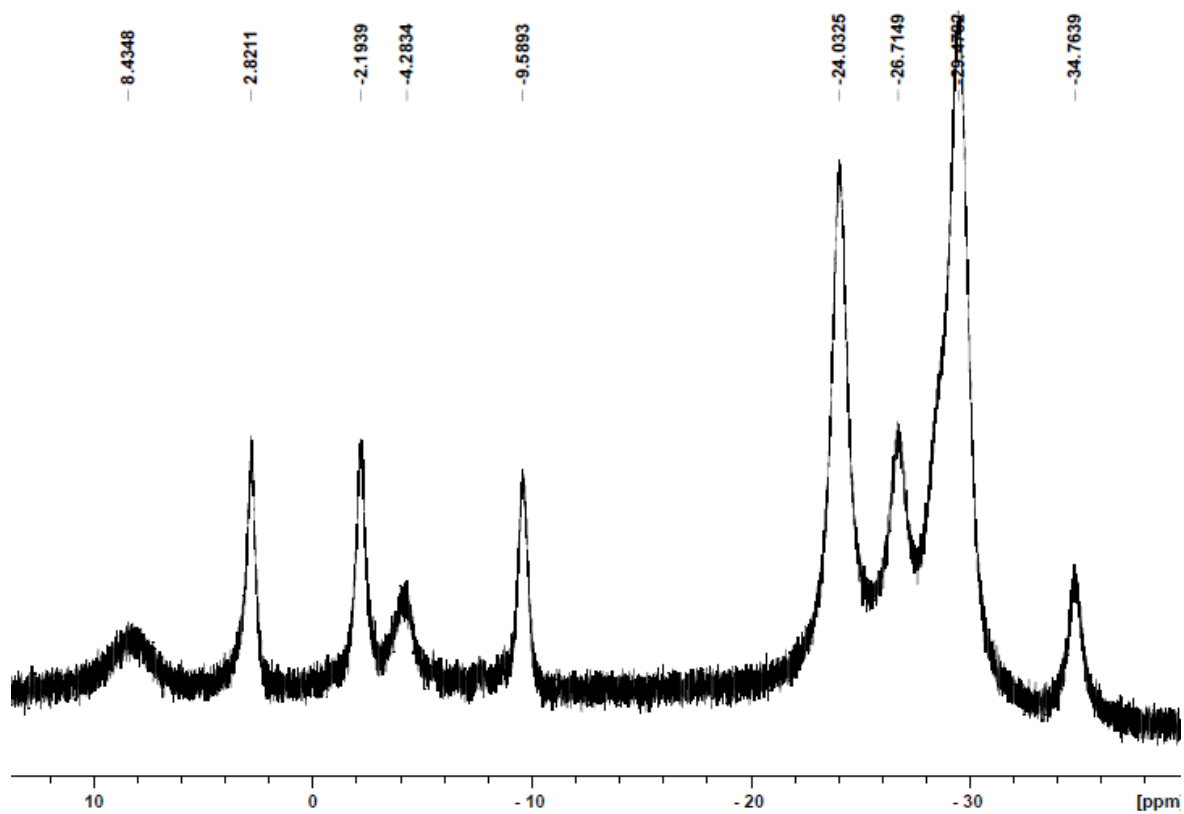


Figure 18: $^{11}\text{B}\{^1\text{H}\}$ and ^{11}B NMR spectra of $\text{Rb}_4[\text{ae-B}_{20}\text{H}_{17}\text{C}_2\text{H}]$.

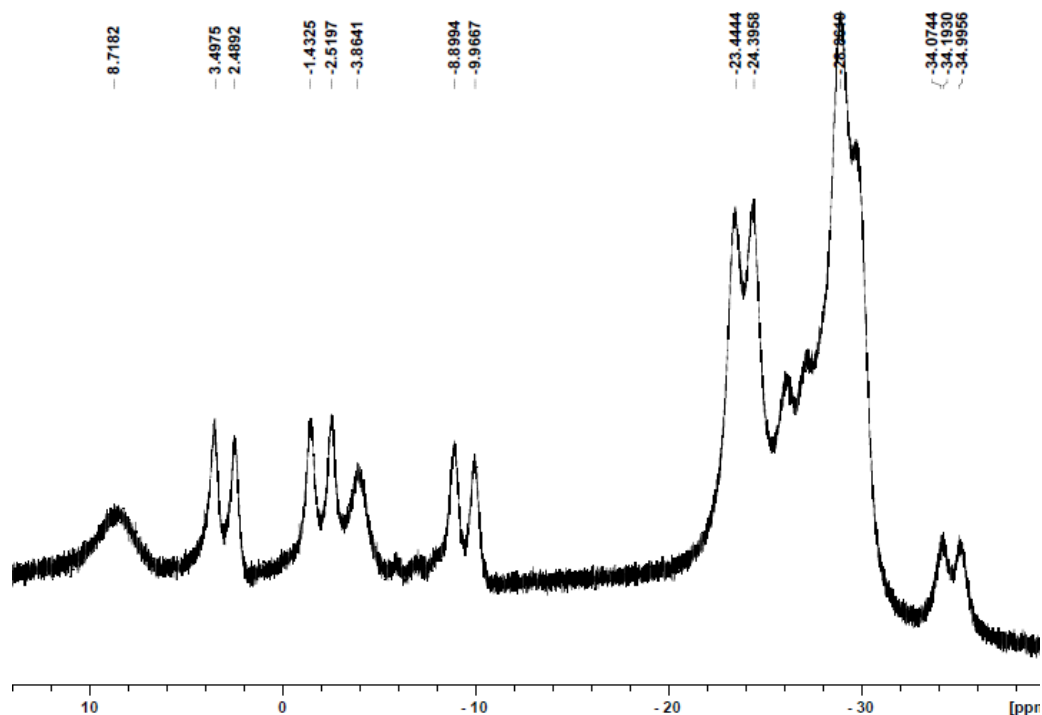


Figure 18: (continued from page 36).

Results regarding $\text{Rb}_4[\text{a}^2\text{-B}_{20}\text{H}_{17}\text{C}_2\text{H}]$. The resulting *ae* isomer was treated with heat and hydrochloric acid, followed by basification, to produce the thermodynamic isomer [$\text{a}^2\text{-B}_{20}\text{H}_{17}\text{C}_2\text{H}$] (**Figure 19**). The product was isolated, recrystallized from water:methanol, and characterized by NMR and IR spectroscopy. The $^{11}\text{B}\{^1\text{H}\}$ NMR spectrum reveals only one signal at -5.9 ppm which is split in the ^{11}B NMR experiment (**Figure 20**). It is possible that one of the two characteristic peaks of the a^2 isomer is overlapping in this region. Just as observed in the previous derivative, the equatorial region of the spectrum demonstrates fewer peaks than the *ae* isomer, a result of the apical-apical bond changing the chemical shift equivalence of these nuclei. The ^1H NMR spectrum exhibits a complicated multiplet between 4.5 to 2.0 ppm as previously observed and attributed to $^1\text{H}\text{-}^{11}\text{B}$ coupling. IR spectroscopy confirms the presence of the B-H bond stretch centered

at 2429 cm^{-1} . The presence of a weak alkyne band expected to be present in the region of $2260\text{-}2100\text{ cm}^{-1}$ cannot be observed because of the overlap of the strong and broad B-H stretch in the same region.²⁹

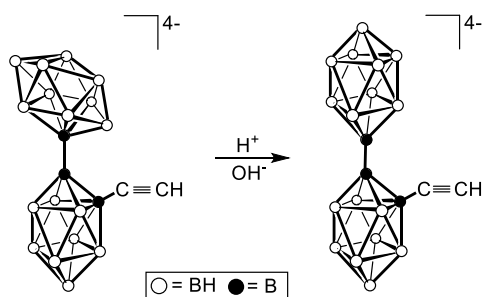


Figure 19: Isomerization of $[\text{B}_{20}\text{H}_{17}\text{C}\equiv\text{CH}]^{4-}$.

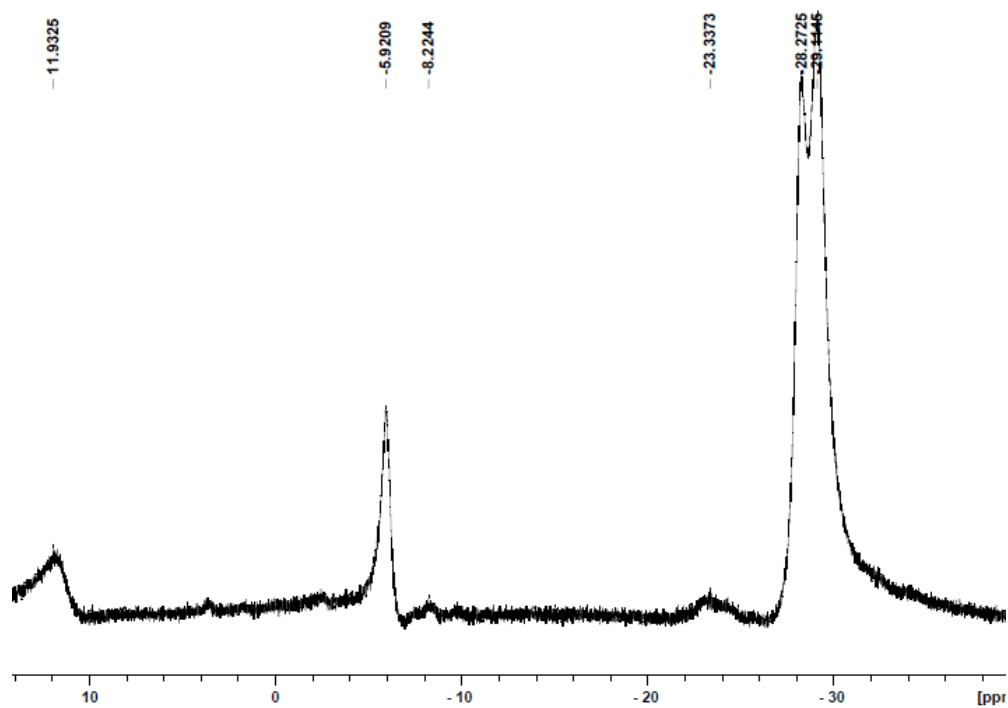


Figure 20: $^{11}\text{B}\{^1\text{H}\}$ and ^{11}B NMR spectra of $\text{Rb}_4[\text{a}^2\text{-B}_{20}\text{H}_{17}\text{C}_2\text{H}]$.

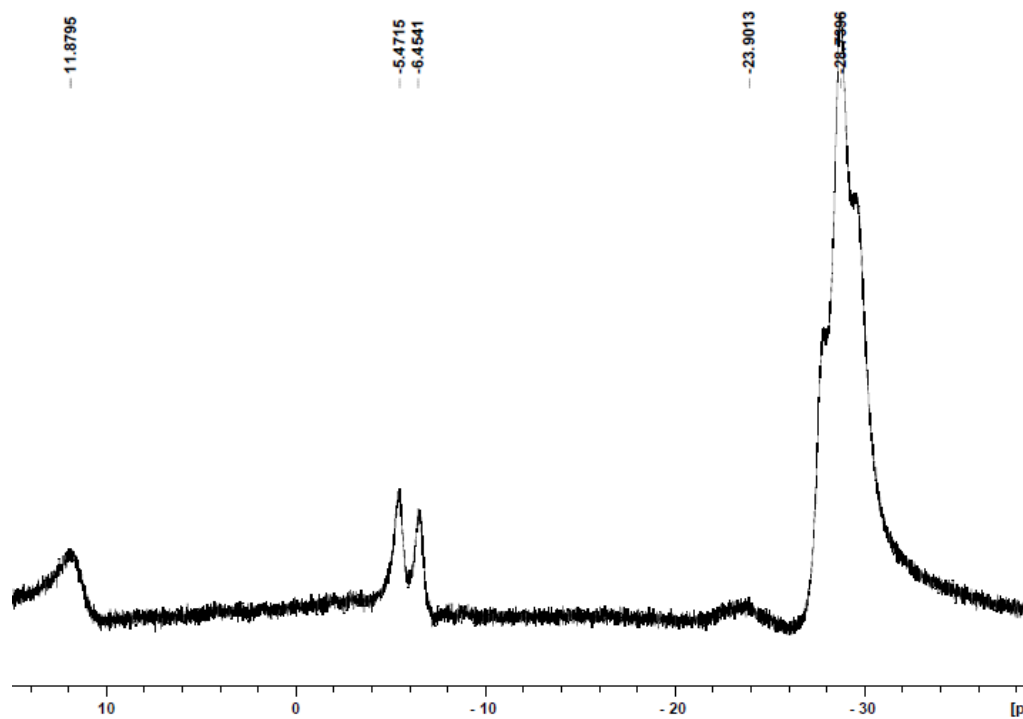


Figure 20: (continued from page 38).

Results regarding $Rb_4[ae-B_{20}H_{17}CH_2CN]$. The reactivity of the $[trans-B_{20}H_{18}]^{2-}$ anion has also been investigated using the $^-CH_2CN$ ion as a potential carbon nucleophile. The nucleophile was prepared from the reaction of *n*-butyllithium and acetonitrile using the method described by Das and Wilkie.³⁰ The deprotonation of an alpha hydrogen from acetonitrile by *n*-butyllithium resulted in the desired anion containing an electron rich carbon atom. The anion was not isolated and the $[trans-B_{20}H_{18}]^{2-}$ ion was allowed to react *in situ* with the $^-CH_2CN$ ion in diethylether to produce the $[ae-B_{20}H_{17}CH_2CN]^{4-}$ ion (**Figure 21**). The product of the reaction was isolated, recrystallized from water:methanol, and characterized by NMR and IR spectroscopy. The $^{11}B\{^1H\}$ NMR experiment verified three signals corresponding to the *ae* isomer at 2.4, -2.5, and -9.9 ppm which were observed as doublets in the ^{11}B NMR experiment (**Figure 22**). The 1H

NMR spectrum exhibited a complicated multiplet between 4.5 to 2.0 ppm as previously observed and attributed to ^1H - ^{11}B coupling. The ^{13}C NMR spectrum does not reveal any peaks. This may be because of the low abundance of ^{13}C atoms and/or the potential peak corresponding to the alpha carbon bonded to the boron atom being broadened by coupling to the quadrupolar nucleus. The beta carbon is a quaternary carbon and would have a lower signal intensity and be difficult to observe. The carbon in the cyano group should be observed in the 110-125 ppm range of the spectrum.²⁹ The IR spectrum revealed the B-H stretch centered at 2438 cm^{-1} . The presence of a weak to medium nitrile band expected to be present in the region of $2260\text{-}2240\text{ cm}^{-1}$ cannot not be observed because of the overlap of the strong and broad B-H stretch in the same region.²⁹

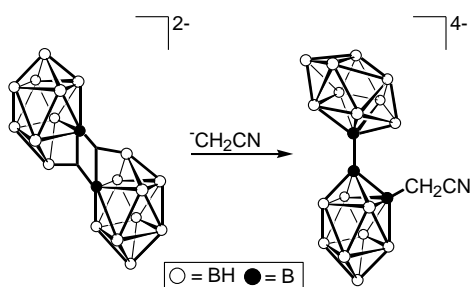


Figure 21: Reaction of CH_2CN^- with $[\text{trans-B}_{20}\text{H}_{18}]^{2-}$.

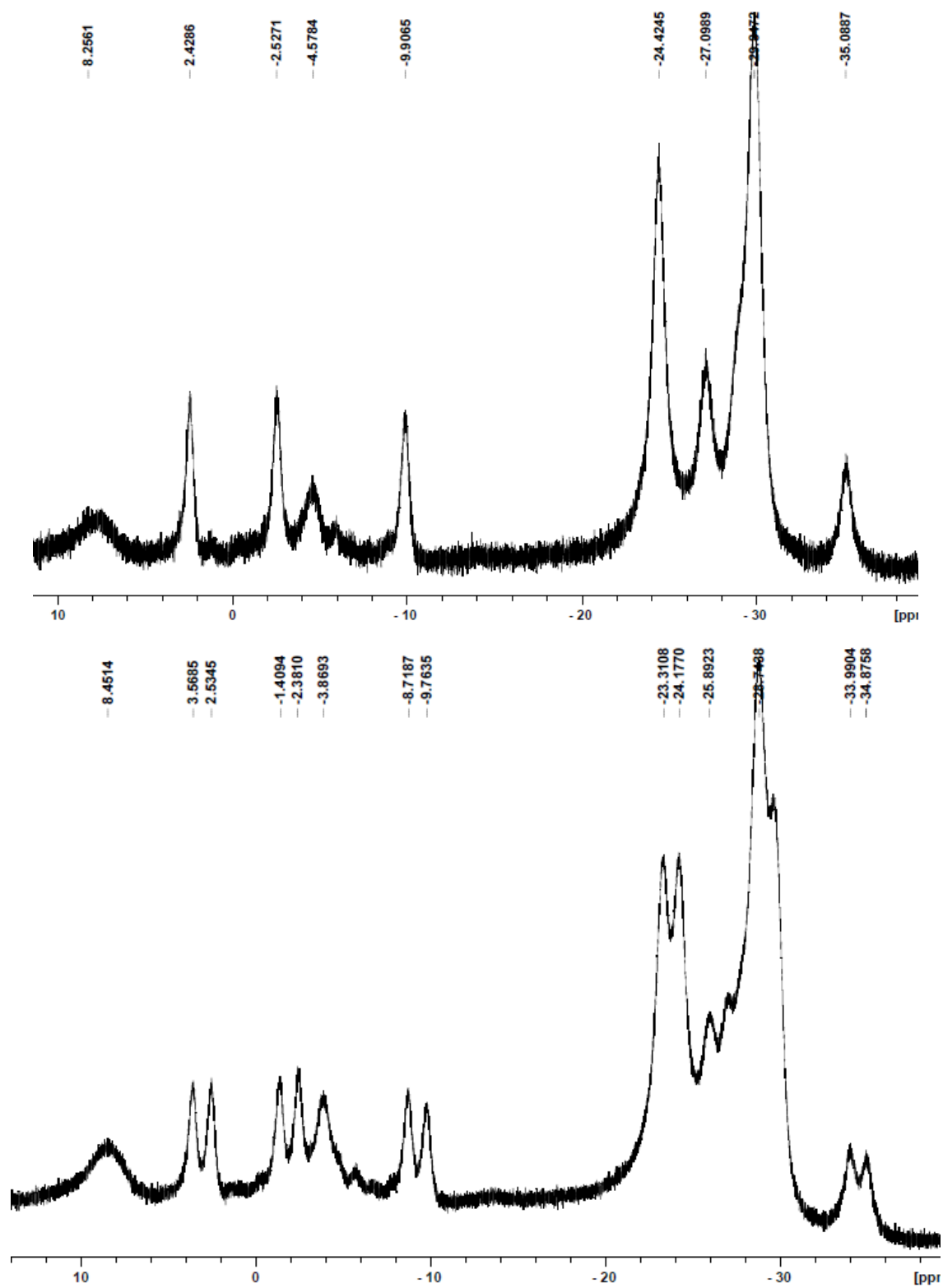


Figure 22: $^{11}\text{B}\{^1\text{H}\}$ and ^{11}B NMR spectra of $\text{Rb}_4[\text{ae-B}_{20}\text{H}_{17}\text{CH}_2\text{CN}]$.

Results regarding $Rb_4[\alpha^2-B_{20}H_{17}CH_2CN]$. The resulting *ae* isomer was treated with heat and hydrochloric acid, followed by basification, to produce the apical-apical isomer, the thermodynamic isomer, as depicted in **Figure 23**. The resulting product was characterized by NMR and IR spectroscopy. The $^{11}B\{^1H\}$ NMR spectrum has a single peak of interest centered at -6.5 ppm (**Figure 24**). As mentioned previously, the lack of the two characteristic peaks of the α^2 isomer could be due to the overlapping of peaks. This peak is observed as a doublet in the ^{11}B NMR experiment, confirming the presence of a B-H bond in the apical region of the NMR spectrum. In addition, the equatorial region of the spectrum demonstrates fewer peaks than the *ae* isomer, a result of the apical-apical bond changing the chemical shift of these nuclei. The 1H NMR spectrum exhibits a complicated multiplet between 4.5 to 2.0 ppm as previously observed and attributed to 1H - ^{11}B coupling. The B-H stretch is observed at 2410 cm^{-1} for this anion. The presence of a weak to medium nitrile band expected to be present in the region of 2260 - 2240 cm^{-1} cannot be observed because of the overlap of the strong and broad B-H stretch in the same region.²⁹

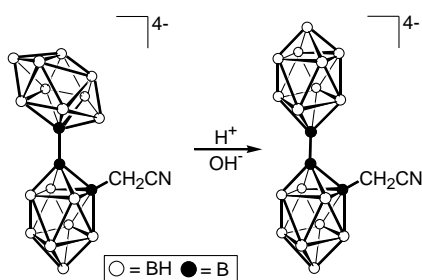


Figure 23: Isomerization of $[B_{20}H_{17}CH_2CN]^{4-}$.

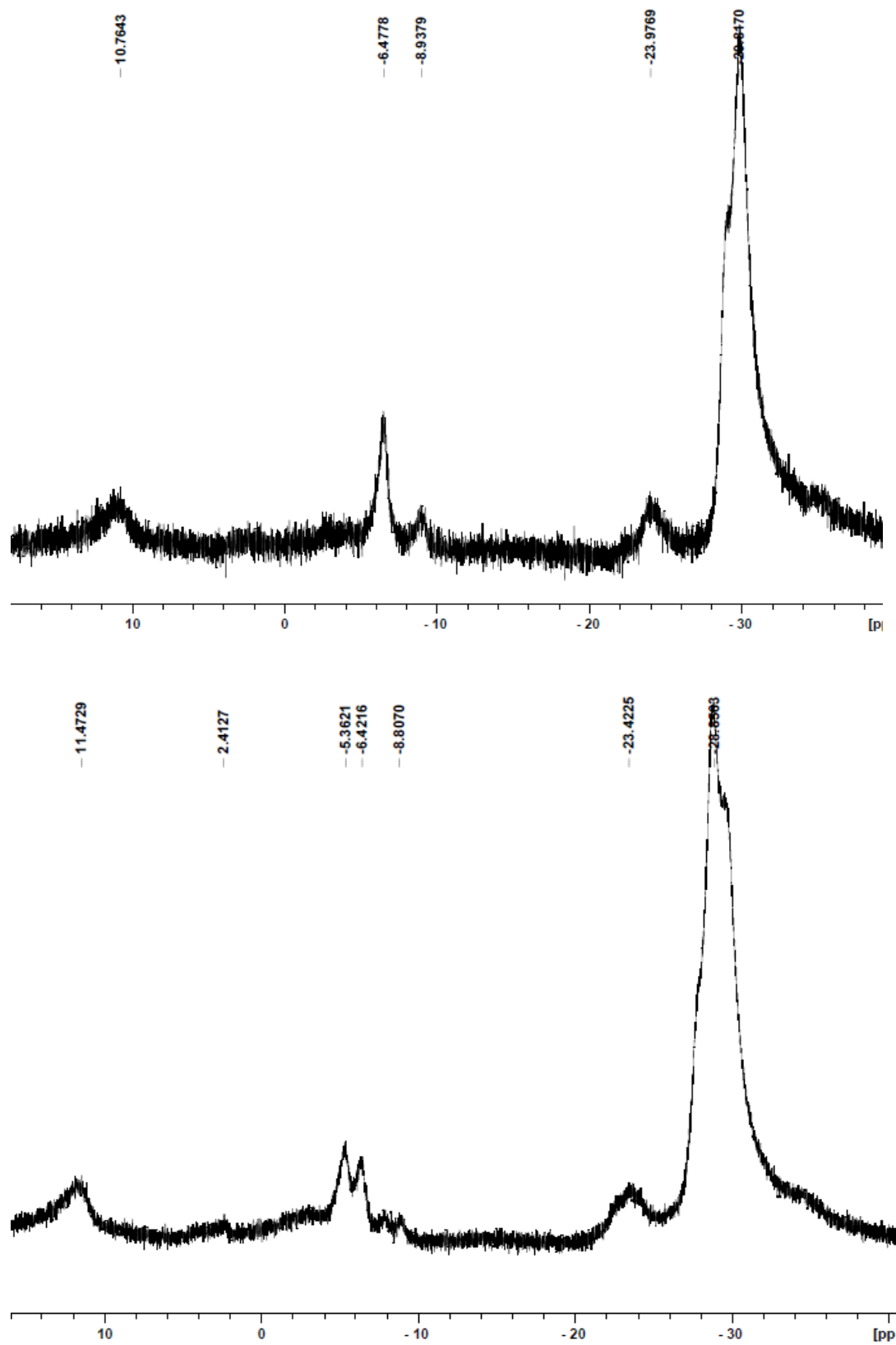


Figure 24: $^{11}\text{B}\{^1\text{H}\}$ and ^{11}B NMR spectra of $\text{Rb}_4[\text{a}^2\text{-B}_{20}\text{H}_{17}\text{CH}_2\text{CN}]$.

In summary, for each of the three selected carbon nucleophiles, ${}^-(\text{CH}_2)_3\text{CH}_3$, ${}^-\text{C}\equiv\text{CH}$, and ${}^-\text{CH}_2\text{CN}$, each of the reactions produced the expected apical-equatorial isomer, the kinetic isomer predicted by the original mechanism proposed by Hawthorne in 1965.¹⁸ The products exhibited the characteristic three apical boron signals in the ${}^{11}\text{B}\{^1\text{H}\}$ NMR spectrum which split into doublets in the ${}^{11}\text{B}$ spectrum. While the ${}^{11}\text{B}$ NMR data exhibited the presence of the desired $[\text{B}_{20}\text{H}_{17}\text{X}]^{4-}$ derivatives, where X is the carbon nucleophile, the ${}^1\text{H}$ and ${}^{13}\text{C}$ NMR data were more complex. In the case of the ${}^1\text{H}$ NMR data, signals were present that appeared to be split by multiple boron atoms within the polyhedral borane cage. In the case of the ${}^{13}\text{C}$ NMR data, only the *n*-butyl derivative exhibited carbon signals at all. While the argument posed earlier for the other two nucleophiles included the potential of significant broadening of the carbon peaks, the fact that the *n*-butyl derivative did exhibit signals places some question on that hypothesis. The rubidium salts had relatively low solubility in water and the lack of carbon signals in the ${}^{13}\text{C}$ NMR spectra could be a result of insufficient concentration of the compounds in the NMR sample. As will be noted in a subsequent section, there is a possibility that the product of the *n*-butyllithium reaction is doubly substituted. In this case, the concentration of the carbon atoms would be higher and may explain the ability to obtain a ${}^{13}\text{C}$ NMR spectrum of this sample. Nevertheless, the one-dimensional ${}^{11}\text{B}$ NMR spectrum gives no indication that the product of the reaction is doubly substituted. The samples have been sent for high resolution mass spectrometry analysis and this will confirm the identity of the reduced compounds.

4.2 Oxidized Derivatives

The determination of reductive substitution of the $[trans\text{-B}_{20}\text{H}_{18}]^{2-}$ ion by a carbon nucleophile has been made based on the resulting one-dimensional ^{11}B NMR spectra, which typically consists of a broad substituted peak in addition to the appropriate number of apical boron atoms signals, corresponding to either the apical-equatorial or apical-apical isomer. The bonding position of the substituent on the boron cage cannot be determined by one-dimensional ^{11}B NMR spectroscopy. The two-dimensional ^{11}B - ^{11}B NMR spectra of the reduced substituted derivatives were not obtained. The calibration of the two dimensional ^{11}B - ^{11}B NMR experiment was performed using a 279 mM aqueous solution of $\text{Na}_2[trans\text{-B}_{20}\text{H}_{18}]^{2-}$ which is centrosymmetric. The symmetry of this molecule results in many chemical shift equivalent nuclei. The reduced products have greatly reduced symmetry in relation to the starting material, resulting in many less chemical shift equivalent nuclei. In addition, the reduced derivatives of the $[trans\text{-B}_{20}\text{H}_{18}]^{2-}$ ion were precipitated as the rubidium salt, $\text{Rb}_4[\text{B}_{20}\text{H}_{17}\text{X}]^{4-}$, where X is the selected carbon nucleophile. As the rubidium salt, these compounds are soluble in water; however not nearly as soluble as the $\text{Na}_2[trans\text{-B}_{20}\text{H}_{18}]^{2-}$ used for the calibration, and a comparable concentration could not be achieved. These differences resulted in the inability to obtain the two-dimensional ^{11}B - ^{11}B NMR spectra of the reduced derivatives. The determination of the point of substitution can be hypothesized by previous investigations, but cannot be confirmed without two-dimensional ^{11}B - ^{11}B NMR data.

To circumvent this issue and create a second series of carbon nucleophile derivatives with the potential for application in BNCT, a series of oxidized products was proposed. Oxidation of the reduced unsubstituted isomers of the $[\text{B}_{20}\text{H}_{18}]^{4-}$ results in the thermodynamic isomer, the $[trans\text{-B}_{20}\text{H}_{18}]^{2-}$ ion, in aqueous solution using Fe^{3+} as the

oxidizing agent at 0 °C.¹ Restoration of the three-center two-electron bond increases the symmetry of the reduced substituted derivative and there is a significant difference in solubility of the oxidized product from the reduced product. There is a trend in cationic affinity of the resulting anions as a direct result of their reduced charge multiplicity. The oxidized product will precipitate from aqueous solution by the addition of an alkyl ammonium salt. The resulting precipitate, with increased organic character, is soluble in the organic solvent, acetonitrile, which greatly increases the solubility of the oxidized product in relation to the reduced product. The increase in chemical shift equivalent nuclei and concentration has allowed for the determination of bonding position of the nucleophile on the boron cage for the *n*-butyl derivative.

Results regarding $(Me_4N)_2[B_{20}H_{17}(CH_2)_3CH_3]$. Oxidation of the reduced *n*-butyl product, $[ae-B_{20}H_{17}(CH_2)_3CH_3]^{4-}$ was achieved by the addition of ferric ion to an aqueous solution of the reduced derivative at 0 °C (**Figure 25**). The product is precipitated from the solution as the tetramethyl ammonium salt.

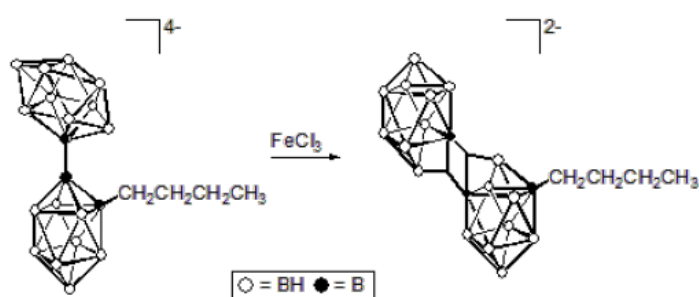


Figure 25: Oxidation of $[ae-B_{20}H_{17}(CH_2)_3CH_3]^{4-}$ to $[trans-B_{20}H_{17}(CH_2)_3CH_3]^{2-}$.

The $^{11}B\{^1H\}$ NMR spectrum is much different than what was expected (**Figure 26**). The peak at 29.9 ppm in the $[trans-B_{20}H_{18}]^{2-}$ ion is a singlet in the $^{11}B\{^1H\}$ NMR

spectrum and a doublet in the ^{11}B NMR spectrum and corresponds to the two apical boron atoms of the molecule which are not involved in three-center two-electron bonding. This signal is not present for this derivative near 30 ppm. Instead the signal shows up at -6.8 ppm, an upfield shift indicating an increase in shielding of this atom. The equatorial boron atom involved in the three center two electron bonds is observed at 13.1 ppm whereas it is 15.6 ppm in the $[\textit{trans}\text{-B}_{20}\text{H}_{18}]^{2-}$ ion. The other unexpected differences can be observed in the equatorial region. The $[\textit{trans}\text{-B}_{20}\text{H}_{18}]^{2-}$ ion has five signals in this region which are all doublets in the ^{11}B NMR spectrum. The oxidized derivative of the *n*-butyl derivative has only four signals, indicating an increase in symmetry. In addition, the signal at -10.4 ppm does not produce a doublet in the ^{11}B NMR spectrum, indicating that it is the potential point of substitution. The ^1H NMR is very resolute and contains three of the four signals expected to resemble an *n*-butyl pattern of splitting: a multiplet centered at 4.1 ppm, a quintuplet centered at 3.3 ppm, a sextuplet which is missing, and a triplet centered at 1.3 ppm. The multiplet centered at 4.1 ppm may correspond to the hydrogen atoms bound to the alpha carbon. The multiplet is very broad, a possible result of coupling to the adjacent quadrupolar boron nucleus. The signal at 3.1 ppm can be attributed to the precipitating counter ion Me_4N^+ , CH_3CN solvent at 2.0 ppm, and TMS at 0.0 ppm. A singlet at 2.2 ppm and a triplet at 0.9 have not been identified. The ^{13}C spectrum exhibits four separate signals for the *n*-butyl chain at 78.0, 47.1, 14.0, and 8.4 ppm. Comparison of the two-dimensional ^{11}B - ^{11}B NMR spectrum of this derivative to the $[\textit{trans}\text{-B}_{20}\text{H}_{18}]^{2-}$ ion reveals that there is a single cross-peak that has appeared. The cross-peak results from the coupling of the signal at -10.4 ppm from the $^{11}\text{B}\{^1\text{H}\}$ NMR spectrum suspected to be the substituted peak, to the

equatorial boron atom involved in three center two electron bonding. The integration of this peak in the ^{11}B NMR spectrum suggests that there are two substitutions on the molecule. The double substitution on the equatorial belt would explain the increase in symmetry and resulting four signals in the $^{11}\text{B}\{^1\text{H}\}$ NMR spectrum. It would also explain the upfield shift of the signal corresponding to the apical boron atoms. The only observation which does not support this analysis is the coupling of non-adjacent boron atoms that is observed in the two dimensional ^{11}B - ^{11}B NMR spectrum. This could possibly be due to a through space interaction. The combination of the chemical shift and integration from the ^{11}B NMR spectrum with the cross-peak observed in the two dimensional ^{11}B - ^{11}B NMR spectrum of the oxidation product, indicate a doubly substituted product. Mass spectral analysis will be able to discern whether the product is singly or doubly substituted. The IR spectrum exhibits the B-H stretch at 2477 cm^{-1} .

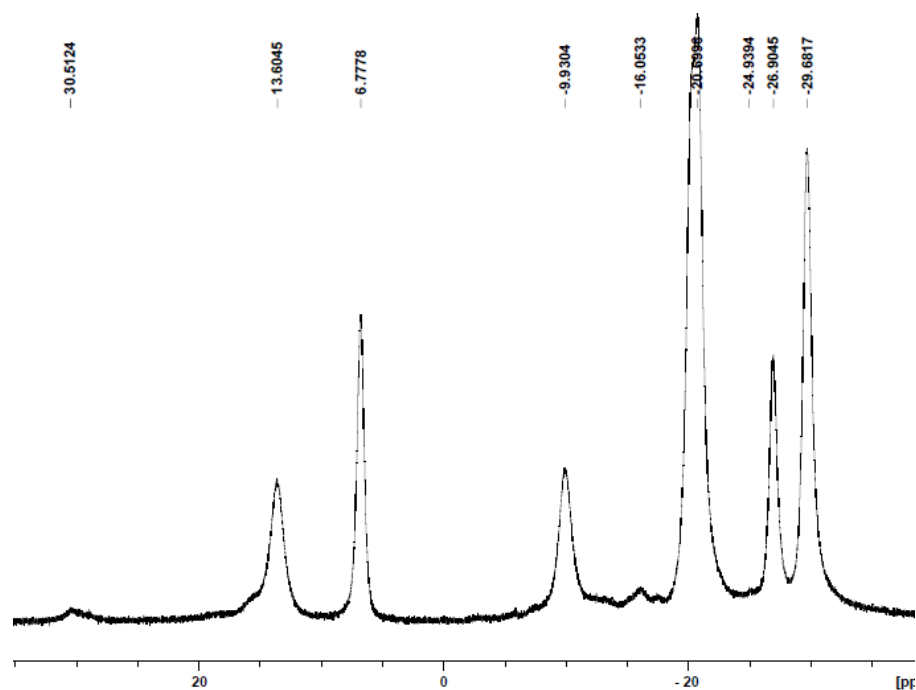


Figure 26: $^{11}\text{B}\{^1\text{H}\}$ and ^{11}B NMR spectra of $(\text{Me}_4\text{N})_2[\text{B}_{20}\text{H}_{17}(\text{CH}_2)_3\text{CH}_3]$.

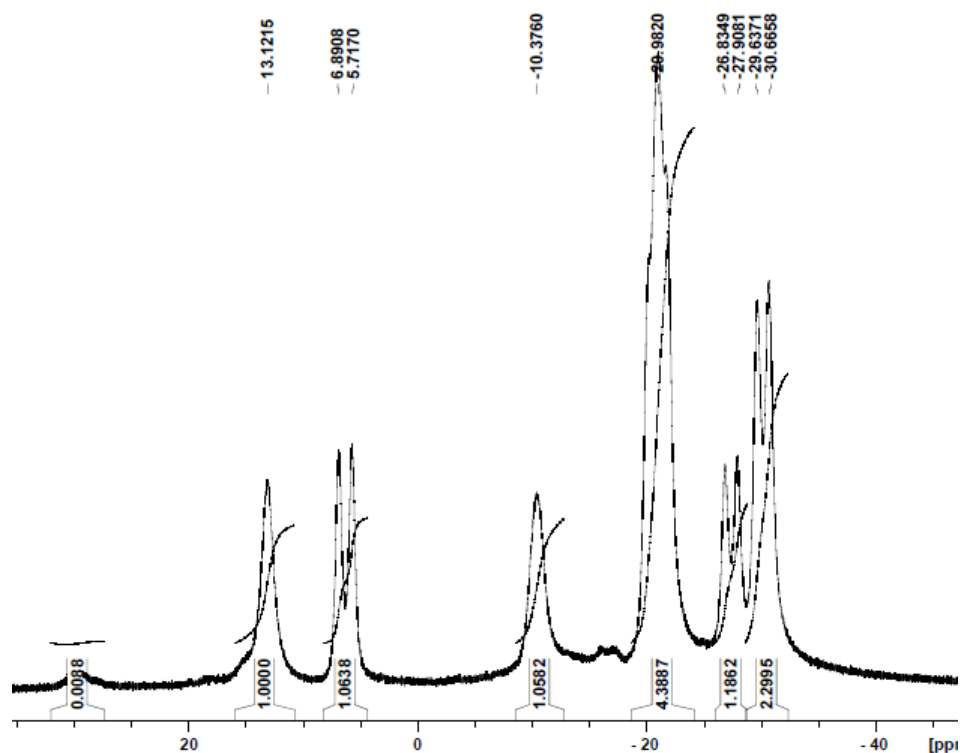


Figure 26: (continued from page 48).

Results regarding $(Bu_4N)_2[B_{20}H_{17}C_2H]$. Oxidation of the $[ae-B_{20}H_{17}(C_2H)]^{4-}$ product to form the $[B_{20}H_{17}(C_2H)]^{2-}$ ion was achieved by reaction of the reduced derivative with the ferric ion in aqueous solution at 0 °C (**Figure 27**). The product is precipitated from the aqueous solution by addition of a solution of tetrabutylammonium bromide in methanol.

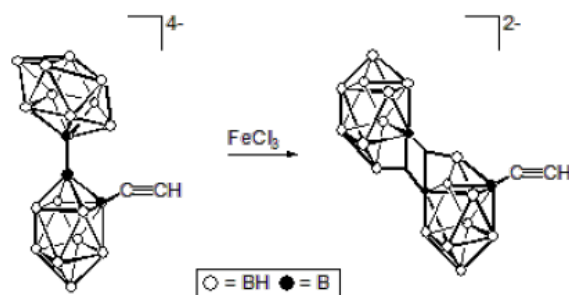


Figure 27: Oxidation of $[ae-B_{20}H_{17}(C_2H)]^{4-}$ to $[trans-B_{20}H_{17}(C_2H)]^{2-}$.

The $^{11}\text{B}\{^1\text{H}\}$ NMR spectrum is very similar to that of the $[\textit{trans}\text{-B}_{20}\text{H}_{18}]^{2-}$ ion. The spectrum exhibits a signal at 29.4 ppm that is a doublet in the ^{11}B NMR experiment (**Figure 28**). This is consistent with the apical boron atoms which appear at 29.9 ppm in the $[\textit{trans}\text{-B}_{20}\text{H}_{18}]^{2-}$ ion. The signal at 14.8 ppm corresponds to the equatorial boron atoms involved in the three center two electron bond, analogous to the signal present in the spectrum of the $[\textit{trans}\text{-B}_{20}\text{H}_{18}]^{2-}$ ion at 15.6 ppm. In addition, the equatorial atoms display the same pattern. The $^{11}\text{B}\{^1\text{H}\}$ NMR spectrum exhibits five signals at -8.0, -13.6, -17.1, -20.5 and -26.8 ppm which are split into doublets in the ^{11}B NMR spectrum. The ^1H NMR spectrum exhibits a complicated multiplet between 6.0 and 4.5 ppm and could be a result of ^1H - ^{11}B coupling. This multiplet is shifted upfield in comparison to the reduced derivative as would be expected by the change in electronic environment due to formation of the three-center two-electron bonds and the concurrent increase in the overall charge on the ion from a -4 to a -2 charge. All other signals can be attributed to the precipitating counter ion and solvent. While the ^{13}C NMR of the product is quite clean, there are no signals corresponding to the substituent on the product observed in the ^{13}C NMR spectrum. All signals were assigned to the reference standard and counter ion. The increased solubility of the oxidized derivative enabled the acquisition of the two-dimensional ^{11}B - ^{11}B NMR spectrum; however the spectrum was more complicated than expected and three cross-peaks were different than the $[\textit{trans}\text{-B}_{20}\text{H}_{18}]^{2-}$ standard.

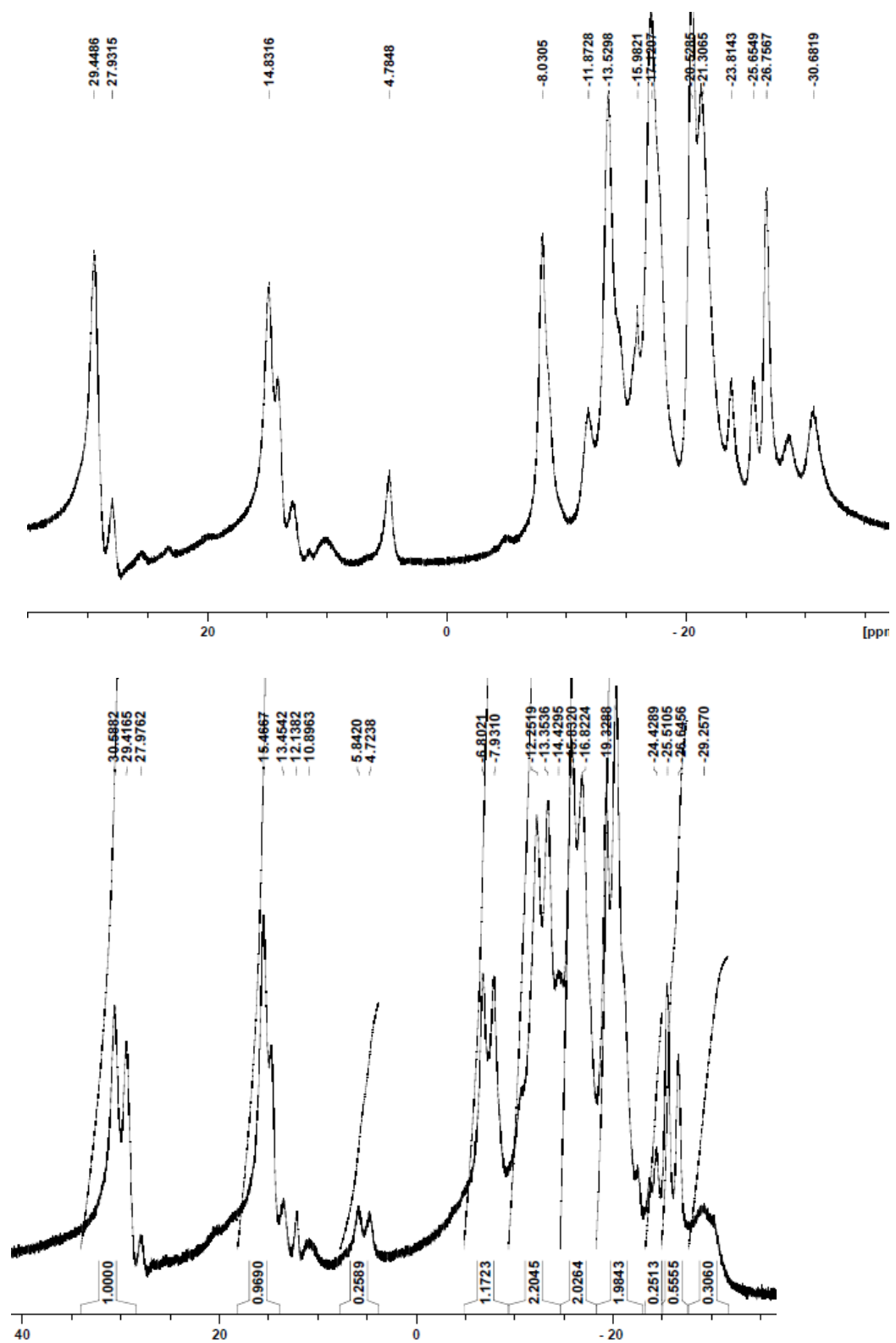


Figure 28: $^{11}\text{B}\{^1\text{H}\}$ and ^{11}B NMR spectra of $(\text{Bu}_4\text{N})_2[\text{B}_{20}\text{H}_{17}\text{C}_2\text{H}]$.

Results regarding $(\text{Bu}_4\text{N})_2 [\text{B}_{20}\text{H}_{17}\text{CH}_2\text{CN}]$. Oxidation of the reduced acetonitrile product, $[\text{ae-B}_{20}\text{H}_{17}\text{CH}_2\text{CN}]^{4-}$ was achieved by the addition of ferric ion to an aqueous solution of the reduced derivative at 0 °C (**Figure 29**). The product is precipitated from the solution as the tetrabutyl ammonium salt.

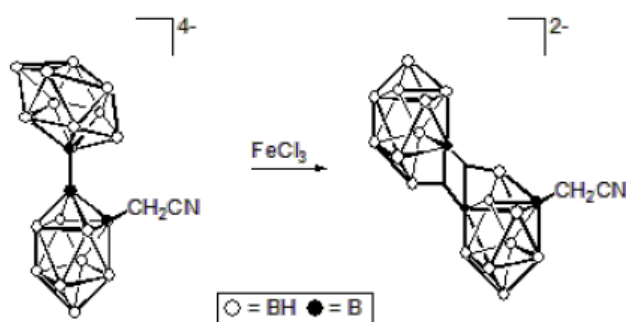


Figure 29: $^{11}\text{B}\{^1\text{H}\}$ and ^{11}B NMR spectra of $(\text{Bu}_4\text{N})_2[\text{B}_{20}\text{H}_{17}\text{CH}_2\text{CN}]$.

The $^{11}\text{B}\{^1\text{H}\}$ NMR spectrum is somewhat similar to that of the $[\text{trans-B}_{20}\text{H}_{18}]^{2-}$ ion. The $^{11}\text{B}\{^1\text{H}\}$ NMR spectrum exhibits a peak at 29.2 ppm that is a doublet in the ^{11}B NMR experiment (**Figure 30**). This is consistent with the apical boron atoms which appear at 29.9 ppm in the $[\text{trans-B}_{20}\text{H}_{18}]^{2-}$ ion. The signal at 11.4 ppm corresponds to the equatorial boron atoms involved in the three center two electron bond, analogous to the signal present in the spectrum of $[\text{trans-B}_{20}\text{H}_{18}]^{2-}$ ion at 15.6 ppm. The ^1H NMR spectrum exhibits a complicated multiplet between 6.0 and 4.5 ppm and could be a result of ^1H - ^{11}B coupling. This multiplet is shifted upfield in comparison to the reduced derivative as would be expected by the change in electronic environment due to formation of the three-center two-electron bonds and the concurrent increase in the overall charge on the ion from a -4 to a -2 charge. While the ^{13}C NMR of the product is resolute, there are no signals corresponding to the substituent on the product observed in

the ^{13}C NMR spectrum. All present signals were assigned to the reference standard and counter ion. Due to the small amount of sample available, a two dimensional ^{11}B - ^{11}B NMR spectrum could not be obtained.

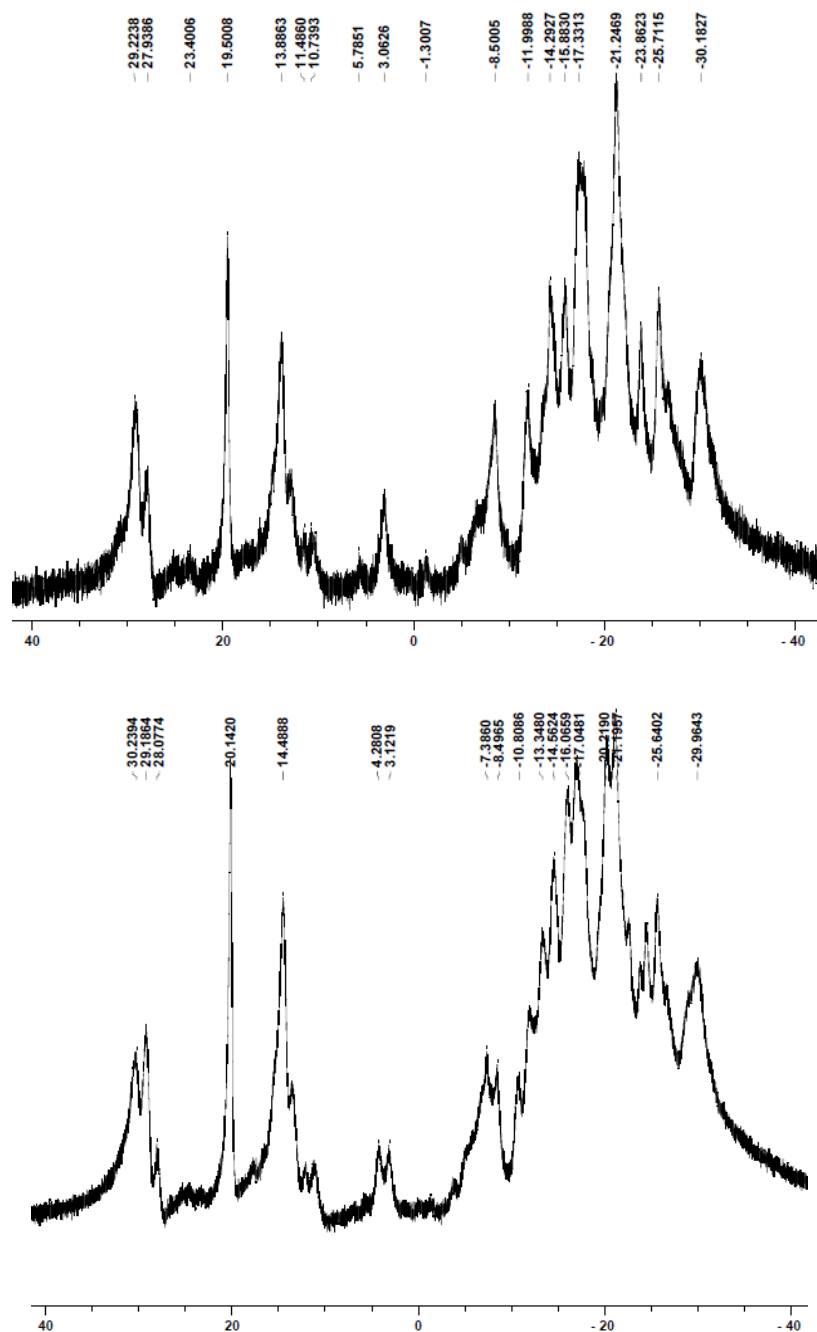


Figure 30: $^{11}\text{B}\{^1\text{H}\}$ and ^{11}B NMR spectra of $(\text{Bu}_4\text{N})_2 [\text{B}_{20}\text{H}_{17}\text{CH}_2\text{CN}]$.

CHAPTER V

CONCLUSIONS

Although the susceptibility of the [*trans*-B₂₀H₁₈]²⁻ ion to nucleophilic attack has been investigated for nucleophiles containing oxygen, nitrogen, and sulfur, no investigations have been reported in the literature for nucleophilic attack by a carbon nucleophile. The products of the proposed reactions are of interest because they provide another means of investigating both the original mechanism of nucleophilic attack proposed by Hawthorne in 1965¹⁸ and the revised mechanism proposed by Hawthorne in 2002,¹ neither of which can explain the unique reactivity of the thiol anions.²⁵ Additionally, the products of the reactions with carbon nucleophiles have the potential to serve as the starting materials for polyhedral borane anions that contain both carboxylic acid and amide substituents. The carboxylic acid and amide substituents may be capable of reacting with amino acids and/or protein substituents once delivered by unilamellar liposomes and thus be retained *in vivo*.

As a result of this interest in the carbon nucleophiles, a series of reactions have been completed to yield both the reduced derivatives of the form [B₂₀H₁₇X]⁴⁻, both the apical-equatorial and the apical-apical isomers, and the oxidized derivatives of the form [B₂₀H₁₇X]²⁻ where X is the carbon nucleophile. The results of this study have confirmed that a carbon nucleophile will react with the [*trans*-B₂₀H₁₈]²⁻ ion. The products

of the reactions have been characterized by NMR spectroscopy, including, as appropriate, one-dimensional ^{11}B , two-dimensional ^{11}B , ^{13}C , and ^1H NMR, and IR spectroscopy.

While final confirmation of the identity of the compounds has not been verified by either elemental analysis or high-resolution mass spectrometry analysis, the compounds have been sent to the laboratories of Dr. Mark Lee at the University of Missouri for high resolution mass spectrometry analysis. The results of this analysis are pending.

The $[\text{ae-B}_{20}\text{H}_{17}\text{X}]^{4-}$ and $[\text{a}^2\text{-B}_{20}\text{H}_{17}\text{X}]^{4-}$ isomers, where X is the selected carbon nucleophile, have been isolated and characterized for each of the three carbon nucleophiles. In each case, the kinetic isomer, the apical-equatorial isomer, was formed as the first product of the reaction, consistent with the original mechanism proposed by Hawthorne.¹⁸ An alkyl shift was not observed as previously hypothesized during nucleophilic attack by the *n*-butyl anion acting as the nucleophile. The apical-equatorial isomers of each product were converted to the thermodynamic isomer, the apical-apical isomer, using a combination of heat and acidic conditions, again consistent with Hawthorne's original mechanism.¹⁸

The reduced substituted derivatives were oxidized using ferric ion in aqueous solution to restore the three-center two-electron bond resulting in a series of oxidized substituted derivatives of the form $[\text{B}_{20}\text{H}_{17}\text{X}]^{2-}$ where X is the selected carbon nucleophile. Two of the oxidized products yielded ^{11}B NMR spectra consistent with the *trans* derivatives, analogous to the $[\text{trans-B}_{20}\text{H}_{18}]^{2-}$ ion and predicted based on the mechanism of the $[\text{ae-B}_{20}\text{H}_{17}\text{OH}]^{4-}$ previously reported by Hawthorne.¹ The ^{11}B NMR spectrum of the oxidized product of the $[\text{B}_{20}\text{H}_{17}(\text{CH}_2)_3\text{CH}_3]^{2-}$ derivative did not match the spectra of the other two products. While the one-dimensional ^{11}B NMR spectrum of the

reduced product is analogous to those reported for other reduced substituted derivatives, the two-dimensional ^{11}B NMR indicates that the product may be doubly substituted. It appears that the *n*-butyl group is attached on the equatorial boron atoms opposite to the boron atoms involved in the B-B-B intercage connection on one polyhedral borane cage. The mechanism of nucleophilic attack on the $[\textit{trans}\text{-B}_{20}\text{H}_{18}]^{2-}$ by the *n*-butyl nucleophile cannot be verified until the determination of the molecular weight of this compound by high resolution mass spectrometry. If the oxidized compound does have two *n*-butyl substituents, that would indicate that the initial observation of the one-dimensional ^{11}B NMR spectrum of the reduced substituted derivative of $[\textit{trans}\text{-B}_{20}\text{H}_{18}]^{2-}$ was insufficient to correctly characterize the reduced isomer as $[\textit{ae}\text{-B}_{20}\text{H}_{17}(\text{CH}_2)_3\text{CH}_3]^{4-}$. The determination of the mass spectral analysis will confirm the degree of substitution. Two substituents on the product of the reaction would not be supported by the currently proposed mechanisms nor the reported chemistry of the $[\textit{trans}\text{-B}_{20}\text{H}_{18}]^{2-}$ ion.

Successful preparation of the desired compounds has provided a series of compounds which could be tested directly for potential application in BNCT, but also provide the starting materials for a new project based on the conversion of the products to both carboxylic acid and amide derivatives. Preparation of the oxidized derivatives is critical towards this goal as the conditions necessary to convert either the acetonitrile derivative or the acetylide derivative to the oxidized derivatives would also oxidize the polyhedral borane cage.

The ^1H NMR spectra of all of the *ae* isomers contain a more resolute splitting pattern from 4.5 ppm to 2.0 ppm in comparison to the *a*² isomer. The resolution of this pattern is different for each nucleophile, but more pronounced in the acetylide and

acetonitrile derivatives. This may be due to the concentration of the individual samples, but could also be indicative of the electronic environment. There is a trend in chemical shift in the ^1H NMR data for the oxidized derivatives. The chemical shift of the peaks corresponding to the hydrogen atoms on the primary carbon of the *n*-butyl and acetonitrile nucleophiles, along with the long range coupling of the hydrogen on the beta carbon of the acetylide nucleophile, have all moved downfield. This trend is in alignment with the shift of the alpha carbon on the *n*-butyl oxidized derivative. It has shifted approximately 10 ppm upfield from approximately 66 ppm to 77 ppm. This can be attributed to the overall decrease in delocalized charge multiplicity of the anion.

CHAPTER VI

FUTURE WORKS

The chemistry of the $[\text{B}_{20}\text{H}_{18}]^{2-}$ isomers remains relatively unexplored. Results of the current project serve as the basis for additional research which may lead to the development of novel target materials. The current mechanisms of tumor accretion have not been exploited to their full potential. The ability of the boron compounds to bind to intracellular proteins is one of the most specific accretion modalities. None of the derivatives studied in the past have contained chemically active functional groups found in the amino acid monomers composing intracellular proteins found in cancer cells. Because of this, it has been proposed that derivatives synthesized by the nucleophilic attack of an appropriate carbon nucleophile will have the potential to be functionalized biologically using established organic chemistry techniques and produce molecules which will have a novel method of conglomeration within a tumor.^{31,32} Future investigations will rely on the established chemistry to convert the recently prepared derivatives to either a carboxylic acid functional group or an amide functional group.

6.1 Acetonitrile Derivatives

In order to make the proposed derivatives biologically available for binding to intracellular proteins, the reactivity of the prepared polyhedral borane anions must be

investigated. Based on previous research by Spielvogel and co-workers for the $[\text{BH}_2\text{CN}]_x$ oligomer,^{31,32} the $[\text{B}_{20}\text{H}_{17}\text{CH}_2\text{CN}]^{4-}$ ion should react with triethyloxonium tetrafluoroborate to produce an intermediate salt (**Figure 31**). When exposed to hot water, the intermediate should yield the carboxylic acid, $-\text{COOH}$, derivative whereas when exposed to hot base, the intermediate should yield the amide, $-\text{CONH}_2$, derivative (**Figure 31**).

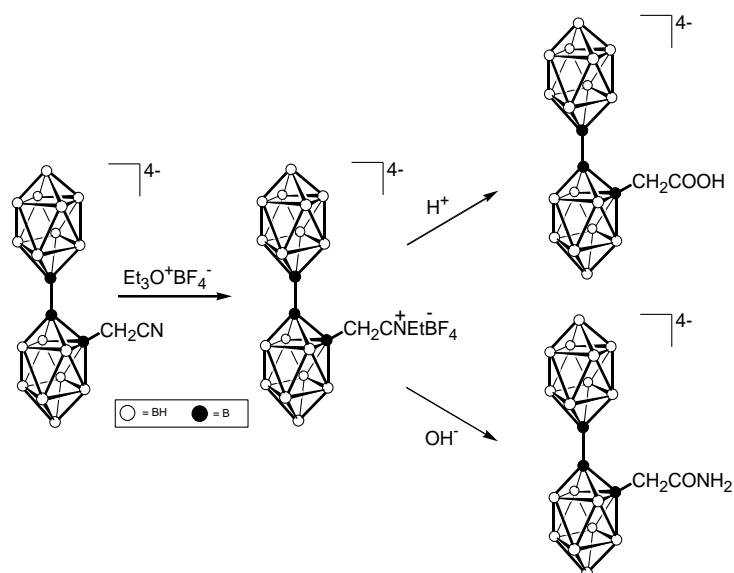


Figure 31: Hydrolysis of $[\text{B}_{20}\text{H}_{17}\text{CH}_2\text{CN}]^{4-}$.

The reactivity of the nitrile group, in the product formed by nucleophilic attack by the deprotonated acetonitrile nucleophile, in subsequent reactions, may be affected by the proximity to the polyhedral borane cage. As a result, additional reactions could be attempted with lithiated nitriles prepared by the reaction of *n*-butyllithium with bromoalkylnitriles, $\text{Br}(\text{CH}_2)_n\text{CN}$, of chain lengths longer than $n=4$ since both bromobutyronitrile ($n=3$) and bromopentane nitrile ($n=4$) are known to cyclize in the

presence of *n*-butyllithium.³³ The reaction of $[trans\text{-B}_{20}\text{H}_{18}]^{2-}$ with the monolithium derivative of phenylacetonitrile, $\text{C}_6\text{H}_5\text{CH}(\text{Li})\text{CN}$, prepared from the reaction of *n*-butyllithium and phenylacetonitrile,³⁰ can also be investigated in a manner analogous to that proposed for the acetonitrile ion.

6.2 Acetylide Derivatives

The acetylide substituted derivatives of the $[trans\text{-B}_{20}\text{H}_{18}]^{2-}$ are predicted to be oxidized in the presence of KMnO_4 based on the investigations by Lee and Chang³⁴ (Figure 32). Oxidation of the acetylide should yield the carboxylic acid derivative.

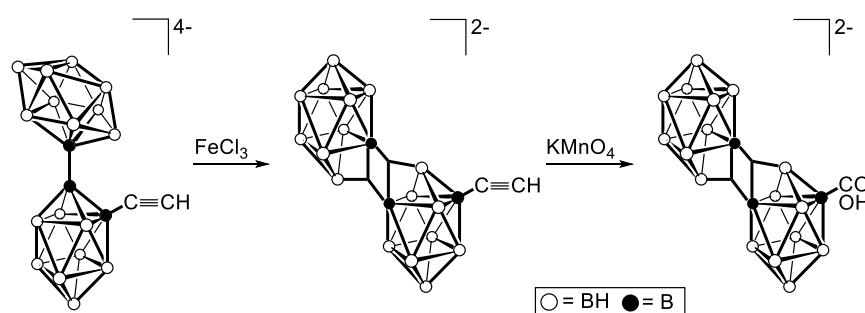


Figure 32: Oxidation of the acetylide functional group of $[trans\text{-B}_{20}\text{H}_{17}\text{C}_2\text{H}]^{2-}$.

6.3 Amino Acid Coupling

The ability of the synthesized carboxylic acid derivatives to react with amino acids could be investigated. Polyhedral borane anions have been shown to interact with serum albumins,³⁵ however, the interaction between the ions and the albumin is largely electrostatic in nature. Only the $[\text{B}_{20}\text{H}_{17}\text{SH}]^{4-}$ ion has exhibited evidence of the formation of a covalent bond with a protein substituent.³⁵ The ability of the polyhedral borane anions to react with representative amino acids should be investigated with the goal of enhancing the understanding of the reactivity of this class of compounds and the potential

to incorporate the ions into molecular targets for application in BNCT. The rubidium salt of the carboxylic acid derivative, $\text{Rb}_4[\text{B}_{20}\text{H}_{17}\text{CH}_2\text{COOH}]$, can be ion-exchanged to the sodium salt to increase the solubility of the compound in a wide variety of solvents. The carboxylic acid reactivity could be tested with a series of representative amino acids, for example, the ethyl ester of tyrosine (**Figure 33**), using dicyclohexylcarbodiimide (DCC) and 4-dimethylaminopyridine (DMAP) for the coupling reaction. While researchers have experience with the coupling reaction,³⁶ the cation of the polyhedral borane anion and the solvent system for the reaction will have to be optimized to yield the desired results.

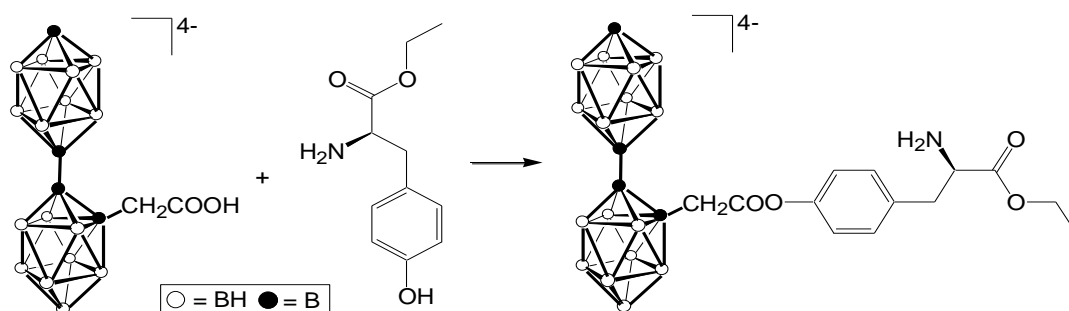
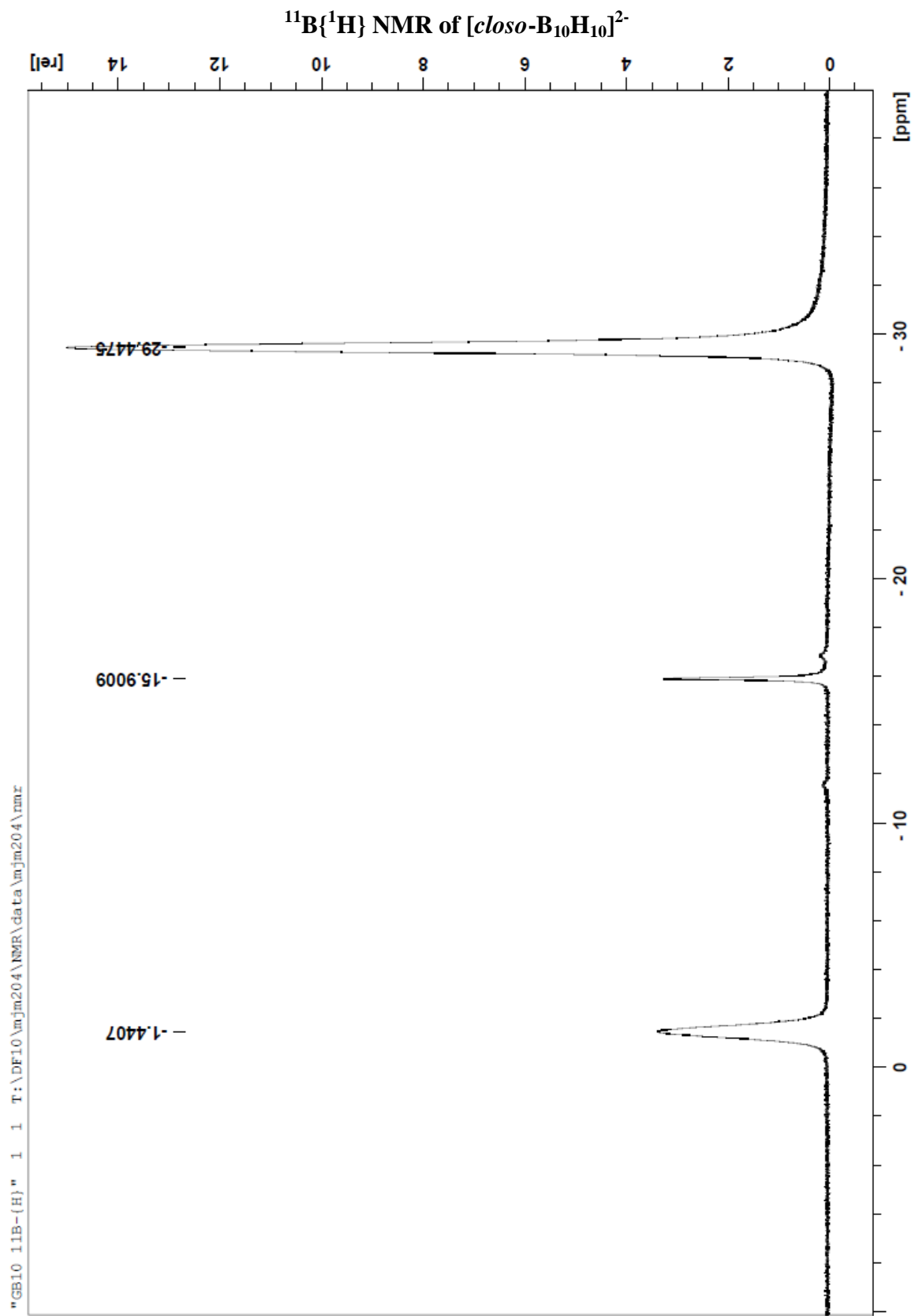
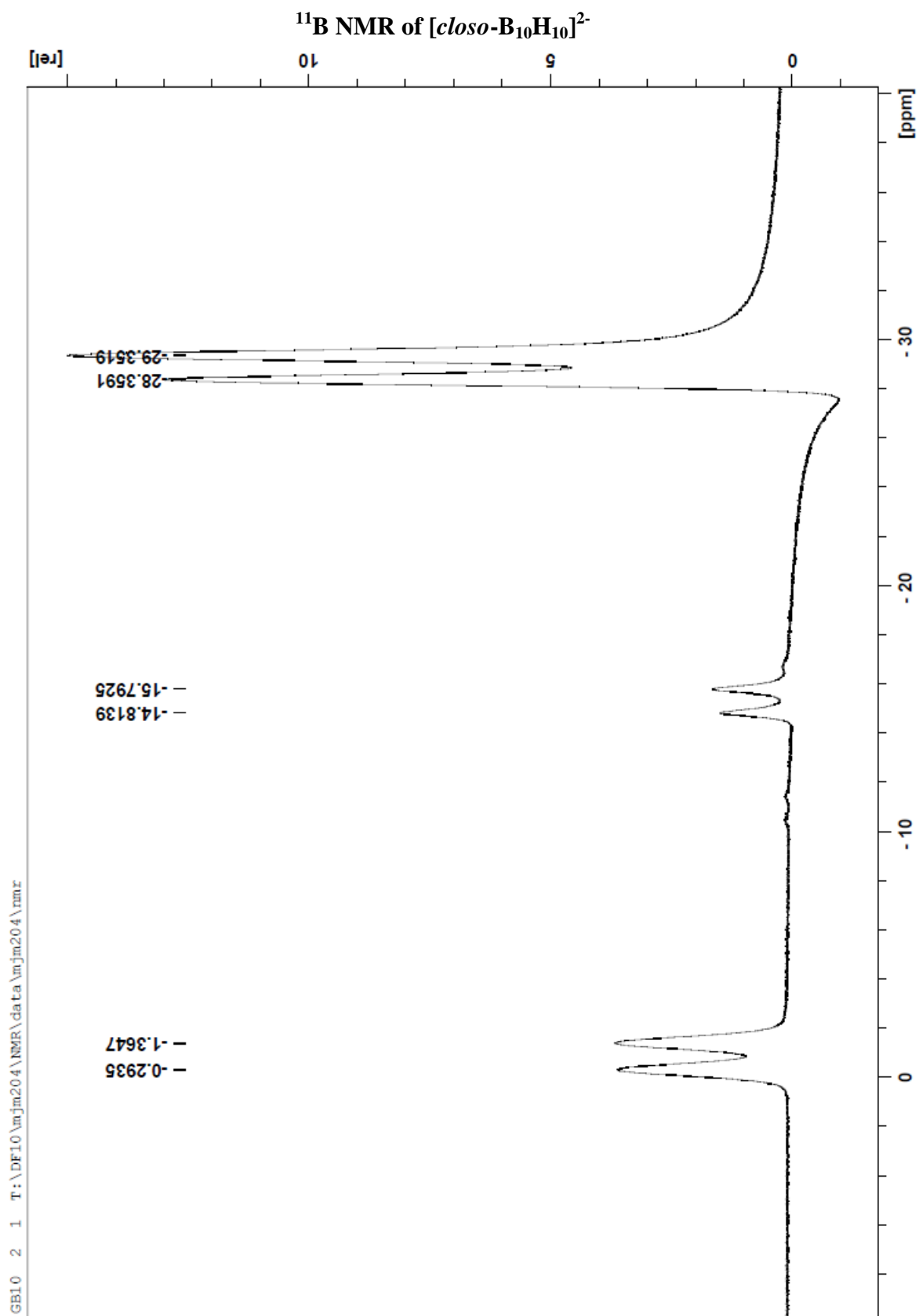
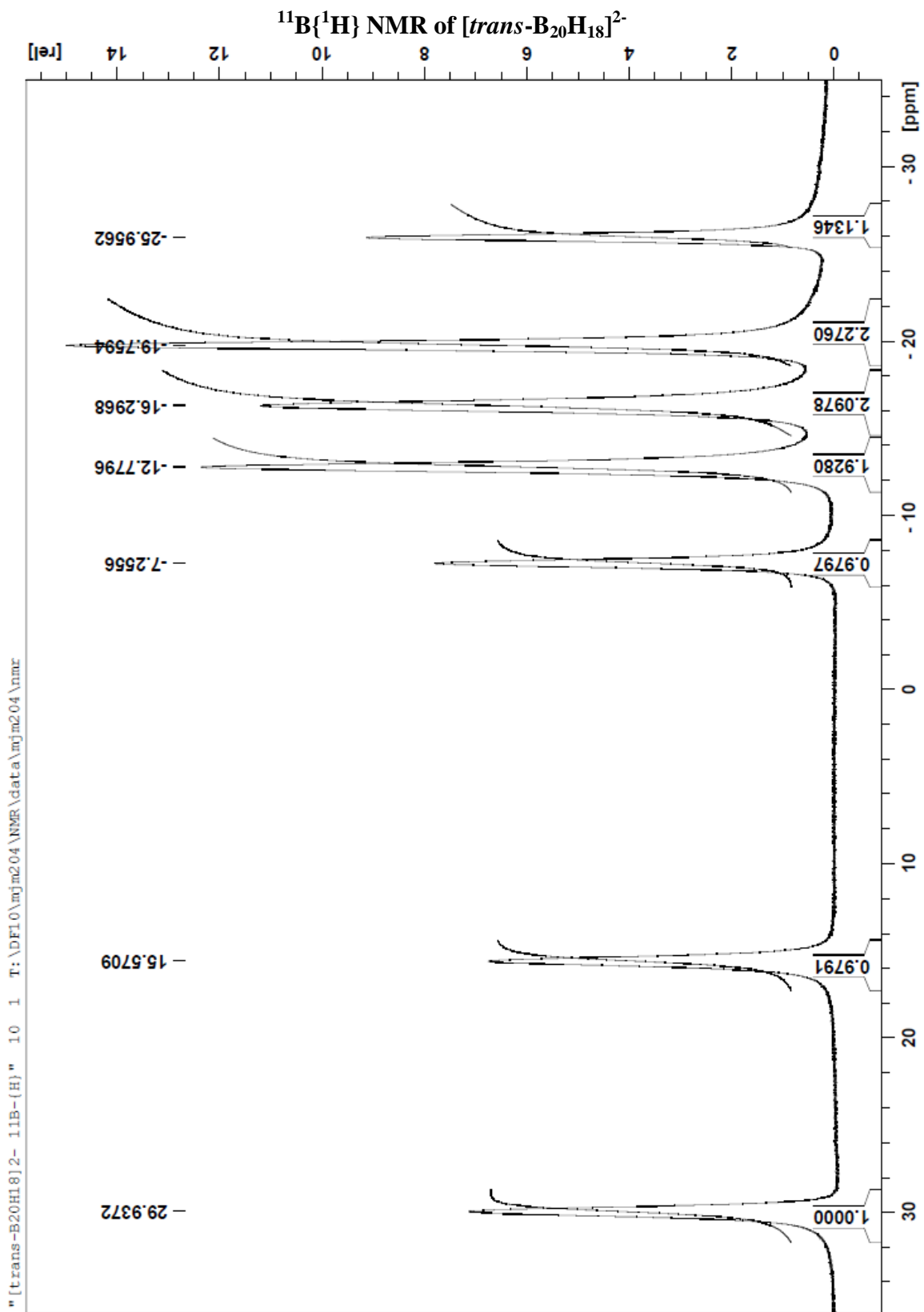


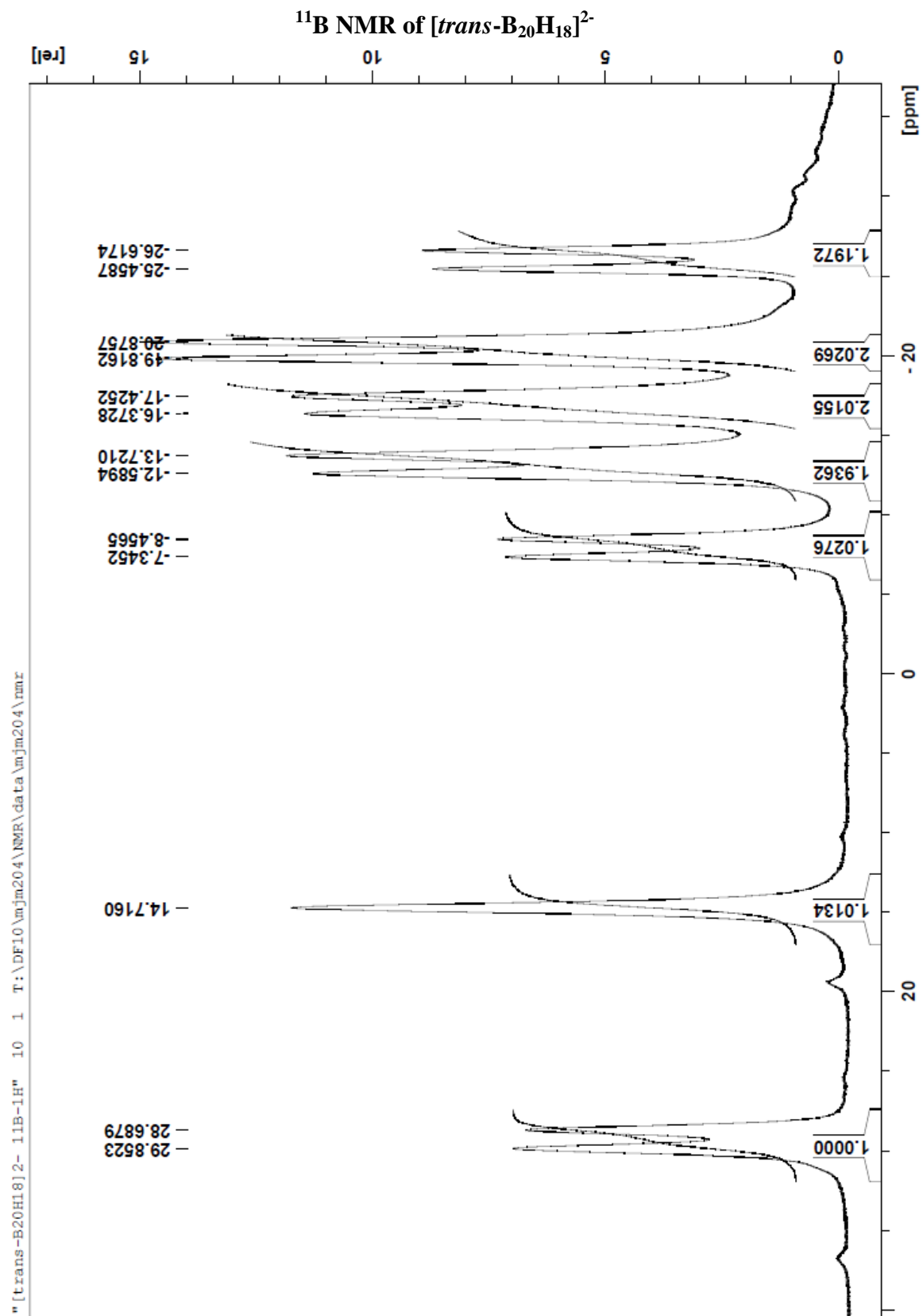
Figure 33: Coupling of carboxylic acid derivative to a representative amino acid, the ethyl ester of tyrosine.

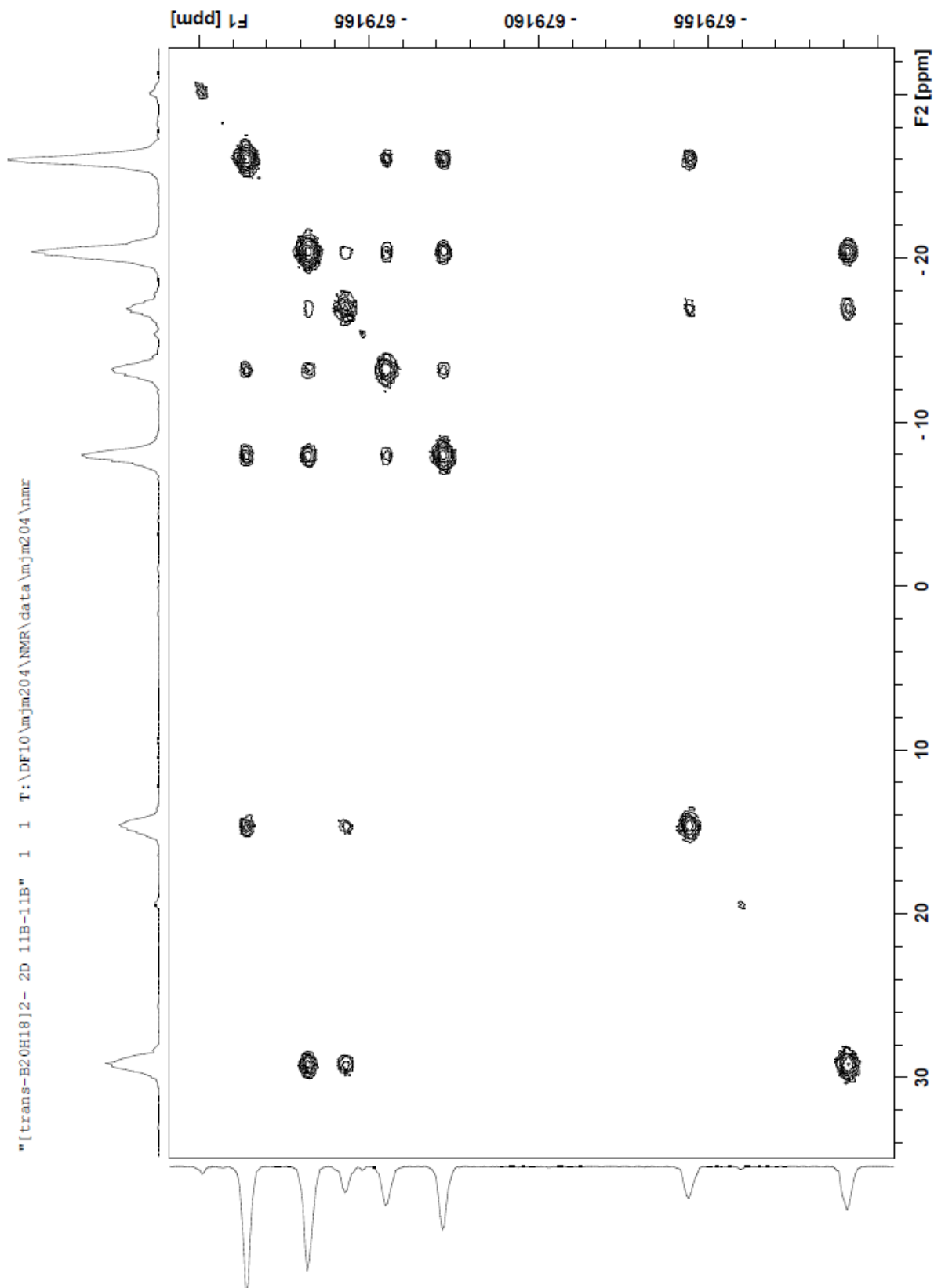
APPENDIX: SPECTRA

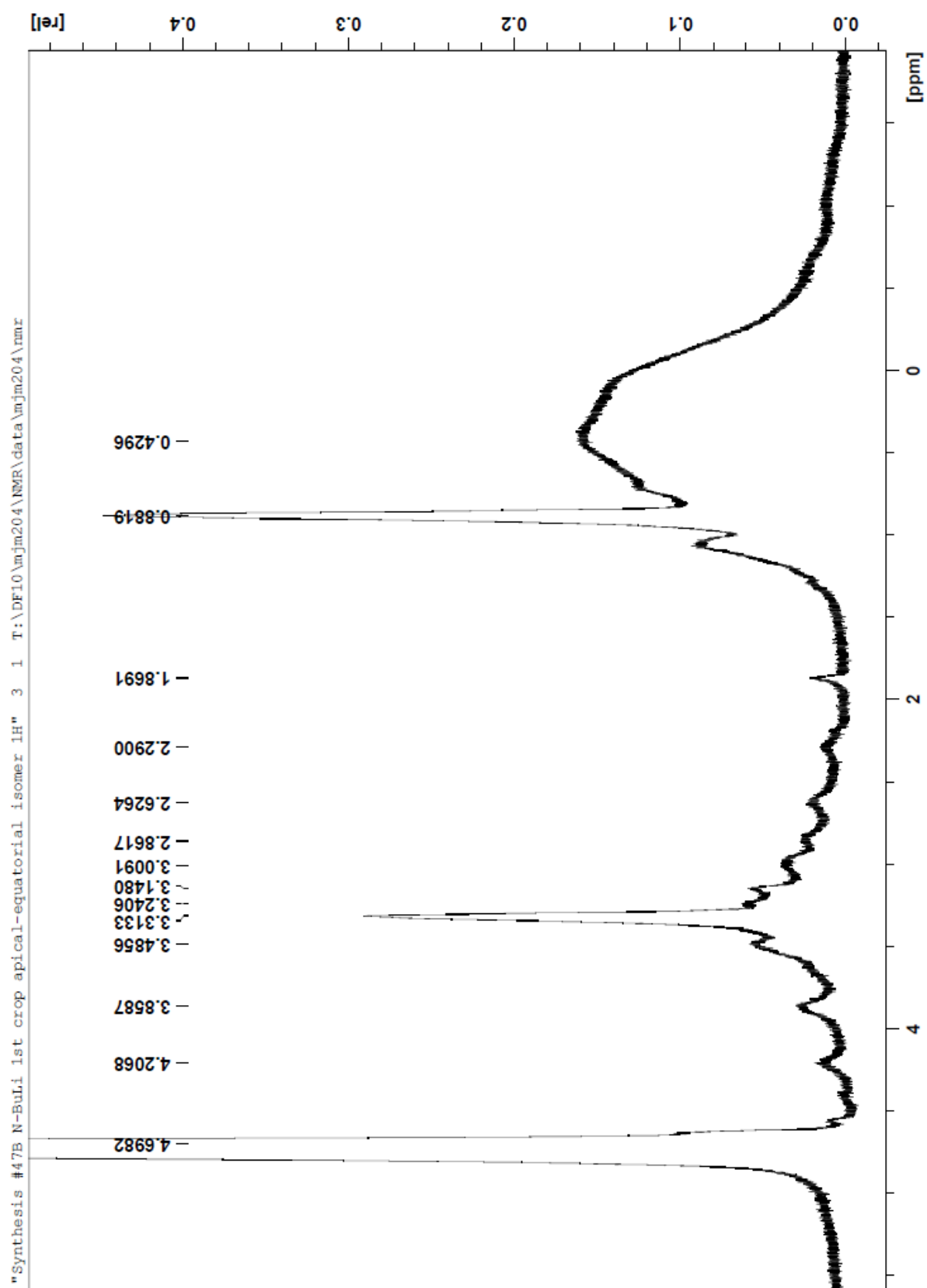


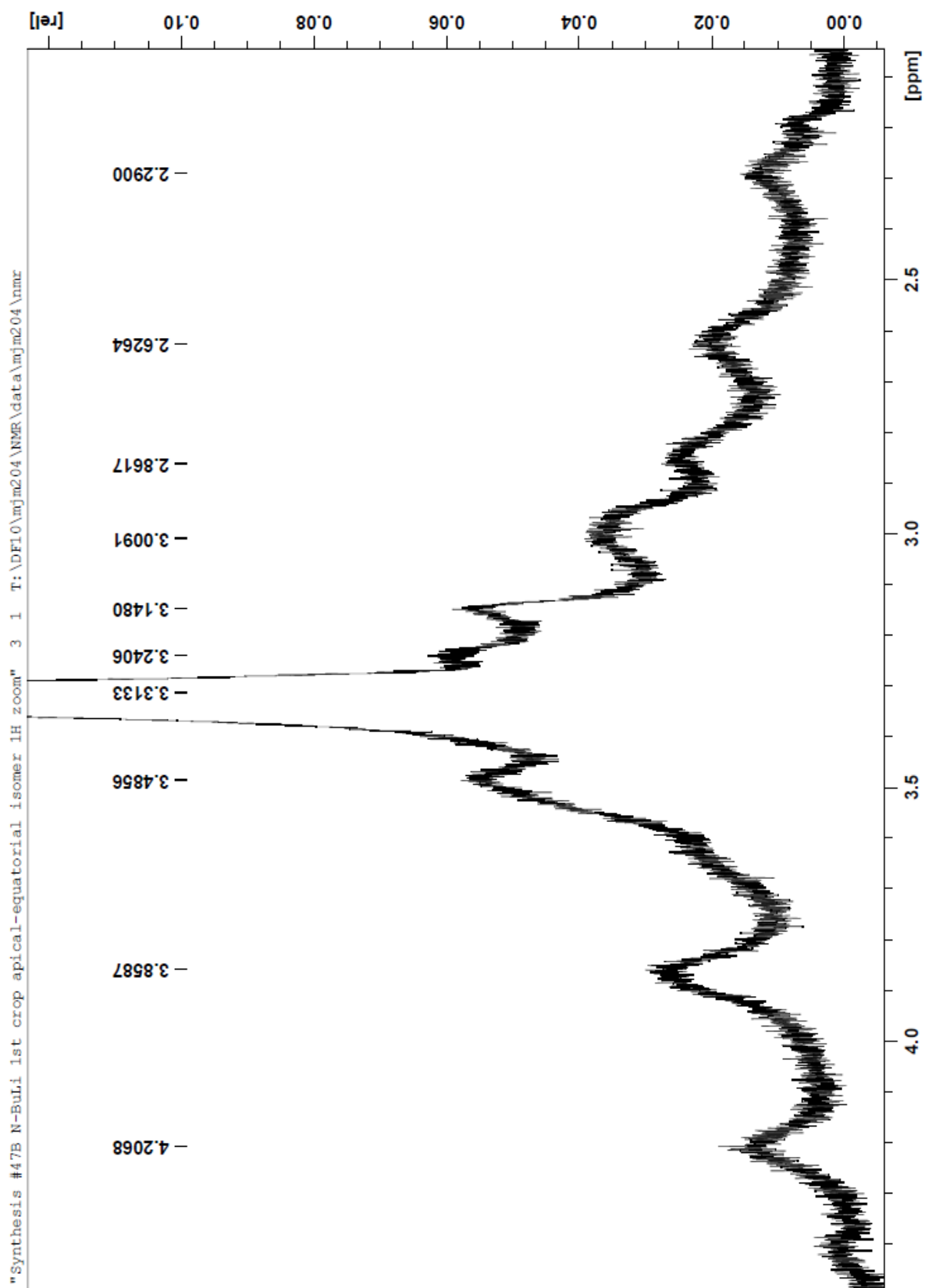


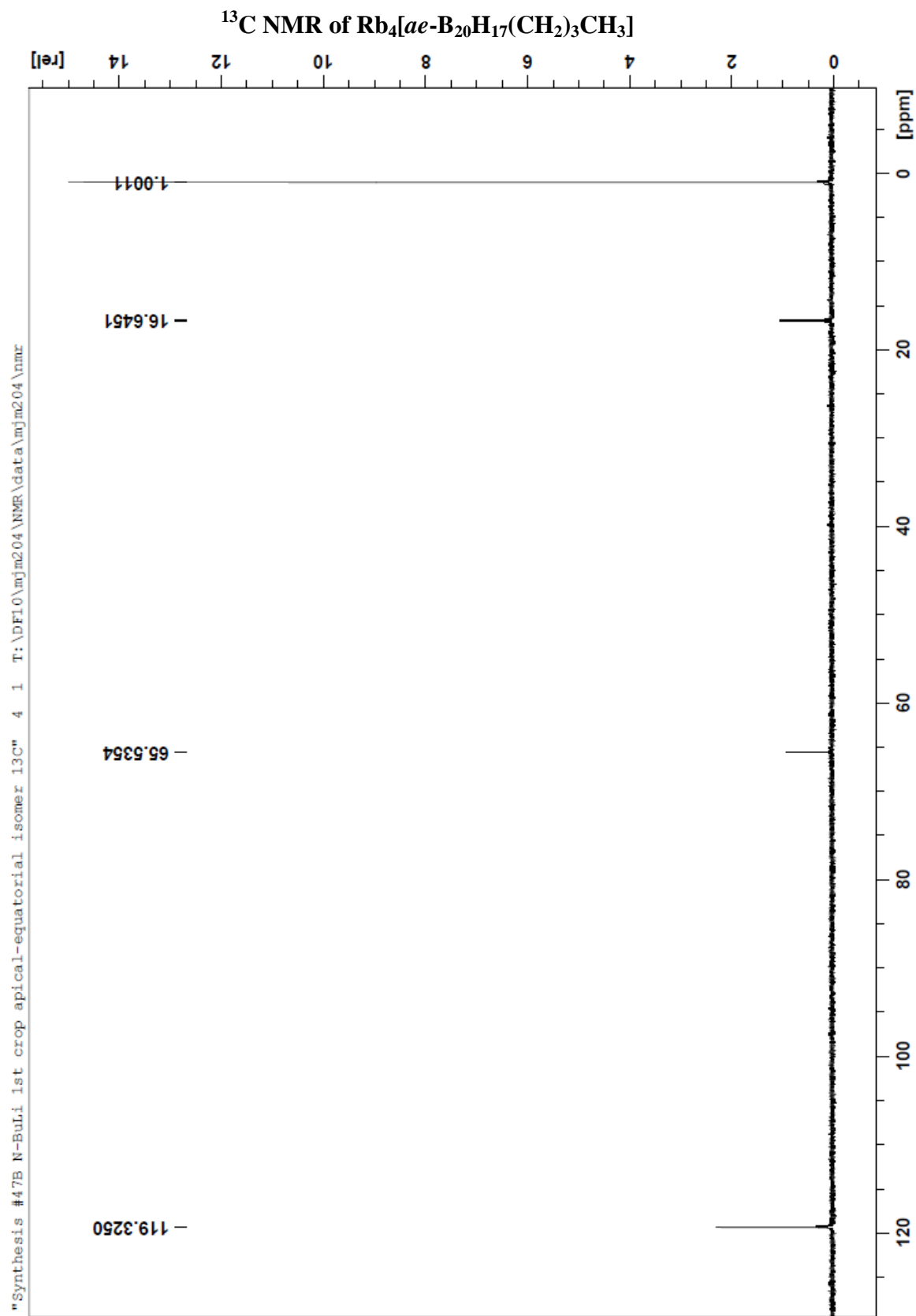


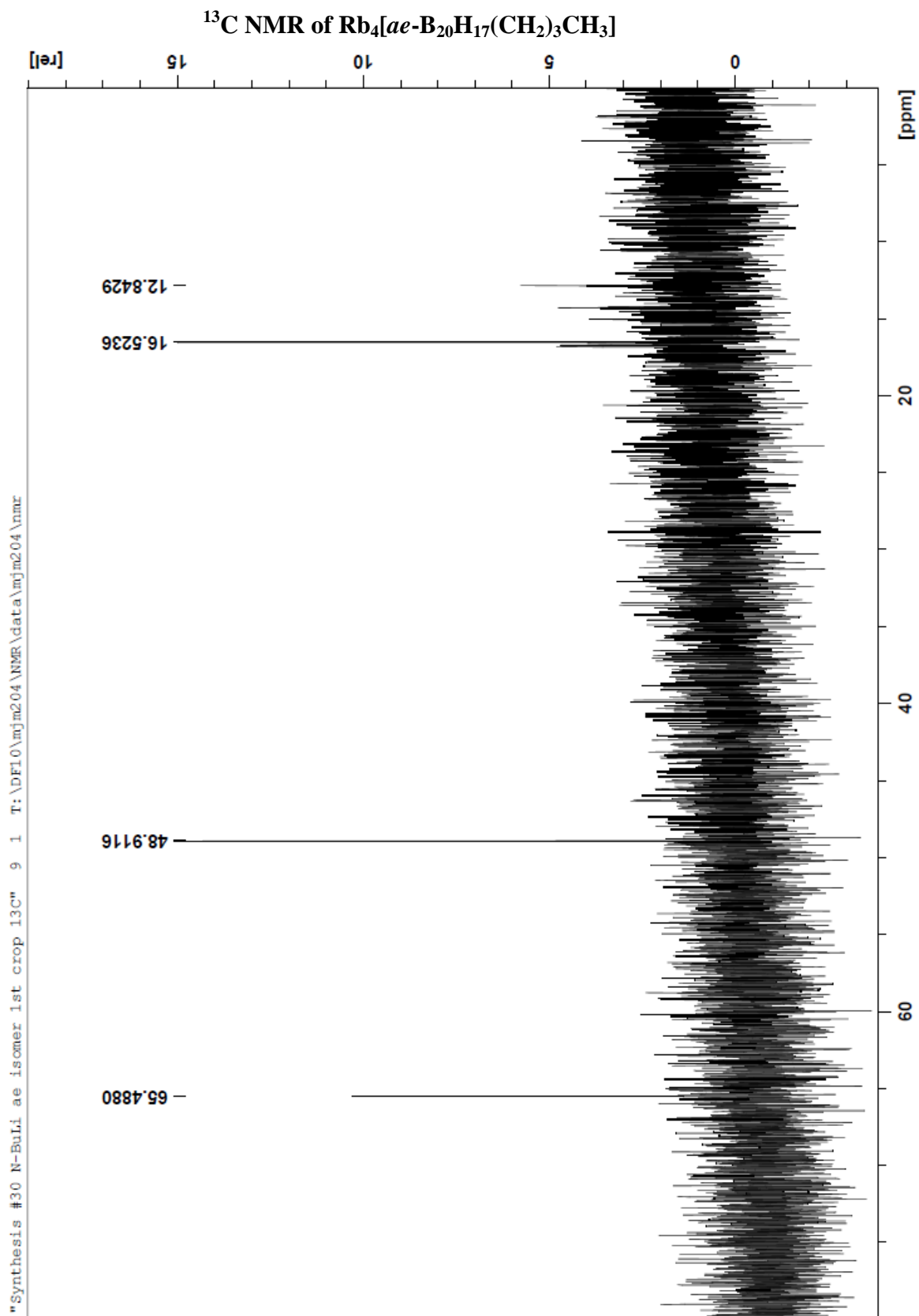


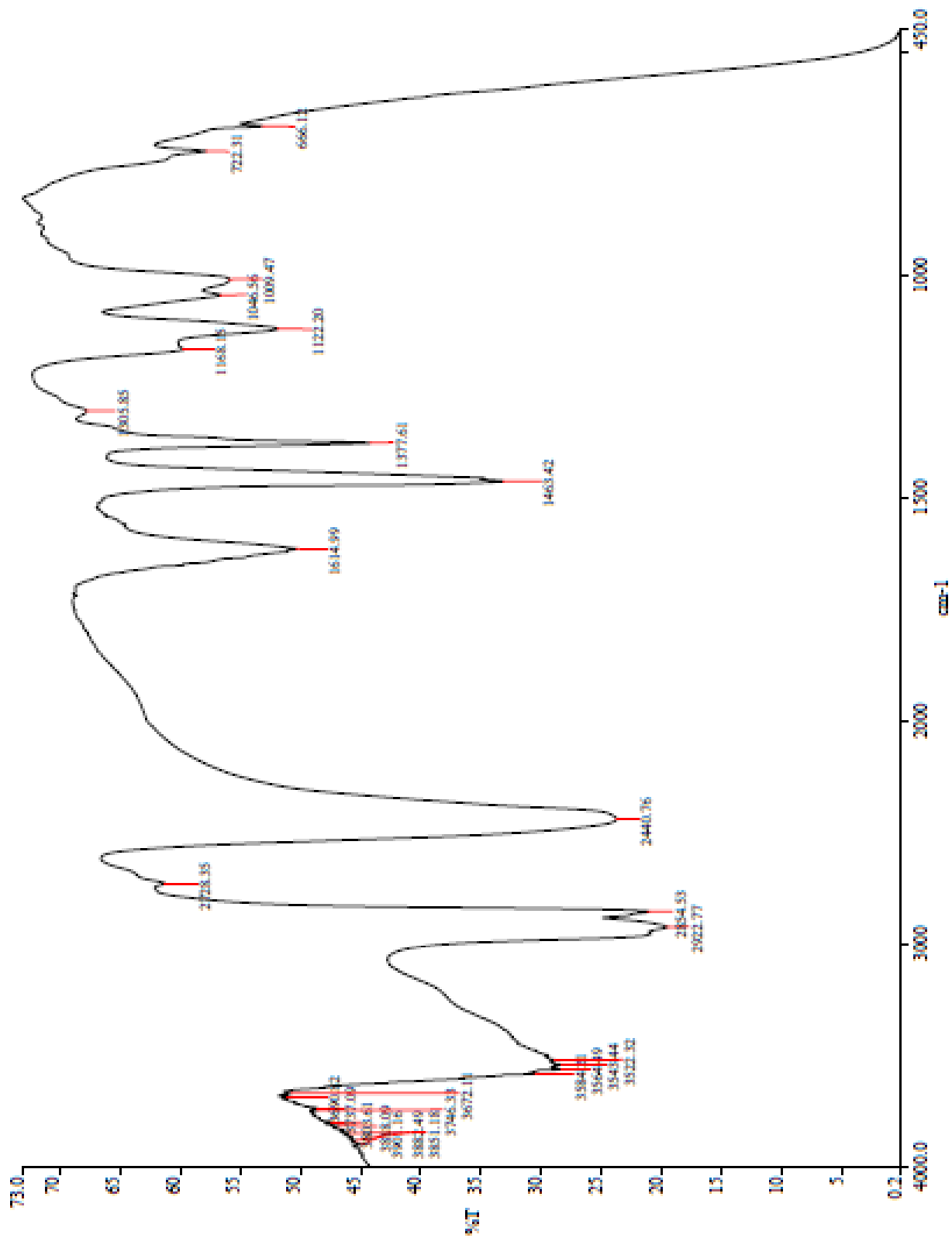
2D ^{11}B - ^{11}B NMR of $[\text{trans-B}_{20}\text{H}_{18}]^{2-}$ 

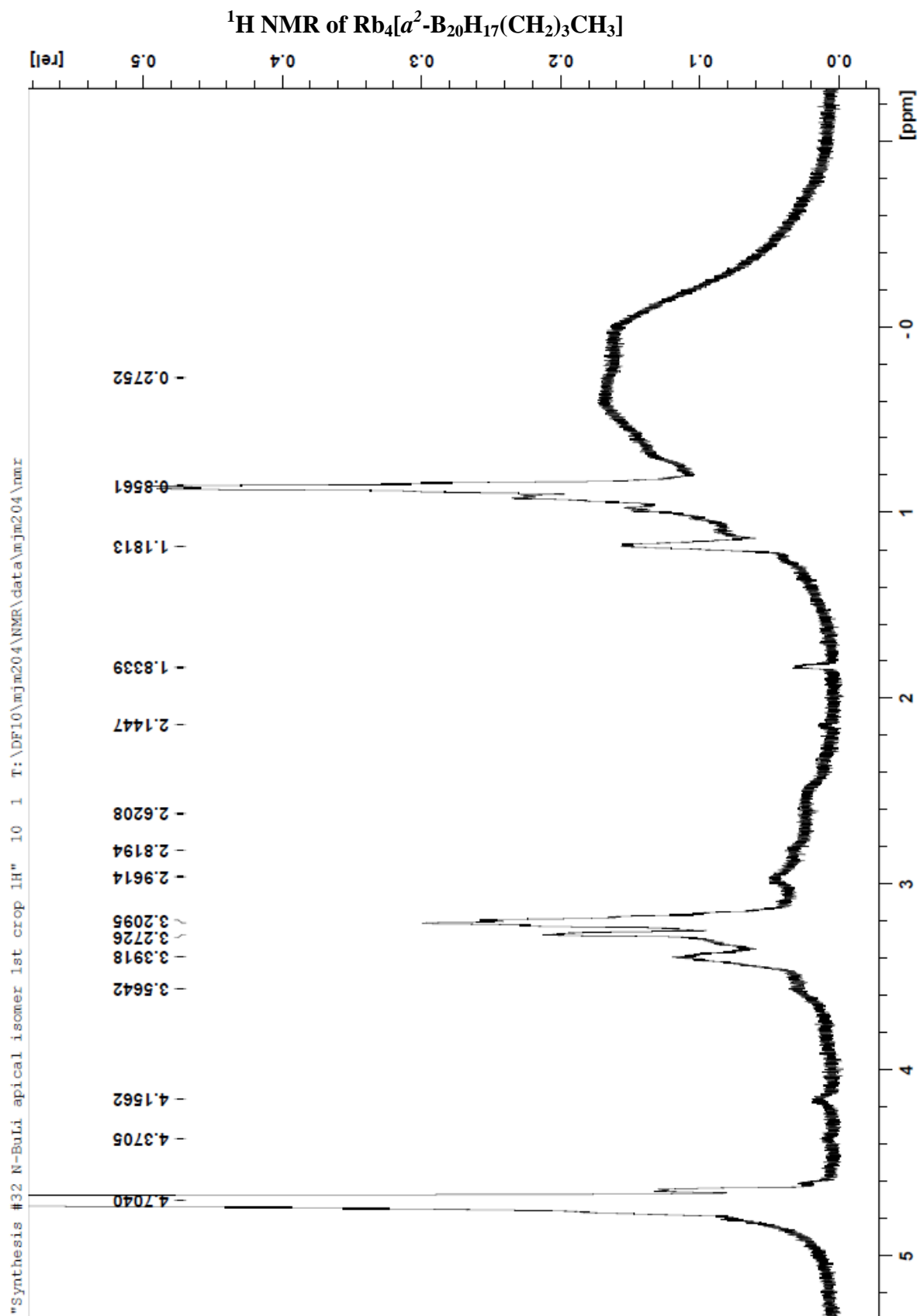
^1H NMR of $\text{Rb}_4[\text{ae-B}_{20}\text{H}_{17}(\text{CH}_2)_3\text{CH}_3]$ 

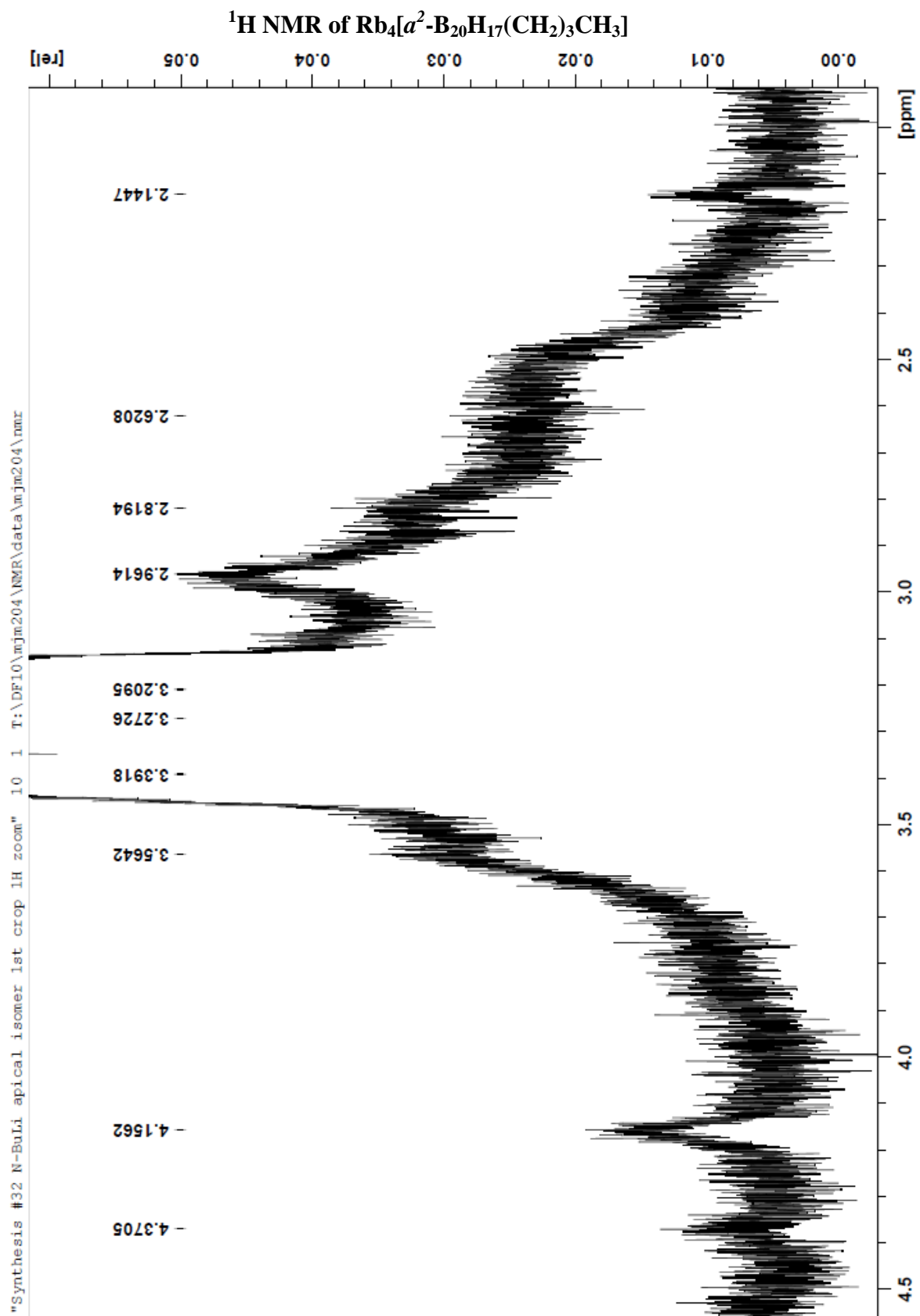
^1H NMR of $\text{Rb}_4[\text{ae-B}_{20}\text{H}_{17}(\text{CH}_2)_3\text{CH}_3]$ 

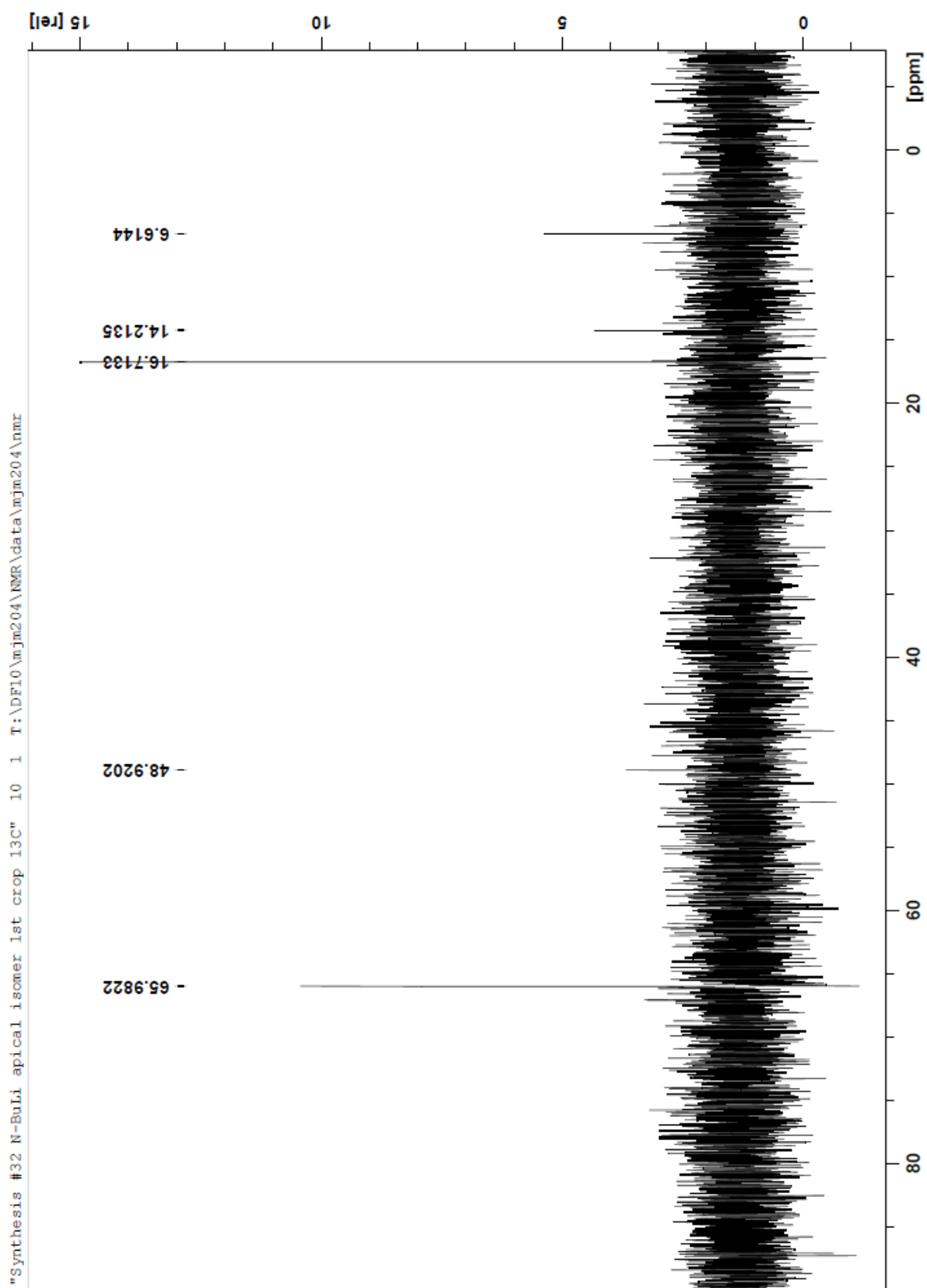


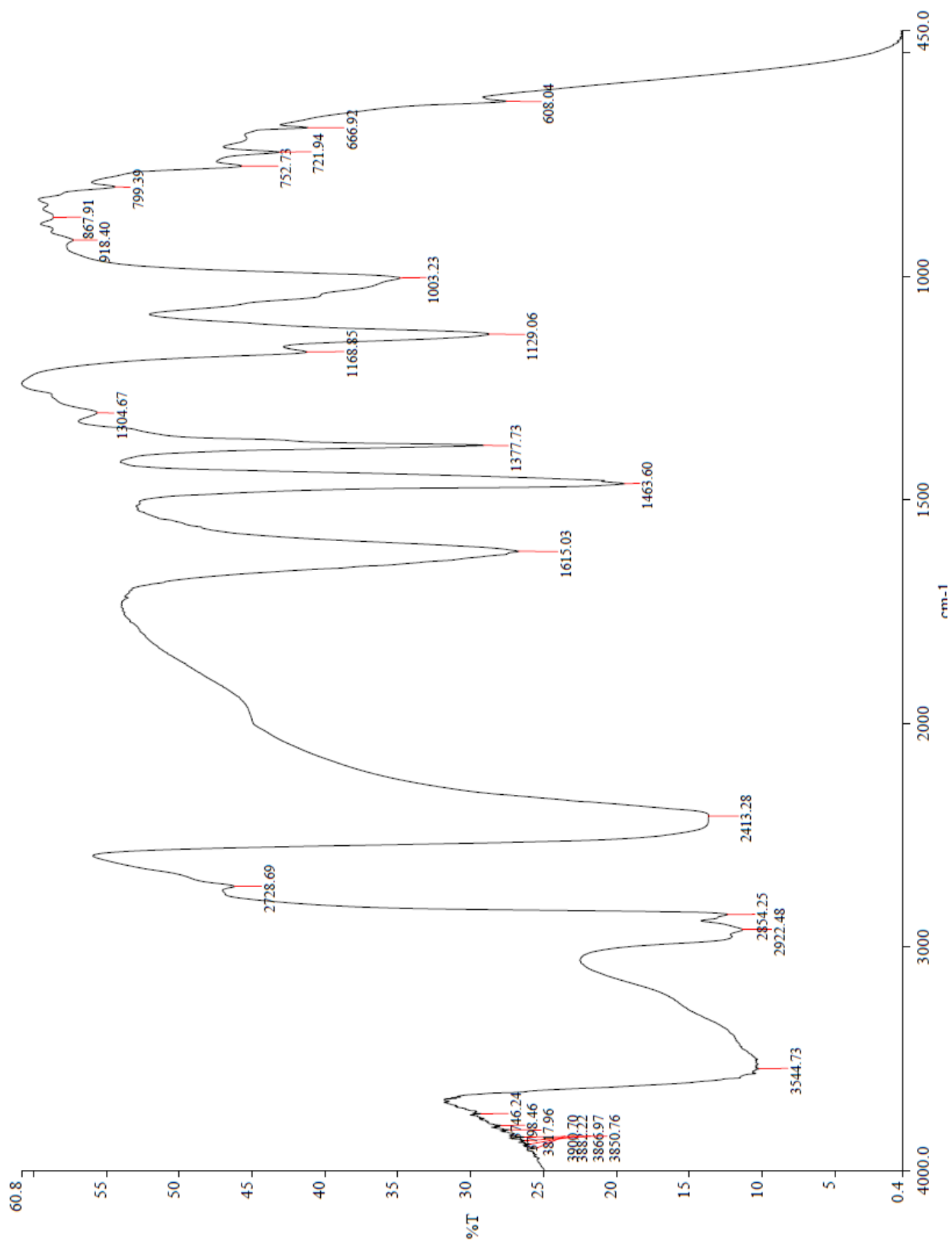


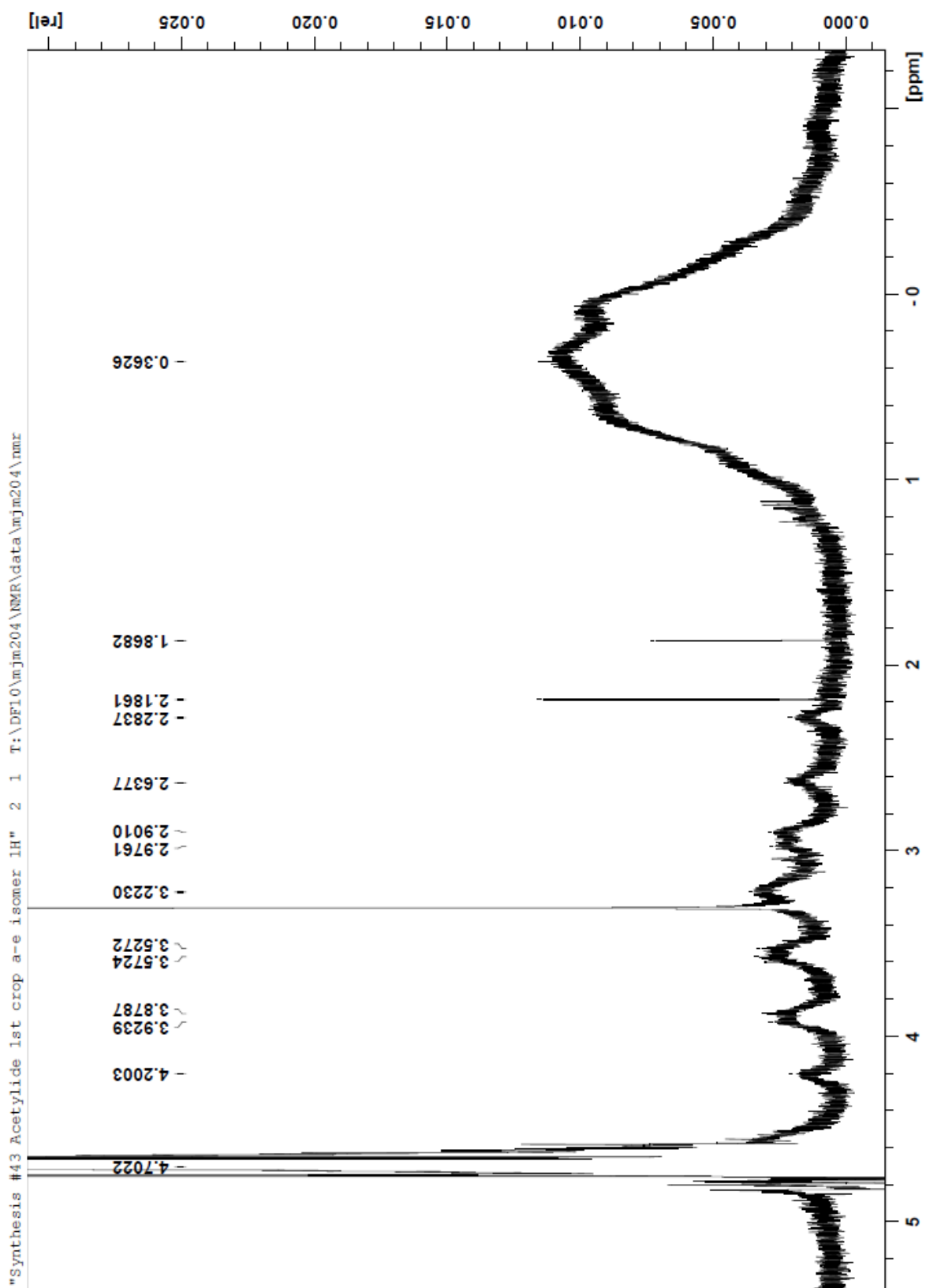
IR of $\text{Rb}_4[\text{ae-B}_{20}\text{H}_{17}(\text{CH}_2)_3\text{CH}_3]$ 

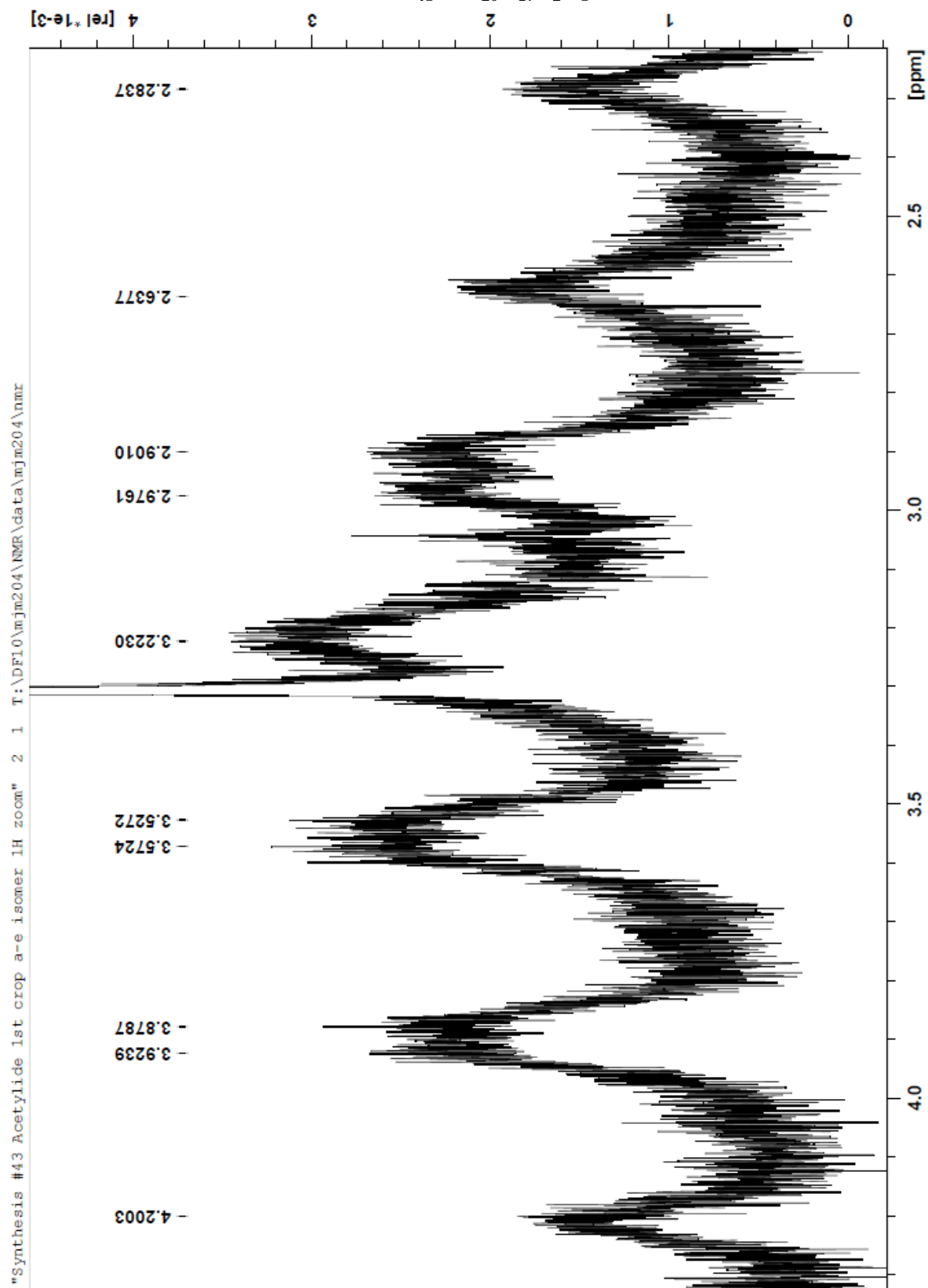


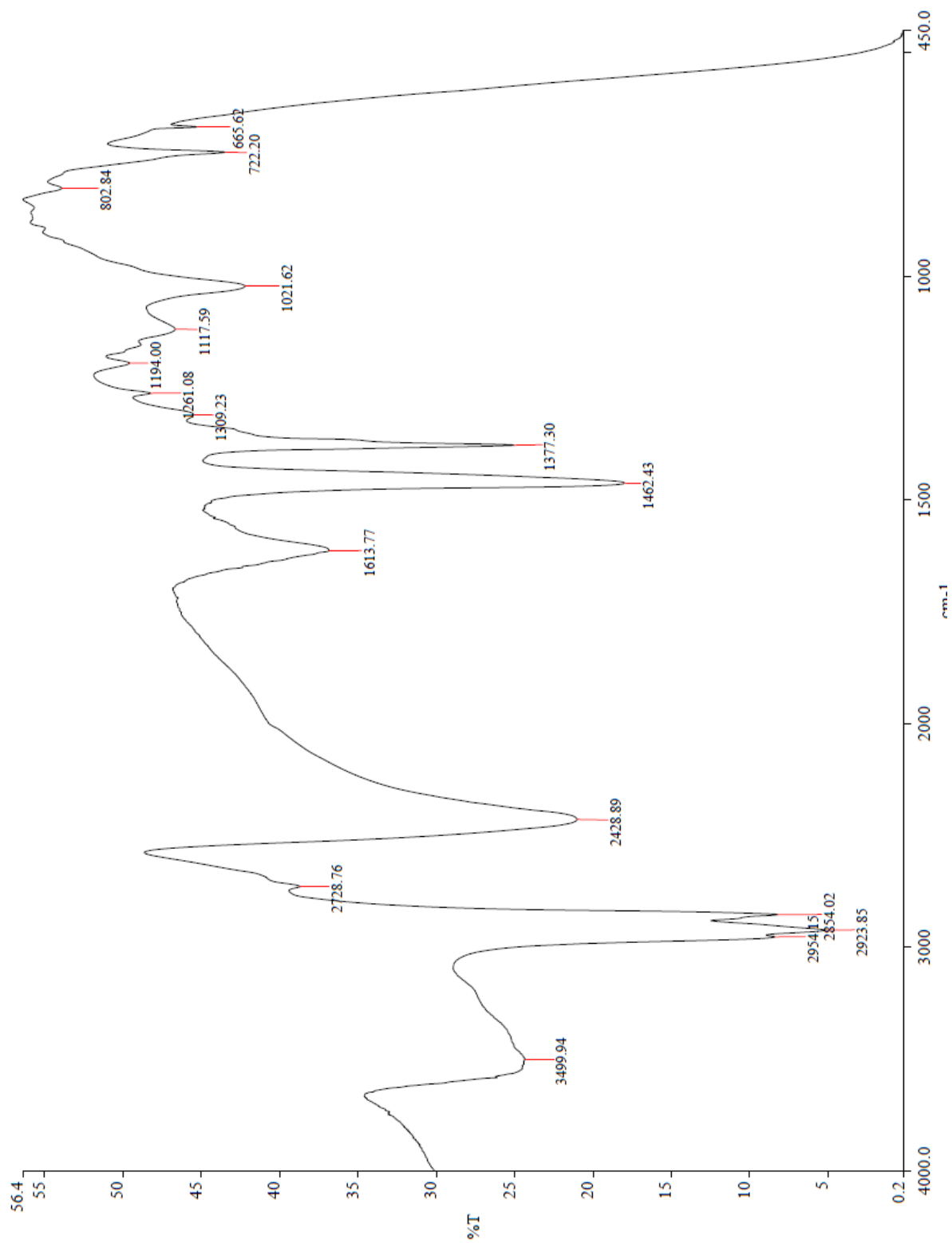


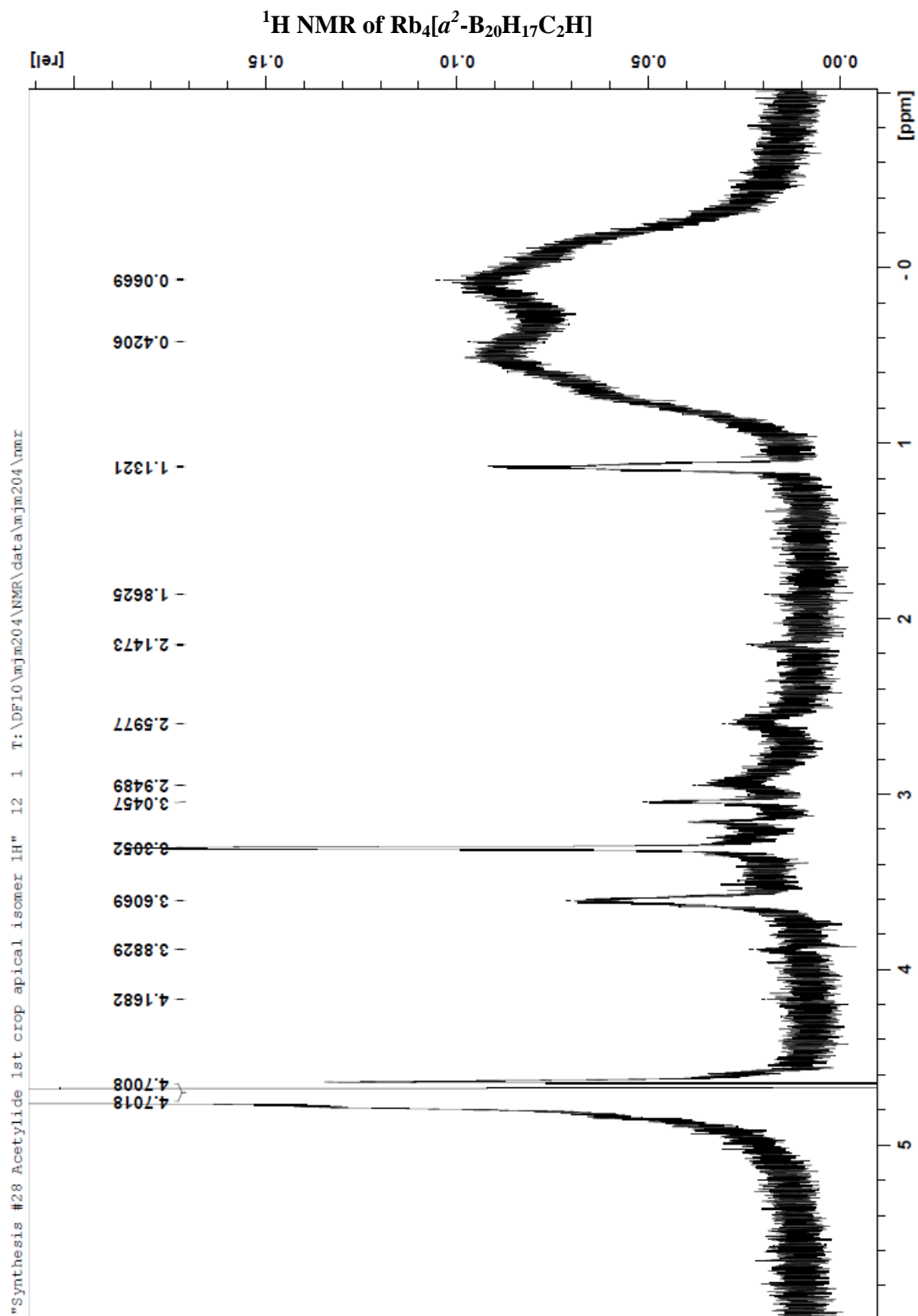
^{13}C NMR of $\text{Rb}_4[\text{a}^2\text{-B}_{20}\text{H}_{17}(\text{CH}_2)_3\text{CH}_3]$ 

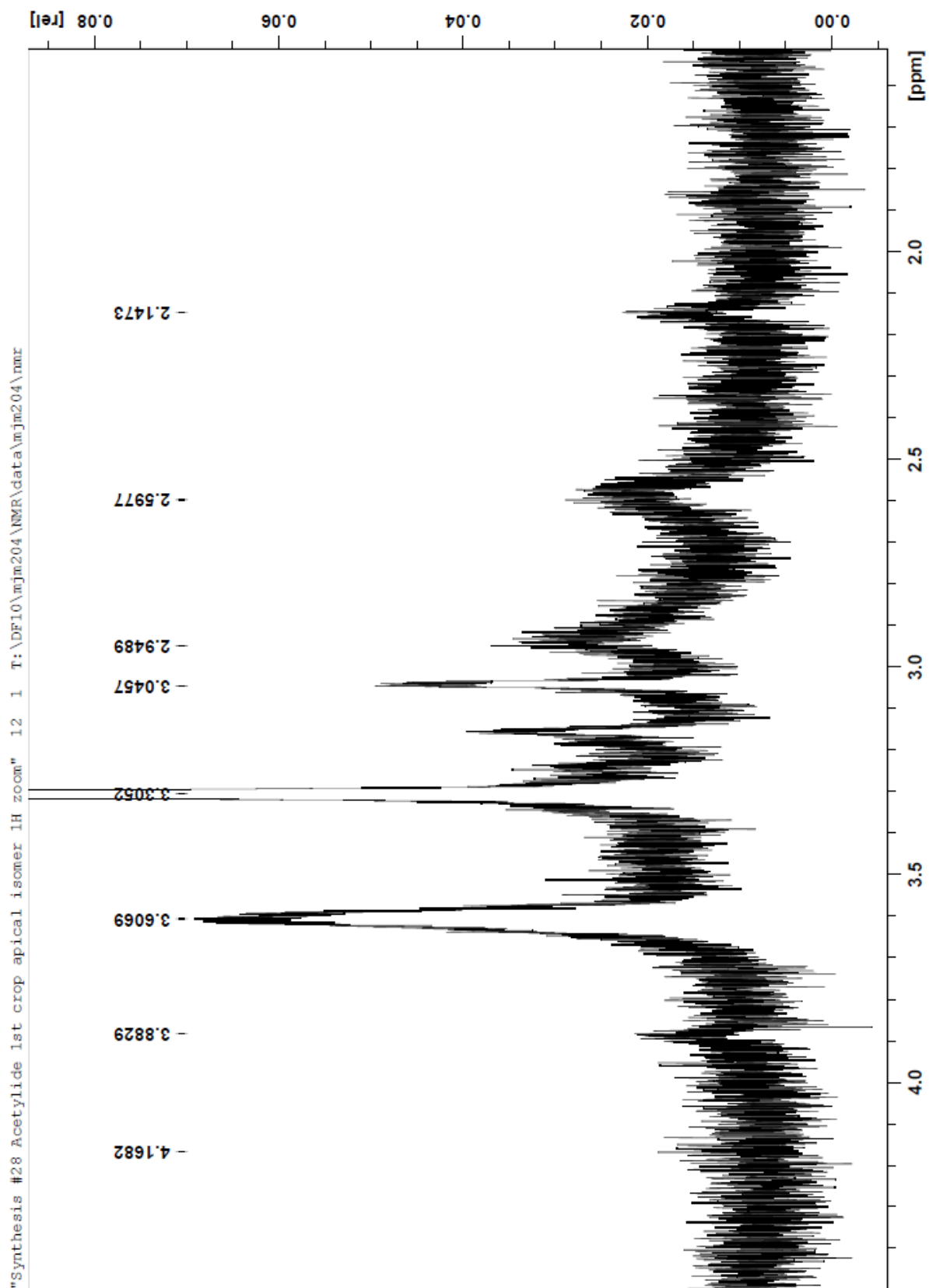
IR of $\text{Rb}_4[\text{a}^2\text{-B}_{20}\text{H}_{17}(\text{CH}_2)_3\text{CH}_3]$ 

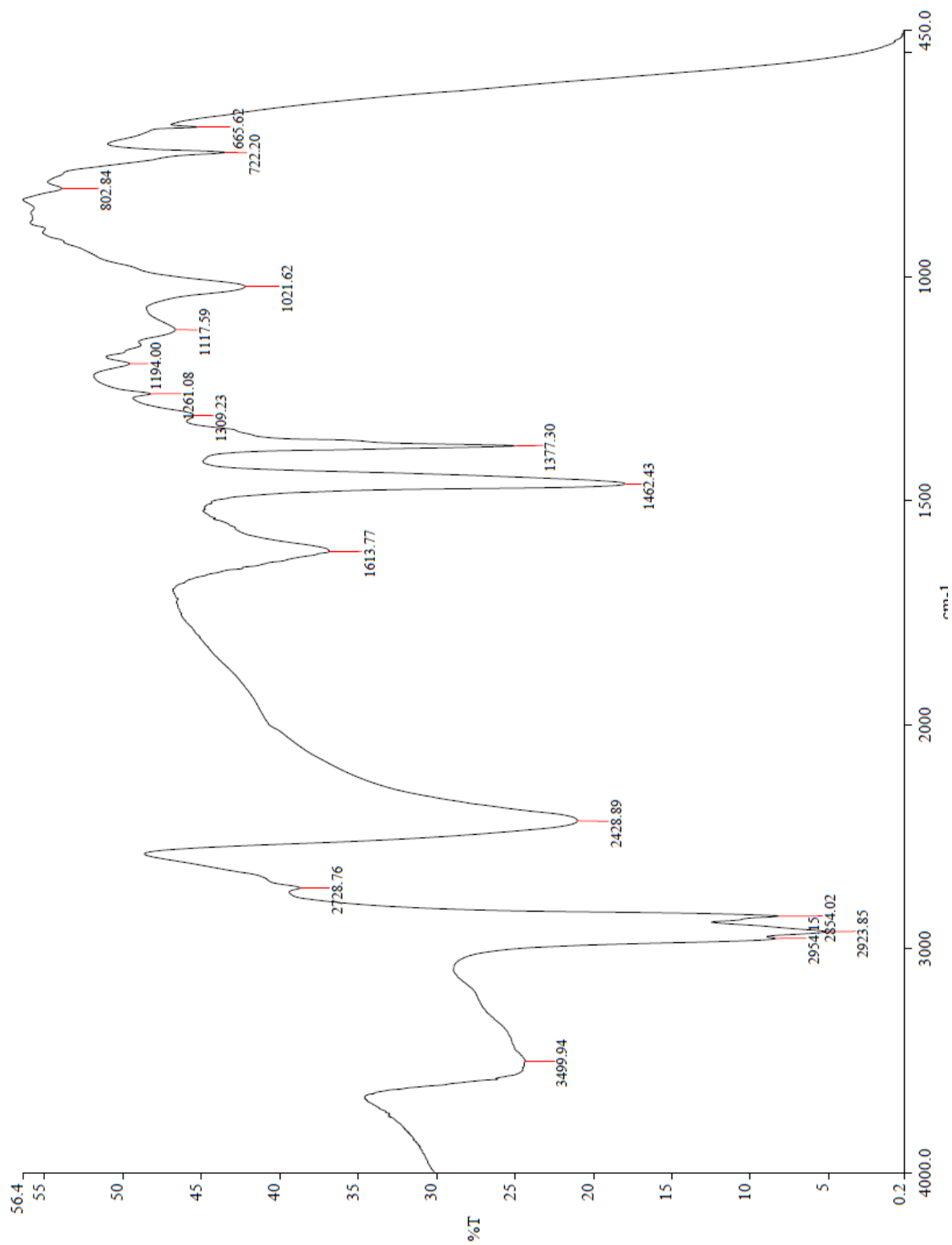
^1H NMR of $\text{Rb}_4[\text{ae-B}_{20}\text{H}_{17}\text{C}_2\text{H}]$ 

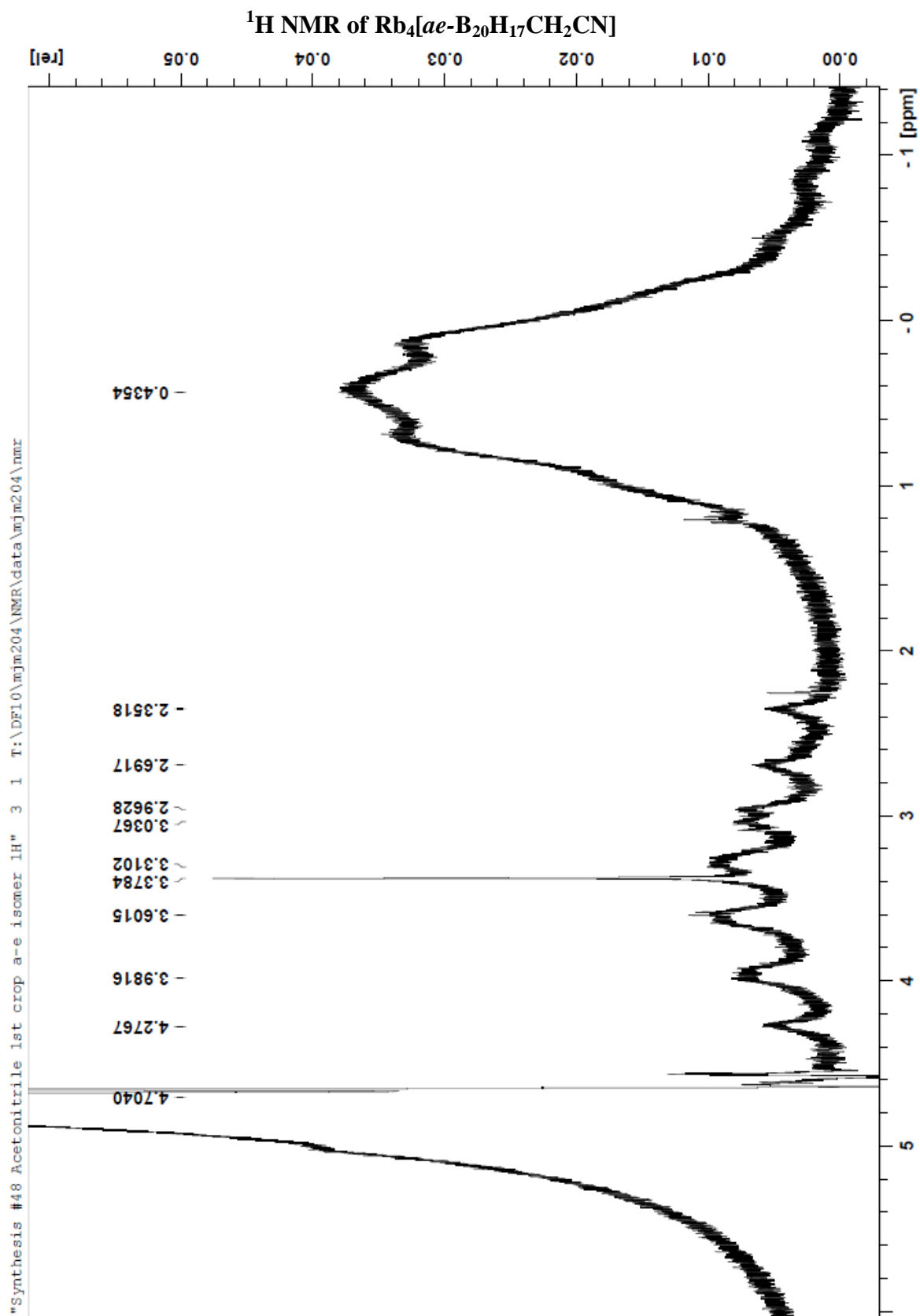
^1H NMR of $\text{Rb}_4[\text{ae-B}_{20}\text{H}_{17}\text{C}_2\text{H}]$ 

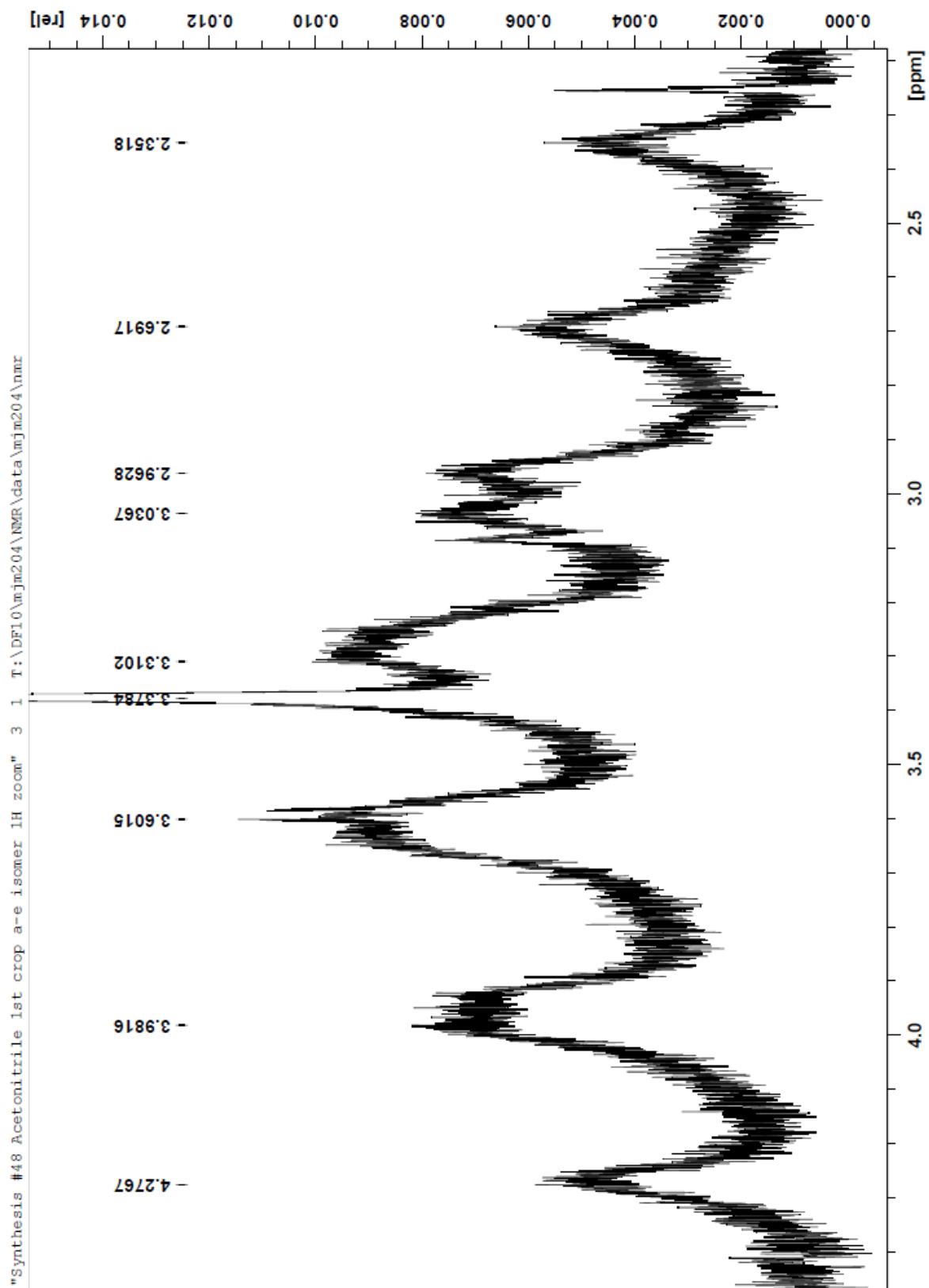
IR of $\text{Rb}_4[\text{ae-B}_{20}\text{H}_{17}\text{C}_2\text{H}]$ 

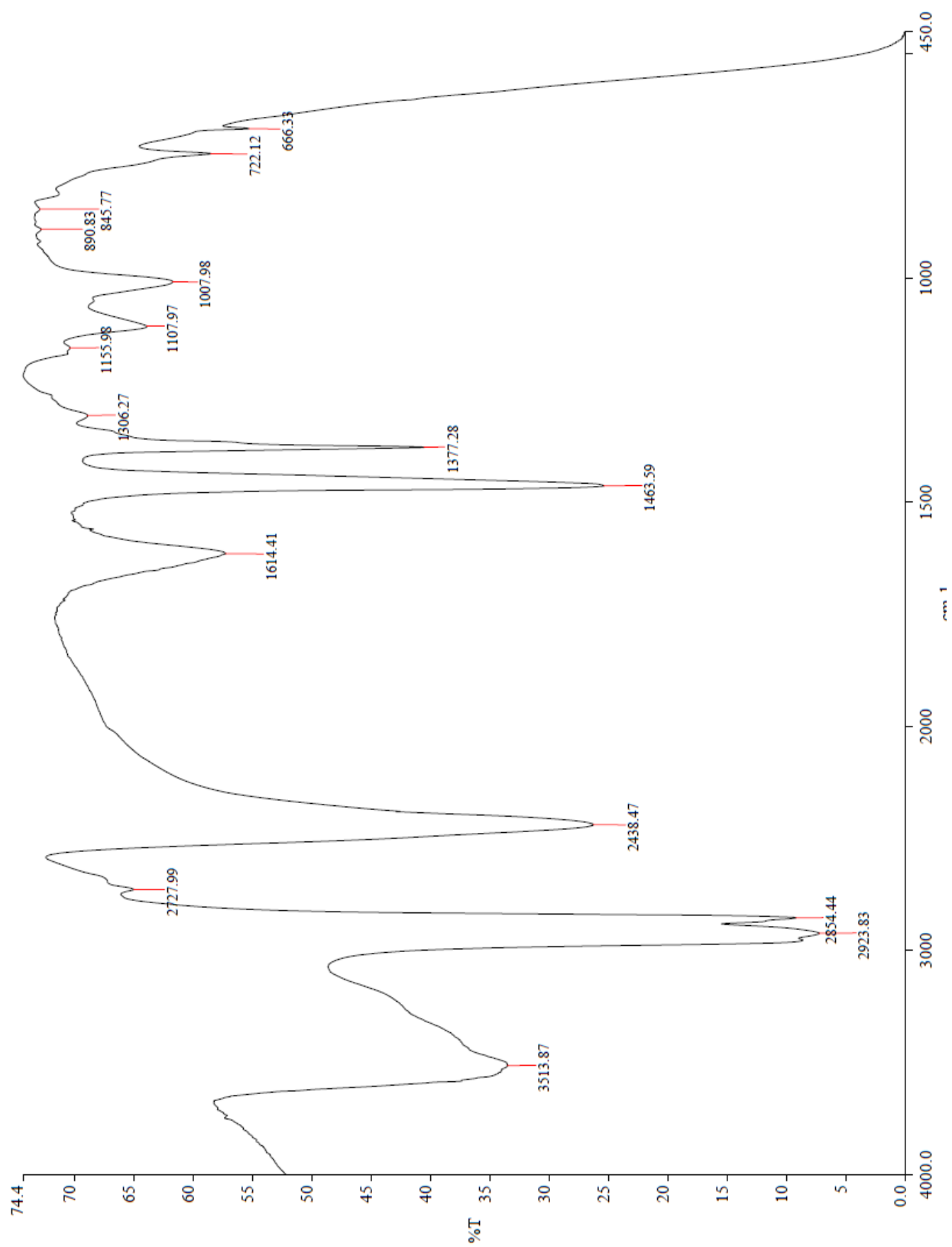


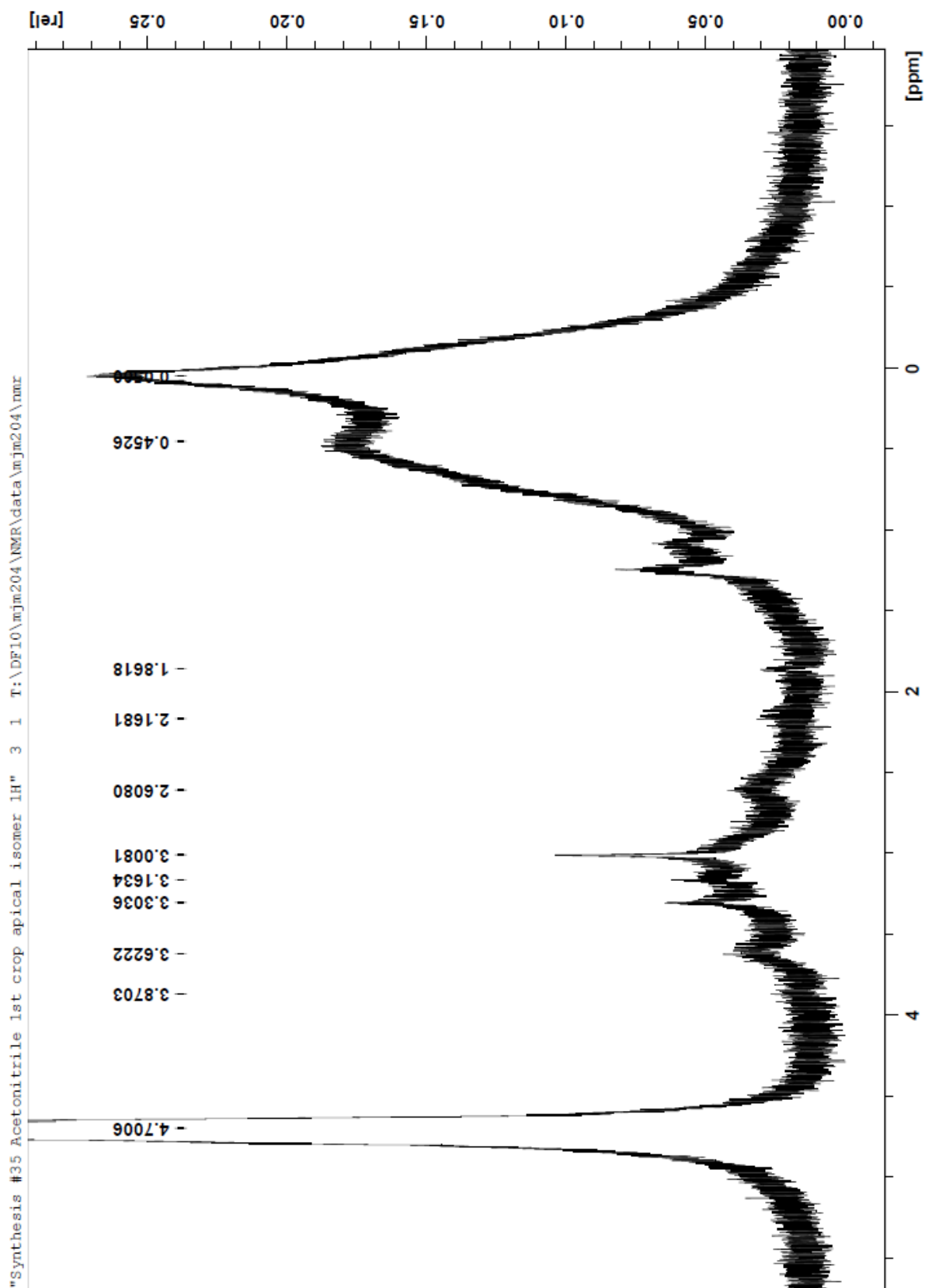
^1H NMR of $\text{Rb}_4[\text{a}^2\text{-B}_{20}\text{H}_{17}\text{C}_2\text{H}]$ 

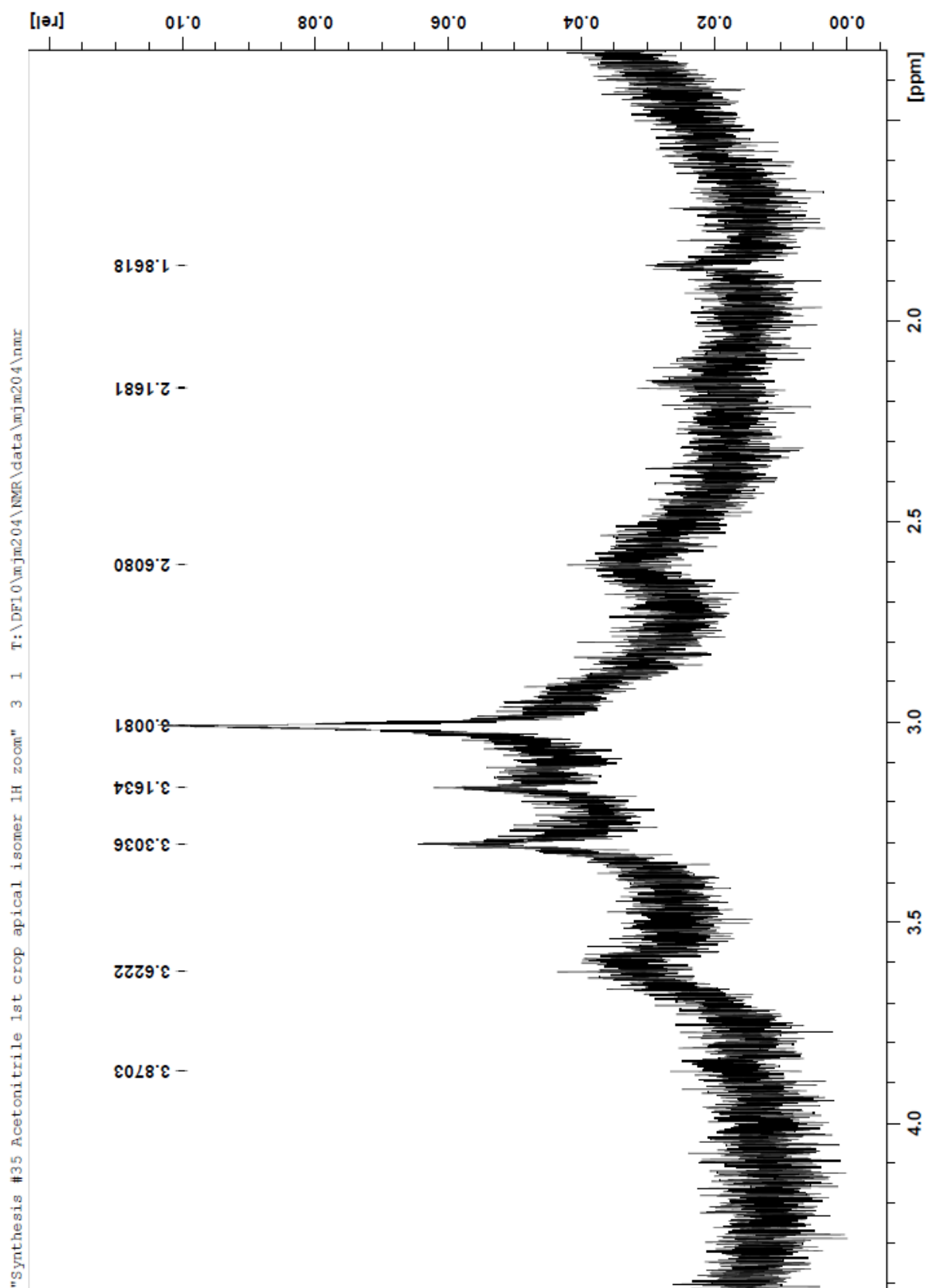
IR of $\text{Rb}_4[\text{a}^2\text{-B}_{20}\text{H}_{17}\text{C}_2\text{H}]$ 

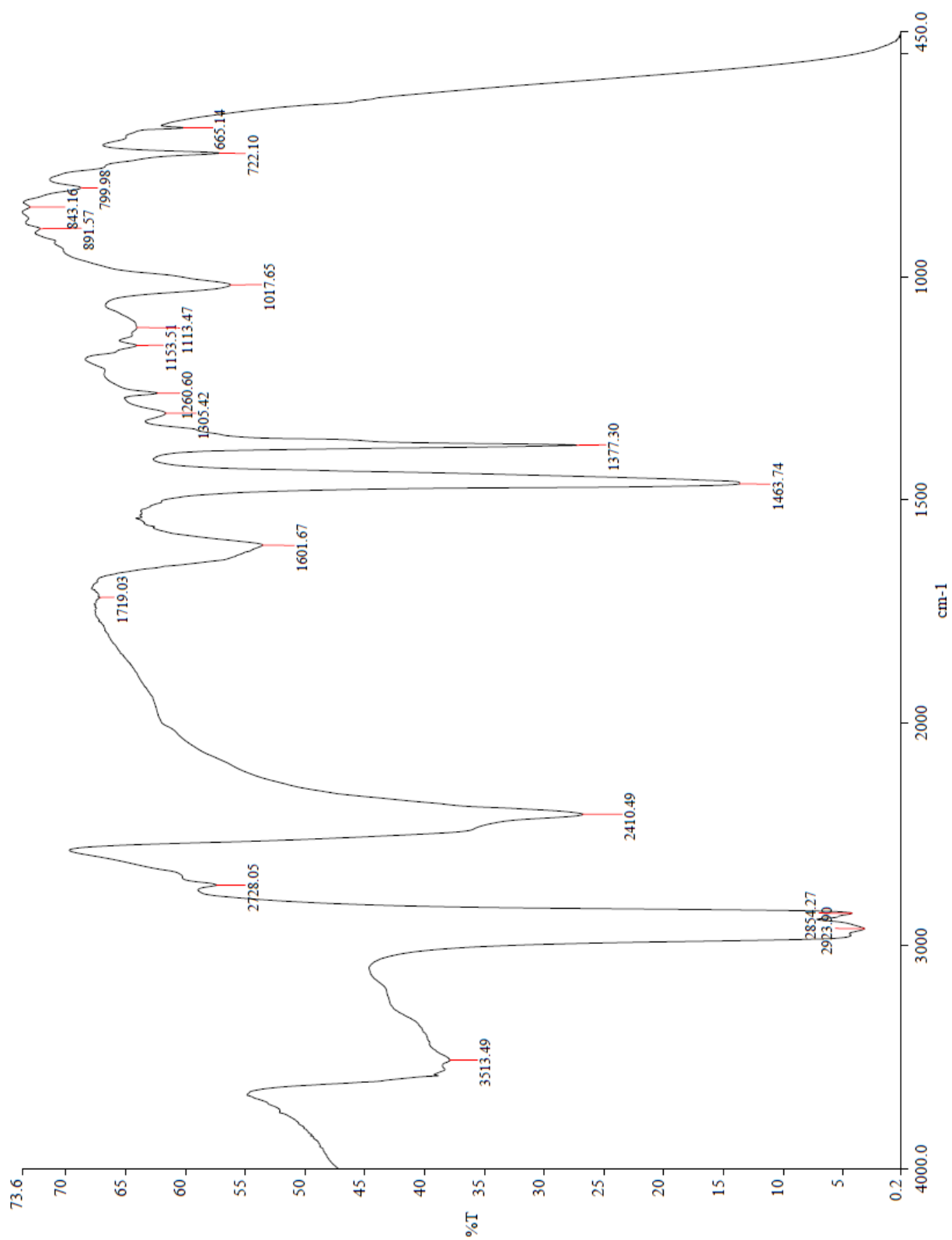


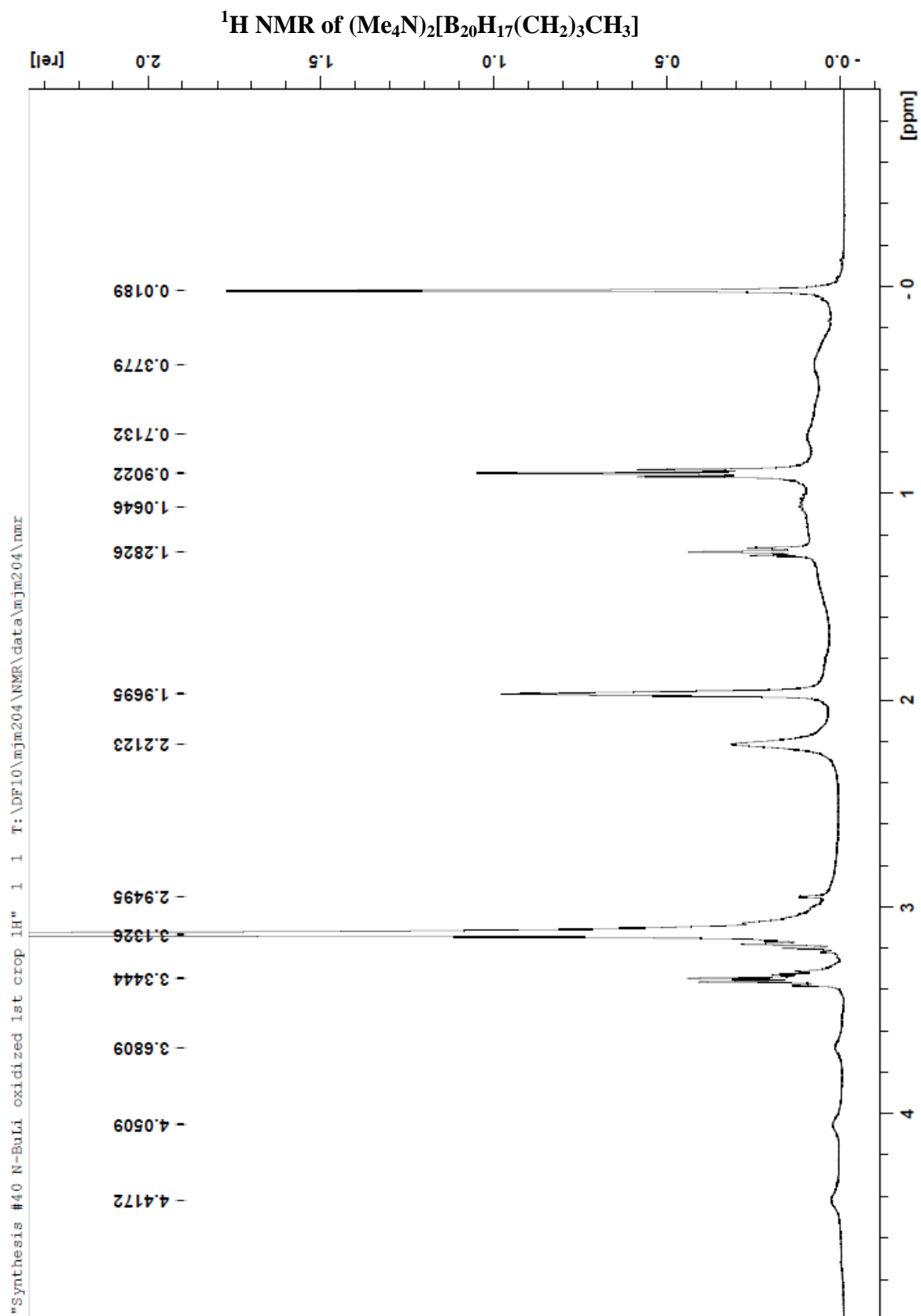
^1H NMR of $\text{Rb}_4[\text{ae-B}_{20}\text{H}_{17}\text{CH}_2\text{CN}]$ 

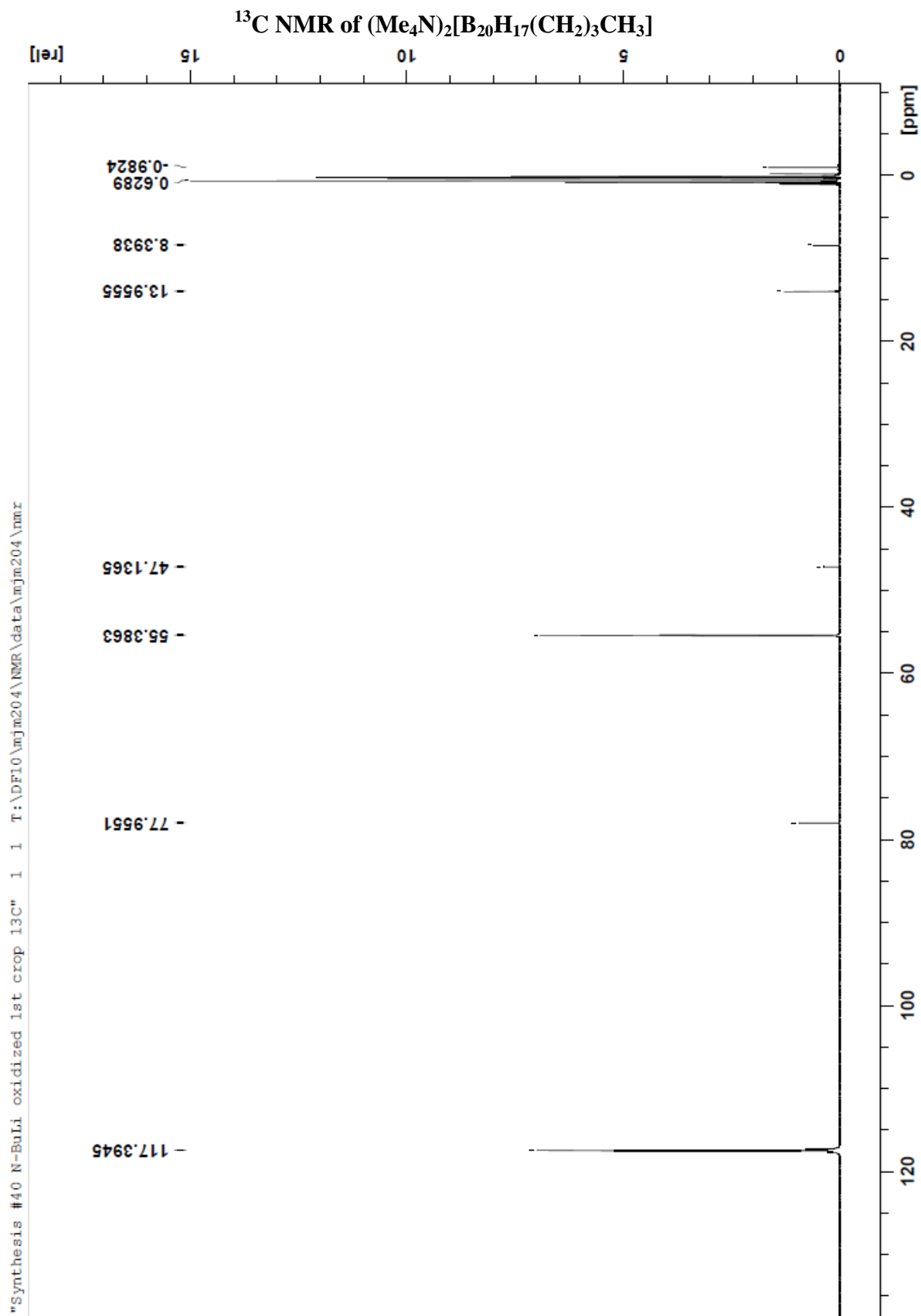
IR of $\text{Rb}_4[\text{ae-B}_{20}\text{H}_{17}\text{CH}_2\text{CN}]$ 

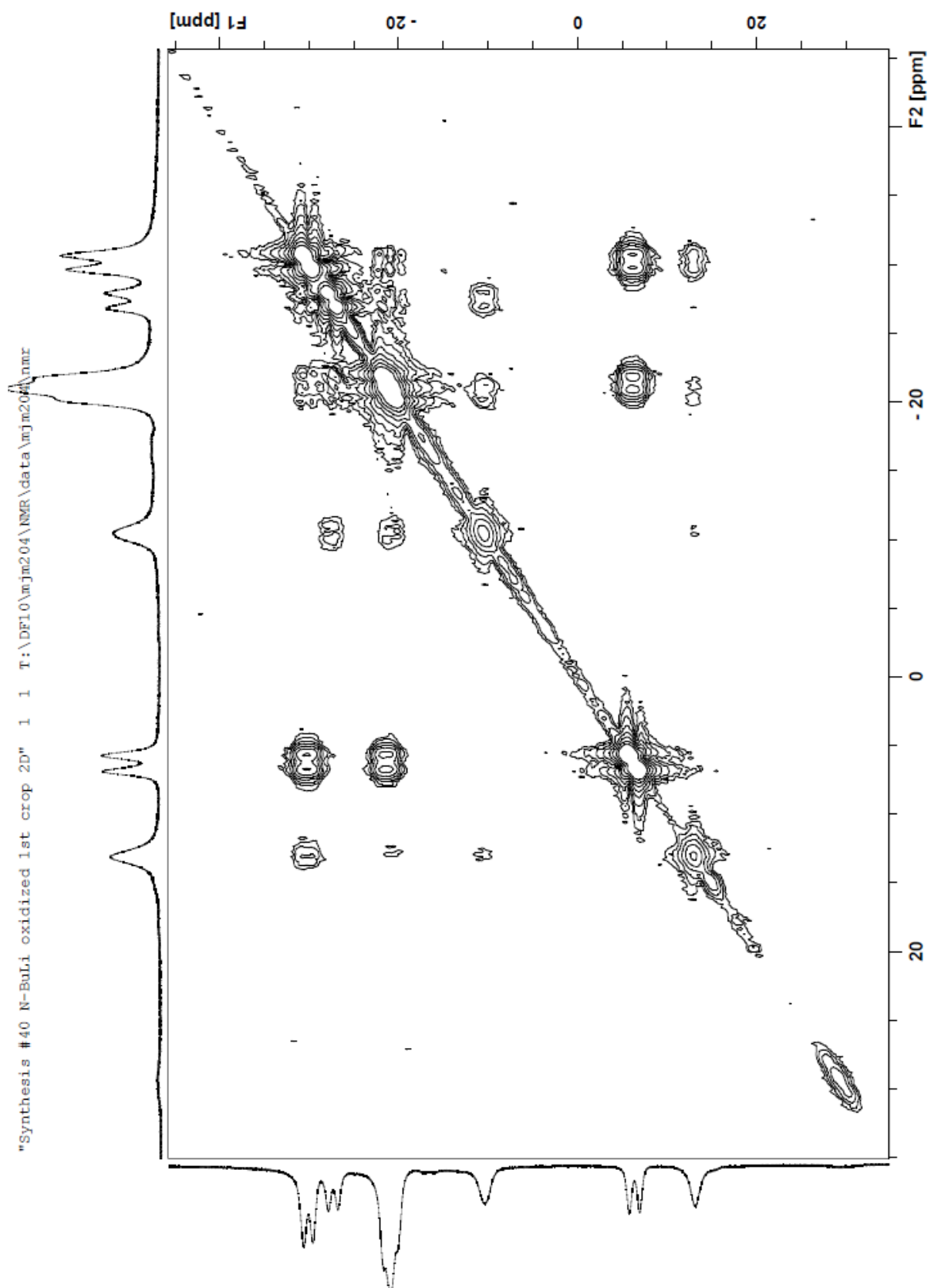
^1H NMR of $\text{Rb}_4[\text{a}^2\text{-B}_{20}\text{H}_{17}\text{CH}_2\text{CN}]$ 

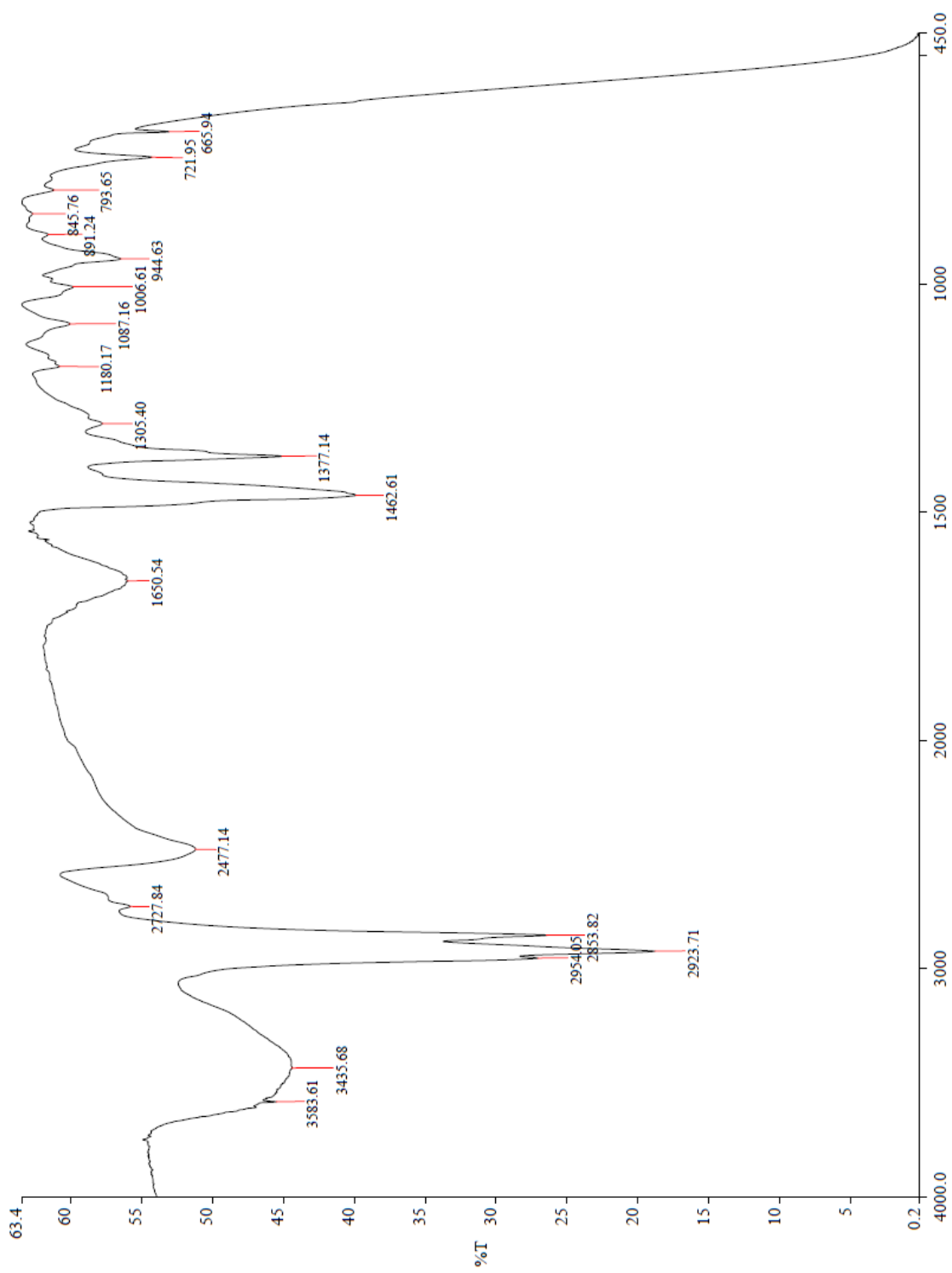
^1H NMR of $\text{Rb}_4[\text{a}^2\text{-B}_{20}\text{H}_{17}\text{CH}_2\text{CN}]$ 

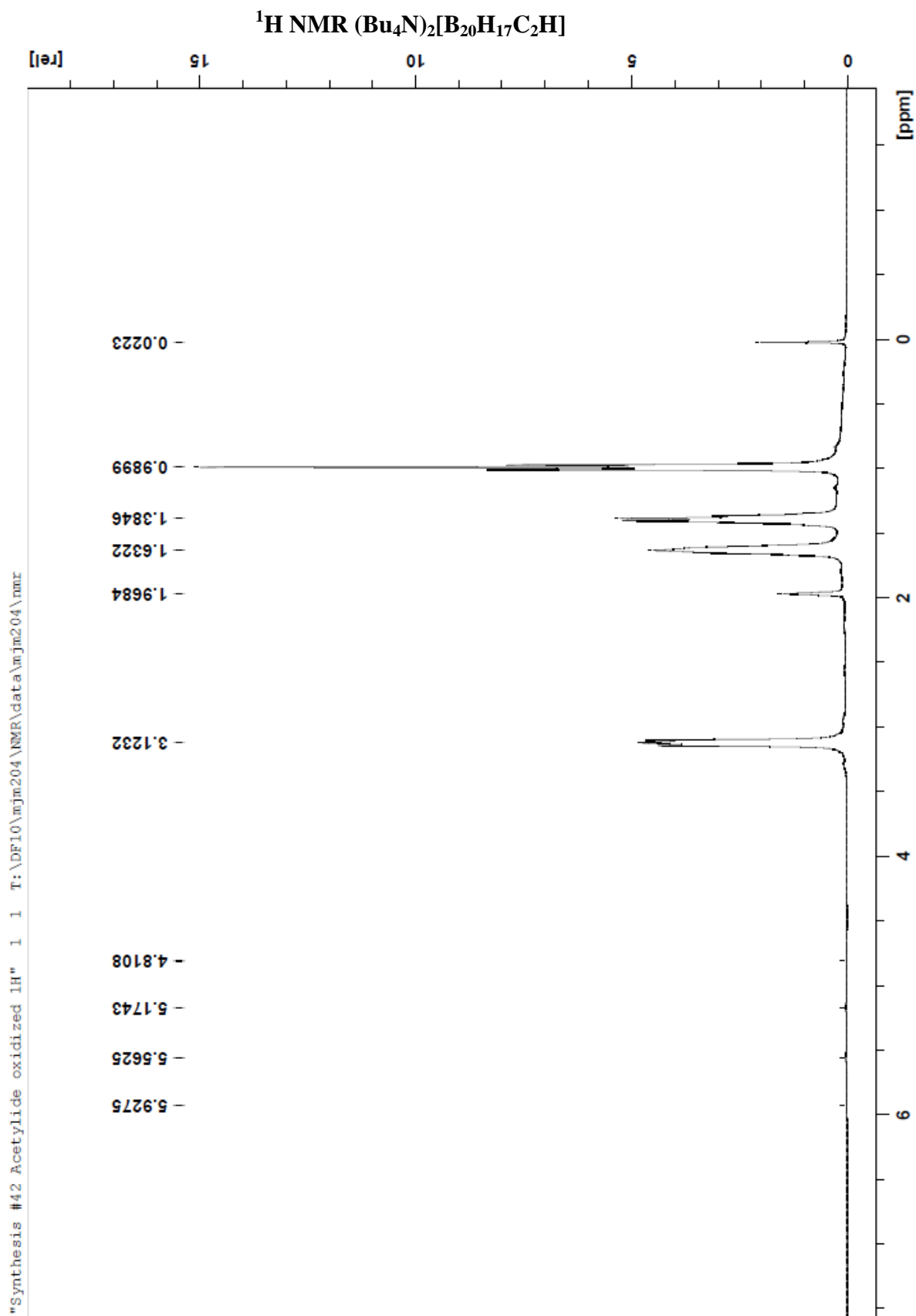
IR of $\text{Rb}_4[\alpha^2\text{-B}_{20}\text{H}_{17}\text{CH}_2\text{CN}]$ 

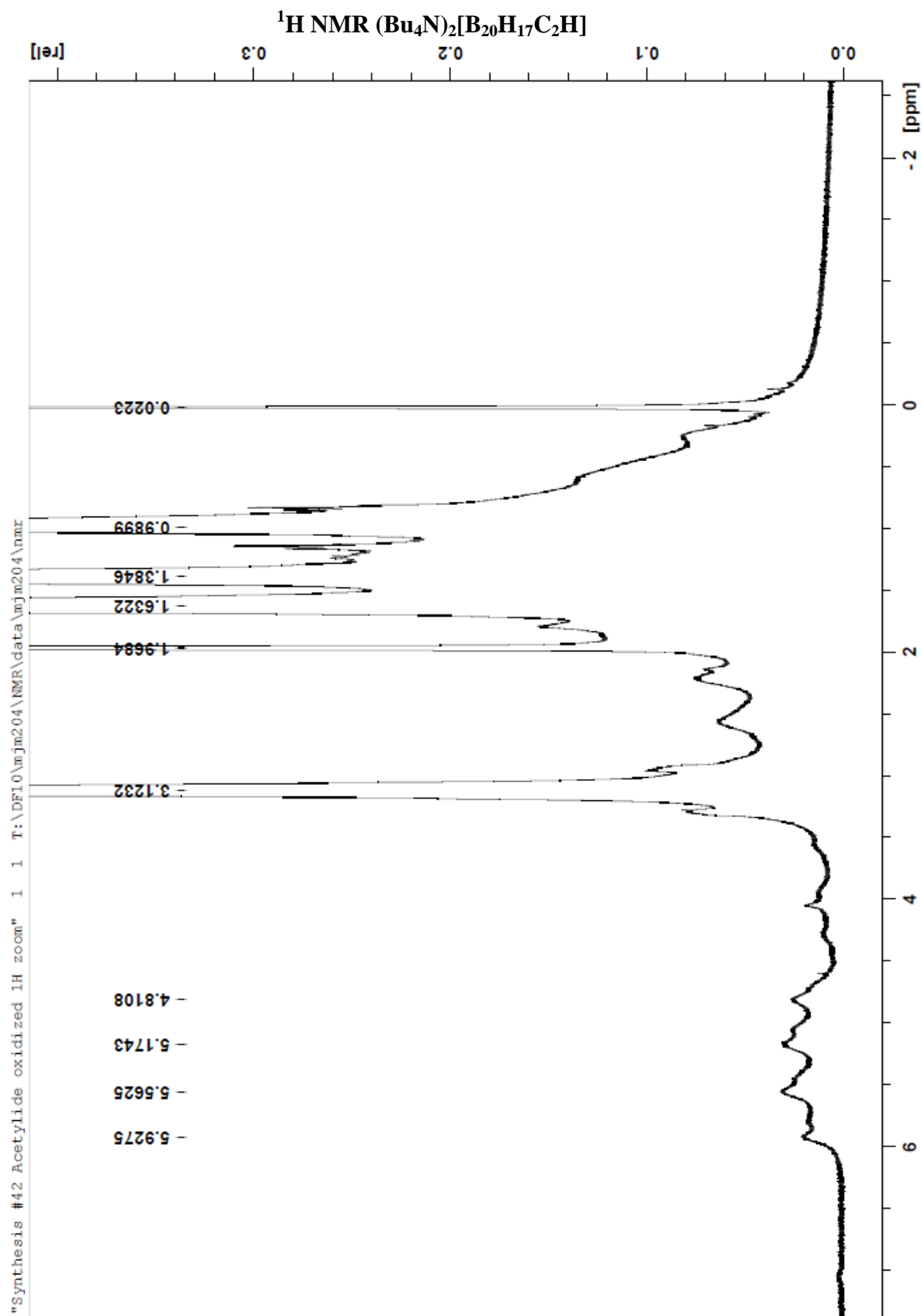


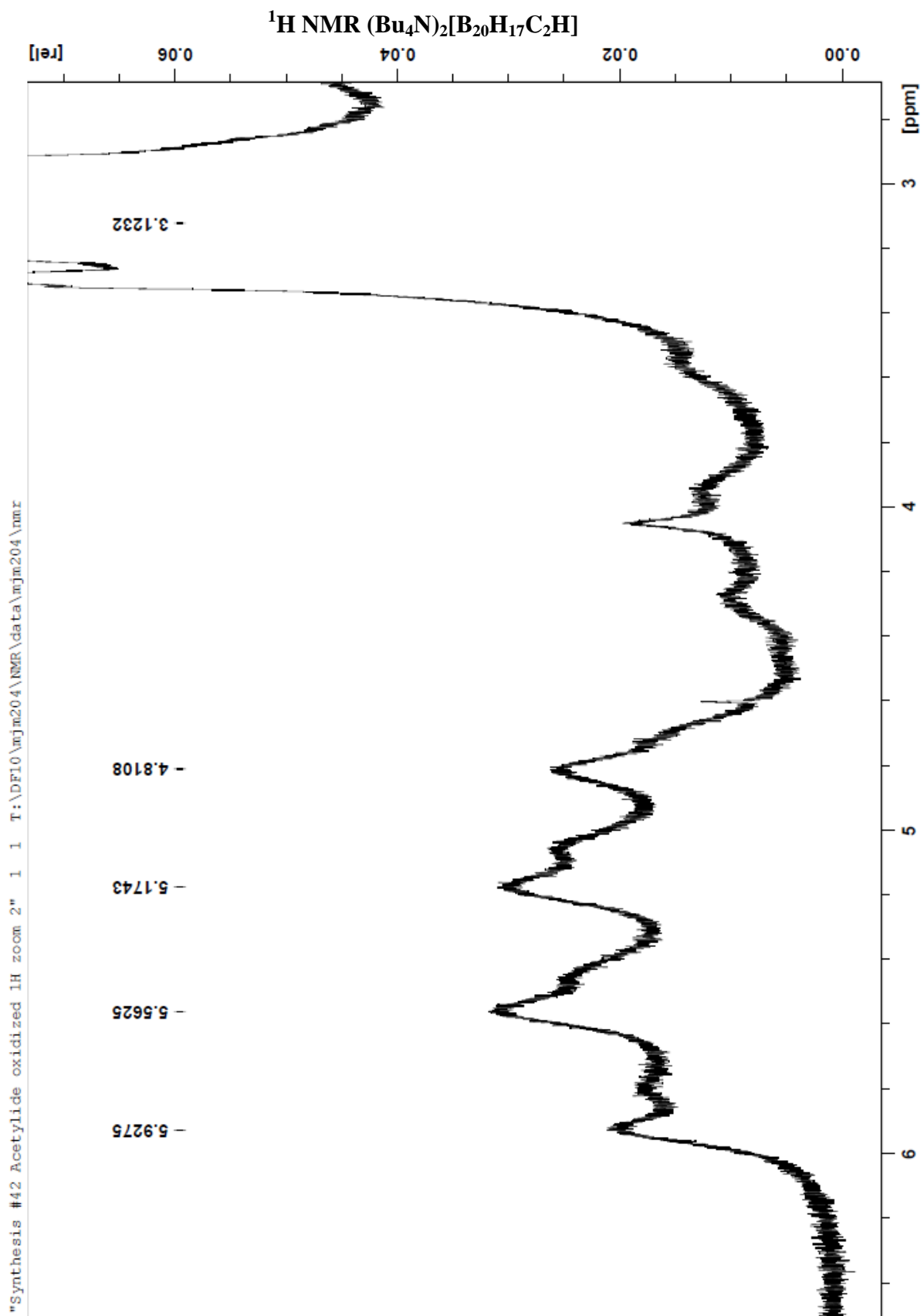


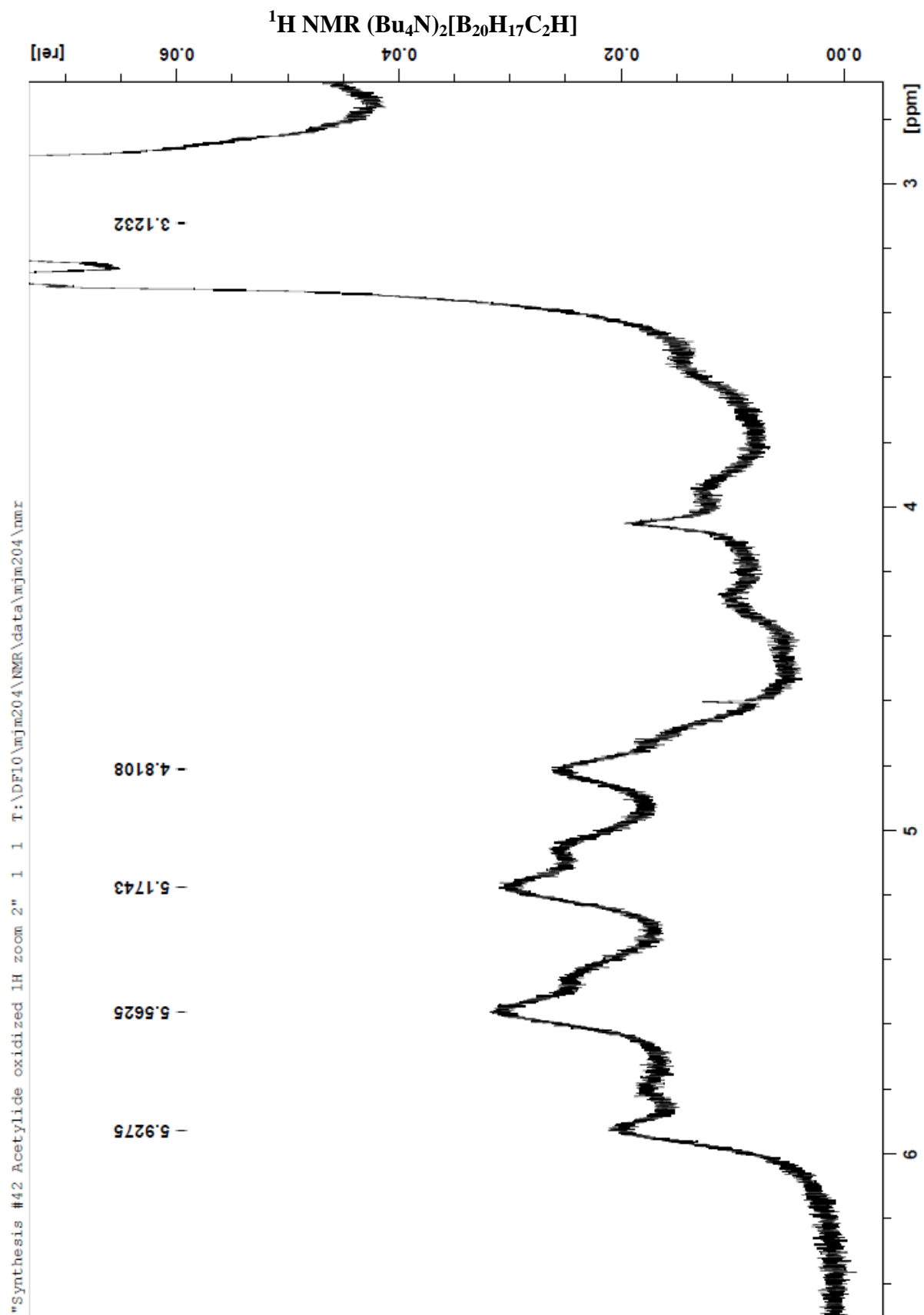
$2D^{11}B-^{11}B$ NMR of $(Me_4N)_2[B_{20}H_{17}(CH_2)_3CH_3]$ 

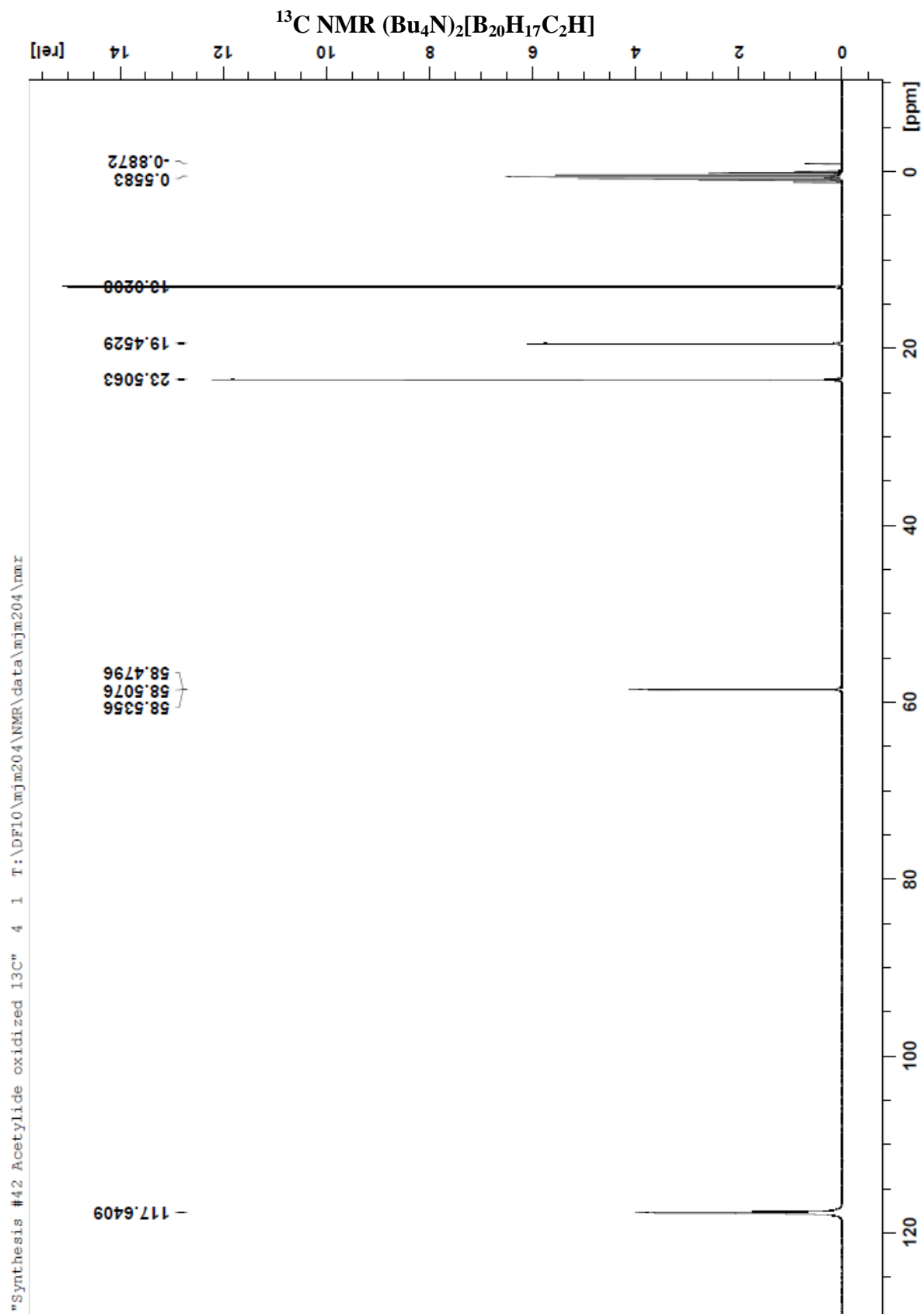
IR of $(\text{Me}_4\text{N})_2[\text{B}_{20}\text{H}_{17}(\text{CH}_2)_3\text{CH}_3]$ 

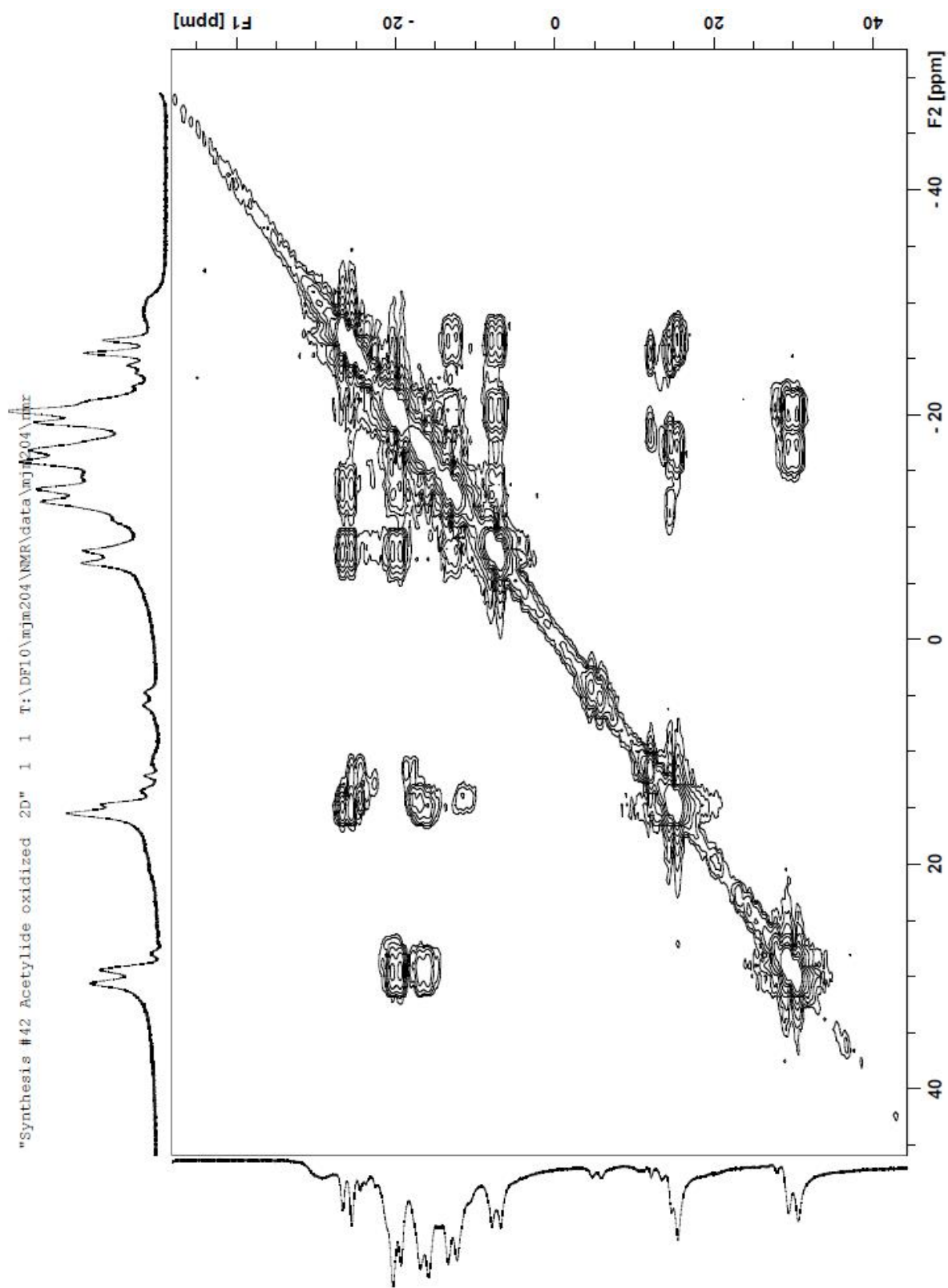


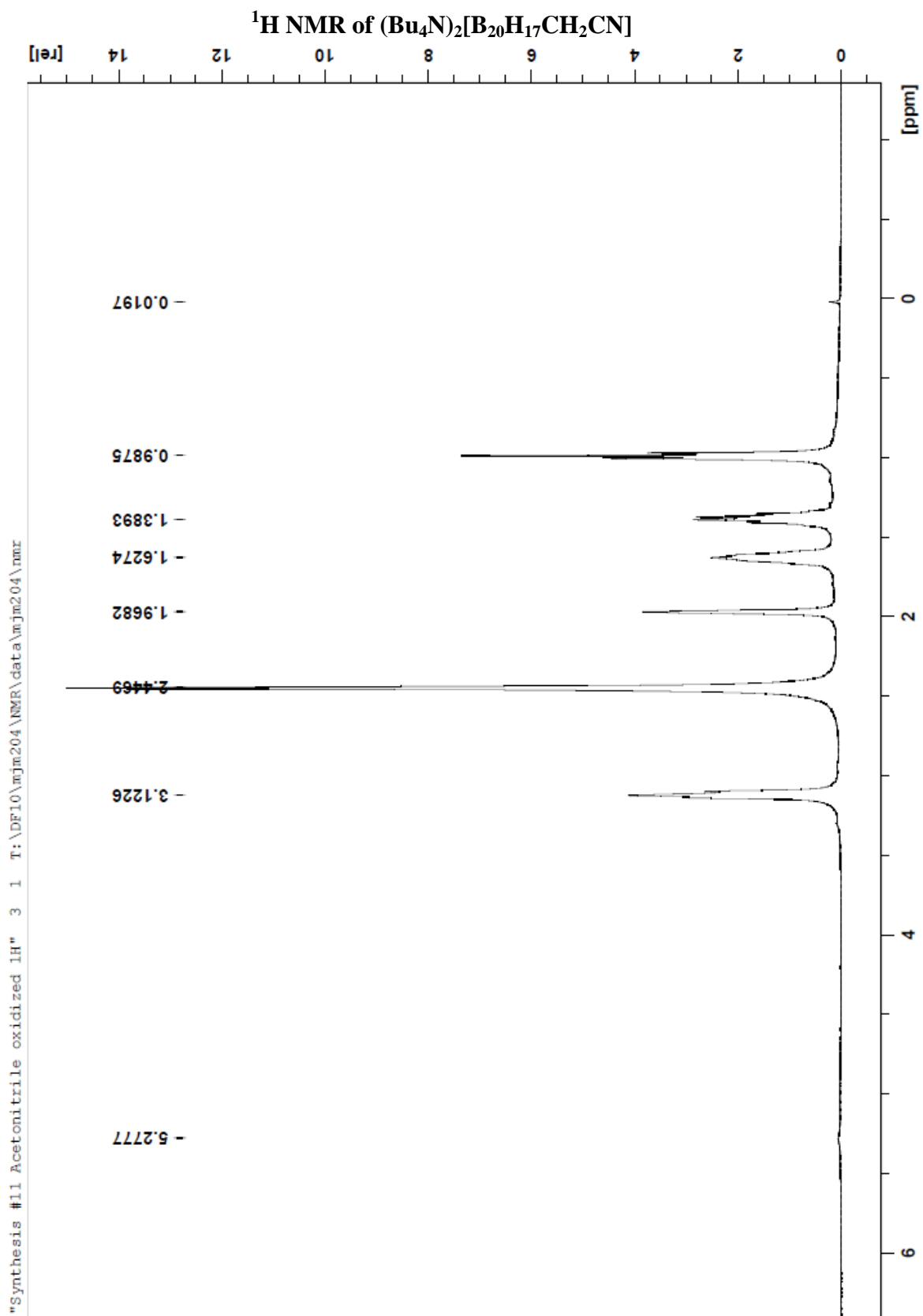


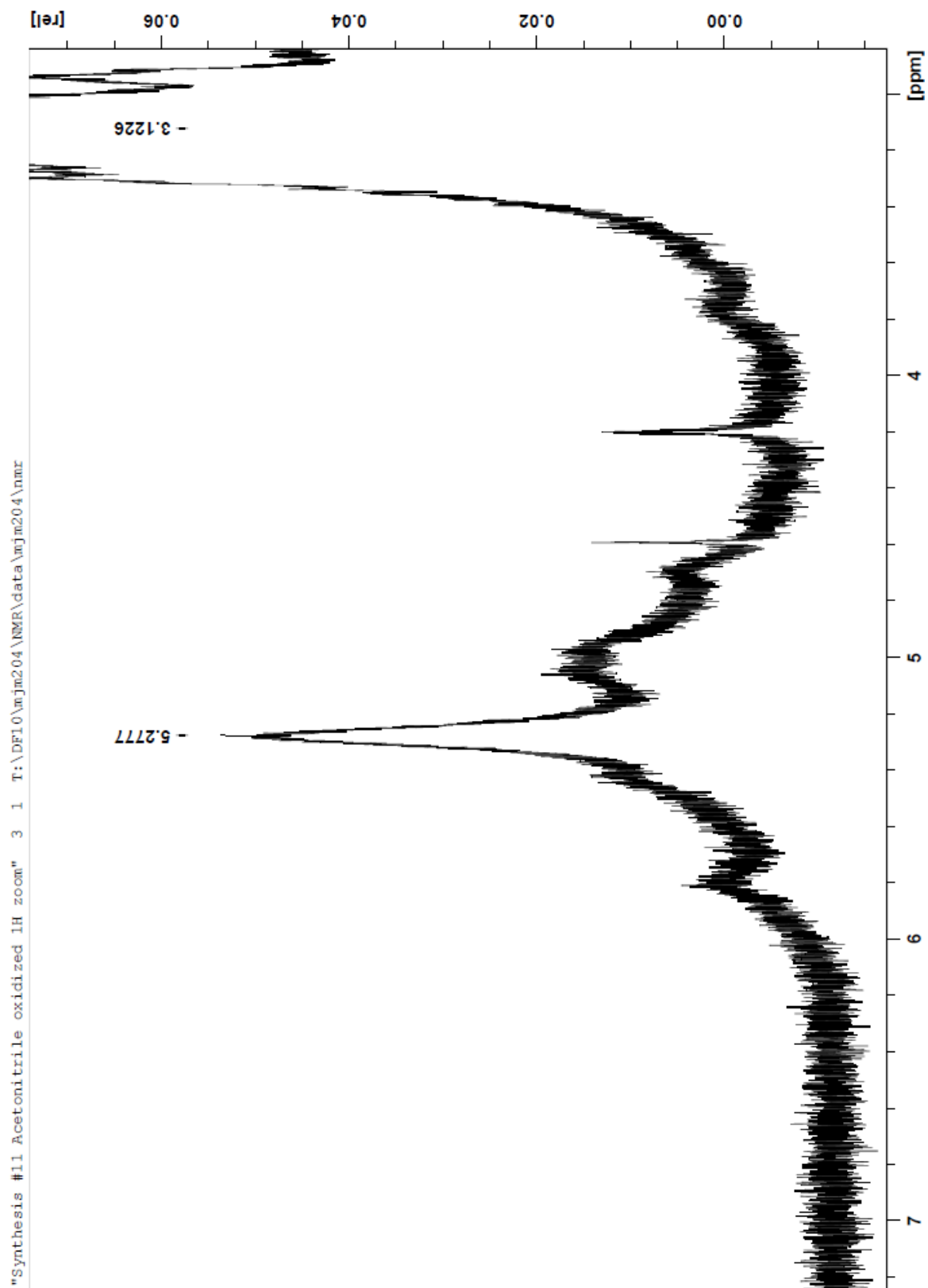






$2D^{11}\text{B}-^{11}\text{B}$ NMR of $(\text{Bu}_4\text{N})_2[\text{B}_{20}\text{H}_{17}\text{C}_2\text{H}]$ 



^1H NMR of $(\text{Bu}_4\text{N})_2[\text{B}_{20}\text{H}_{17}\text{CH}_2\text{CN}]$ 

REFERENCES

1. Hawthorne, M. F.; Shelly, K.; Li, F., The Versatile Chemistry of the $[\text{B}_{20}\text{H}_{18}]^{2-}$ Ions: Novel Reactions and Structural Motifs. *Chem. Commun.* **2002**, (6), 547-554.
2. Wade, K. *Electron Deficient Compounds*. Springer: 1971.
3. Watson-Clark, R. A.; Shelly, K.; and Hawthorne, M. F. The Synthesis and Characterization of Bis-Substituted Derivatives of the $[\text{a}^2\text{-B}_{20}\text{H}_{18}]^{4-}$ Anion and the Interconversion of Isomers. *Inorg. Chem.* **2000**, 39 (9), 1901-1906.
4. Lipscomb, W. N. *The Boranes and Their Relatives*. Harvard University: Cambridge, Massachusetts 1976; Vol. Chemistry.
5. Stock, A. *Hydrides of Boron and Silicon*. Cornell University Press: Ithaca, NY, 1933.
6. Hoffmann, R., Lipscomb, W. N. Theory of Polyhedral Molecules. I. Physical Factorizations of the Secular Equation. *J. Chem. Phys.* **1962**, 36 (8), 2179.
7. Lipscomb, W. N.; Pitochelli, A. R.; and Hawthorne, M. F. Probable Structure Of The $[\text{B}_{10}\text{H}_{10}]^{2-}$ Ion. *J. Am. Chem. Soc.* **1959**, 81, 5833.
8. Hawthorne, M. F.; and Pitochelli, A. R. The Reactions of Bis-Acetonitrile With Amines. *J. Am. Chem. Soc.* **1959**, 82, 5833.
9. Hawthorne, M. F.; and Pitochelli, A. R. The Isolation Of The Icosahedral $[\text{B}_{12}\text{H}_{12}]^{2-}$ Ion. *J. Am. Chem. Soc.* **1960**, 82, 3228.
10. Hawthorne, M. F.; and Pilling, R. L. Bis(Triethylammonium)Decahydrodecaborate(2-). *Inorg. Synth.* **1967**, 9, 16-19.
11. Kaczmarczyk, A.; Dobrott R. D., and Lipscomb, W. N. Reactions of $[\text{B}_{20}\text{H}_{18}]^{2-}$ Ion. *Proc. Natl. Acad. Sci.* **1962**, 48, 729-733.

12. Hawthorne, M. F.; Pilling, R. L.; and Stokely, P. F. The Preparation and Rearrangement of the Three Isomeric $[\text{B}_{20}\text{H}_{18}]^{4-}$ Ions. *J. Am. Chem. Soc.* **1965**, *87* (9), 1893-1899.
13. Pitochelli, A. R.; Lipscomb, W. N.; and Hawthorne, M. F. Isomers of the $[\text{B}_{20}\text{H}_{18}]^{2-}$ Isomer. *J. Am. Chem. Soc.* **1962**, *84*, 3026-3027.
14. Pilling R. L.; and Hawthorne, M. F. Photoisomerization of the $[\text{B}_{20}\text{H}_{18}]^{2-}$ Ion. *J. Am. Chem. Soc.* **1966**, *88* (17), 3873-3874.
15. Li, F.; Shelly, K.; Knobler, C. B.; and Hawthorne, M. F. The Synthesis of $[\text{Me}_4\text{N}]_2[\text{a}^2\text{-B}_{20}\text{H}_{16}(\text{NH}_3)_2]$ and $[\text{trans-B}_{20}\text{H}_{16}(\text{NH}_3)_2]$ from $[\text{Me}_3\text{NH}][\text{cis-B}_{20}\text{H}_{17}\text{NH}_3]$ and Their Structural Characterization. *Inorg. Chem.* **1999**, *38*, 4926-4927.
16. Li, F.; Shelly, K.; Knobler, C. B.; and Hawthorne, M. F. A New Isomer of the $[\text{B}_{20}\text{H}_{18}]^{2-}$ Ion: Synthesis, Structure, and Reactivity of *cis*- $[\text{B}_{20}\text{H}_{18}]^{2-}$ and *cis*- $[\text{B}_{20}\text{H}_{17}\text{NH}_3]$. *Angew. Chem. Int. Ed.* **1998**, *37* (12/14), 1868-1871.
17. Hawthorne, M. F.; Pilling, R. L.; Stokely, P.F.; and Garrett, P. M. The Isolation and Characterization of $[\text{B}_{20}\text{H}_{19}]^{3-}$ and $[\text{B}_{20}\text{H}_{18}]^{4-}$ Ions. *J. Am. Chem. Soc.* **1963**, *85*, 3704-3705.
18. Hawthorne, M. F.; Pilling, R. L.; and Garrett, P. M. A Study of the Reaction of Hydroxide Ion with $[\text{B}_{20}\text{H}_{18}]^{2-}$. *J. Am. Chem. Soc.* **1965**, *87* (21), 4740-4746.
19. Hawthorne, M. F.; Pilling, R. L.; Stokely, P.F.; and Garrett, P. M. The Reaction of the $[\text{B}_{20}\text{H}_{18}]^{2-}$ Ion with Hydroxide Ion. *J. Am. Chem. Soc.* **1963**, *85*, 3704.
20. Georgiev, E. M.; Shelly, K.; Feakes, D. A.; Kuniyoshi, J.; Romano, S.; and Hawthorne, M. F. Synthesis of Amine Derivatives of the Polyhedral Borane Anion $[\text{B}_{20}\text{H}_{18}]^{4-}$. *Inorg. Chem.* **1996**, *35*, 5412-5416.
21. Soloway, A. H.; Tjarks, W.; Barnum, B. A.; Rong, F. G.; Barth, R. F.; Codogni, I. M.; and Wilson, J. G. The Chemistry of Neutron Capture Therapy. *Chem. Rev.* **1998**, *98* (4), 1515-1562.
22. Hawthorne, M. F. The Role of Chemistry in the Development of Boron Neutron Capture Therapy. *Angew. Chem. Int. Ed.* **1993**, *32* (7), 950-984.
23. Feakes, D. A.; Shelly, K.; Knobler, C. B.; and Hawthorne, M. F. $\text{Na}_3[\text{B}_{20}\text{H}_{17}\text{NH}_3]$: Synthesis and Liposomal Delivery to Murine Tumors. *Proc. Nati. Acad. Sci. USA* **1994**, *91* (Medical Sciences), 3029-3033.

24. Feakes, D. A.; Waller, R. C.; Hathaway, D. K.; and Morton, V. S. Synthesis and in vivo Murine Evaluation of $\text{Na}_4[1-(1'\text{-B}_{10}\text{H}_9)\text{-6-SHB}_{10}\text{H}_8]$ as a Potential Agent for Boron Neutron Capture Therapy. *Proc. Natl. Acad. Sci. USA* **1999**, *96* (Medical Sciences), 6406–6410.
25. Smits, J. P.; Mustachio, N.; Newell, B.; and Feakes, D. A. Synthesis and Investigation of $[\text{B}_{20}\text{H}_{17}\text{O}(\text{CH}_2)_5]^{3-}$, a Novel Solvent Complex of the $[\text{B}_{20}\text{H}_{18}]^{4-}$ ion. *Inorg. Chem.* **2012**, *51* (15), 8468-72.
26. Unpublished Results.
27. Shelly, K.; Feakes, D. A.; Hawthorne, M. F.; Schmidt, P. G.; Krischt, T. A.; and Bauer, W. F. Model Studies Directed Toward the Boron Neutron-Capture Therapy of Cancer: Boron Delivery to Murine Tumors with Liposomes. *Proc. Natl. Acad. Sci. USA* **1992**, *89* (Medical Sciences), 9039-9043.
28. Lee, M. W. and Hawthorne, M. F. A Critical Assessment of Boron Target Compounds for Boron Neutron Capture Therapy. *JNO* **2003**, *62*, 33–45.
29. Silverstein, B. *Spectrometric Identification of Organic Compounds 4th Ed.* John Wiley and Sons: United States, 1981.
30. Wilkie, C. and Das, R. Monolithium Derivatives of Acetonitrile and Phenylacetonitrile. *J. Am. Chem. Soc.* **1972**, *94* (13), 4555.
31. Spielvogel, B. F.; Wajnowich, L.; Das, M. K.; McPhail, A. T.; Hargrave, K. D.; Boron Analogues of Amino Acids. Synthesis and Biological Activity of Boron Analogues of Betaine. *J. Am. Chem. Soc.* **1976**, *98* (18), 5702-5703
32. Spielvogel, B. F.; Harchelroad Jr, F.; and Wisian-Neilson, P. Synthesis of Some Cyano-, Amido, and Carboxyborane Adducts of Amines and Diamines. *J. Inorg. Nuc. Chem.* **1979**, *41*, 1222-1227.
33. Gallulo, V.; Dimas, L.; Zezza, C. A.; and Smith, M. B. Cyclization of Alpha Halonitriles with Organolithiums. *Org. Prep. Proc. Intl.* **1989**, *21*, 297-301.
34. Chang, V. S. and Lee, D. G. Oxidation of Hydrocarbons. 9. The Oxidation of Alkynes by Potassium Permanganate. *J. Org. Chem.* **1979**, *44* (15), 2726-2730.
35. McVey, W. J.; Matthews, B.; Motley, D. M.; Linse, K. D.; Blass, D. P.; Booth, R. E; and Feakes, D. A. Investigation of the Interactions of Polyhedral Borane Anions with Serum Albumins. *J. Inorg. Biochem.* **2008**, *102* (4), 943-51.

36. Feakes, D. A.; Shelly, J. K.; and Harris, F. R. Synthesis of Boron Containing Cholesterol Derivatives for Incorporation into Unilamellar Liposomes and Evaluation for Potential Agents for BNCT. *Tetrahedron* **1999**, *55*, 11177-11186.

VITA

Martin James Mantz was born in Beaumont, Texas, on October 12, 1987, the son of Dr. Peter A. Mantz and Marina Custer. After completion of public school at Nederland High School, Nederland, Texas in 2006, he entered Lamar University in Beaumont, Texas. From fall 2008 to spring 2009 he attended the University of Texas at Dallas, but returned to Lamar University in fall 2009 to complete a Bachelor of Science degree in Chemistry and graduated in May 2011. That fall he entered the Graduate College of Texas State.

Permanent address: martinmantz@hotmail.com

This thesis was typed by Martin J. Mantz